

## General Disclaimer

### One or more of the Following Statements may affect this Document

- This document has been reproduced from the best copy furnished by the organizational source. It is being released in the interest of making available as much information as possible.
- This document may contain data, which exceeds the sheet parameters. It was furnished in this condition by the organizational source and is the best copy available.
- This document may contain tone-on-tone or color graphs, charts and/or pictures, which have been reproduced in black and white.
- This document is paginated as submitted by the original source.
- Portions of this document are not fully legible due to the historical nature of some of the material. However, it is the best reproduction available from the original submission.

**LTV RESEARCH CENTER**

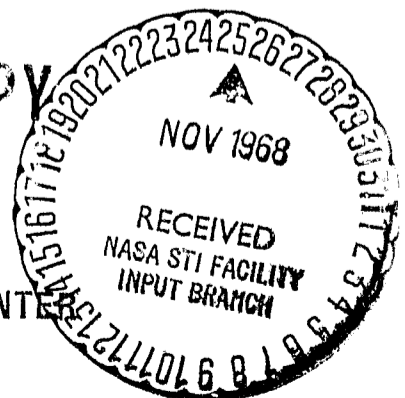
FACILITY FORM 602

<b>N 69-11258</b> (ACCESSION NUMBER)	
<u>153</u> (PAGES)	(THRU)
<u>69-92384</u> (NASA CR OR TMX OR AD NUMBER)	<u>14</u> (CATEGORY)

**LIBRARY COPY**

MAR 27 1967

MANNED SPACECRAFT CENTER  
HOUSTON, TEXAS



NASA CR 72354

LIV BETA-BREMSSTRAHLUNG SPECTROMETER  
FOR GEMINI XII

Contract No. NAS9-5765  
Final Report

O-71000/7R-1  
March, 1967

Prepared by: B. G. Farmer  
B. G. Farmer  
Senior Scientist

Approved by: J. H. Johnson  
J. H. Johnson  
Manager-Nuclear Sciences

N. E. Chappell  
N. E. Chappell  
Research Scientist

H. B. Gibbons  
H. B. Gibbons  
Director

R. G. Bagwell  
R. G. Bagwell  
Research Associate

W. J. Rainwater  
W. J. Rainwater  
Research Scientist

TABLE OF CONTENTS

	<u>Page</u>
INTRODUCTION . . . . .	1
THEORY OF OPERATION . . . . .	3
<u>GENERAL</u> . . . . .	3
<u>PARTICLE DETECTION PROCESSES</u> . . . . .	3
<u>ELECTRONICS</u> . . . . .	4
ELECTRICAL DESIGN . . . . .	5
<u>GENERAL DESIGN SPECIFICATIONS</u> . . . . .	5
<u>PHOTOMULTIPLIER CIRCUIT (N100-10900)</u> . . . . .	5
<u>LINEAR AMPLIFIER (N100-13900)</u> . . . . .	7
<u>HIGH SPEED LEVEL DETECTORS (N100-12900)</u> . . . . .	8
<u>LOGIC AND OUTPUT CIRCUITS (N100-13900)</u> . . . . .	9
<u>LOW VOLTAGE POWER SUPPLY (N100-14900)</u> . . . . .	9
<u>TESTING AND MONITORING</u> . . . . .	11
PACKAGE DESIGN . . . . .	12
<u>DESIGN SPECIFICATIONS</u> . . . . .	12
<u>EXTERNAL DESIGN</u> . . . . .	12
<u>INTERNAL DESIGN</u> . . . . .	12
ANALYSIS OF DATA . . . . .	16
<u>DATA REDUCTION EQUATIONS</u> . . . . .	16
<u>EXPERIMENTAL DISTRIBUTIONS</u> . . . . .	17
<u>BETA RESPONSE MATRIX <math>R_Y</math></u> . . . . .	19
<u>BETA EFFICIENCY MATRIX <math>\epsilon_\beta</math></u> . . . . .	20
<u>BETA CROSS-TALK RESPONSE MATRIX <math>C_\beta</math></u> . . . . .	21

TABLE OF CONTENTS (continued)

	<u>Page</u>
<u>BETA CROSS-TALK EFFICIENCY MATRIX</u> $f_{\beta}$ . . . . .	22
<u>GAMMA RESPONSE MATRIX</u> $R_{\gamma}$ . . . . .	22
<u>GAMMA EFFICIENCY MATRIX</u> $\epsilon_{\gamma}$ . . . . .	22
<u>GAMMA CROSS-TALK RESPONSE MATRIX</u> $C_{\gamma}$ . . . . .	24
<u>GAMMA CROSS-TALK EFFICIENCY MATRIX</u> $f_{\gamma}$ . . . . .	24
<u>TEST SPECTRA</u> . . . . .	24
<u>Beta Spectrum</u> . . . . .	25
<u>Bremsstrahlung Spectrum</u> . . . . .	26
<u>FINAL SYSTEM CALIBRATION</u> . . . . .	26

## INTRODUCTION

Throughout the Gemini program a number of radiation monitoring devices have been employed both inside and outside the spacecraft to measure radiation exposure to the astronauts. These have been both active and passive devices, sensitive to a variety of radiations expected in near earth orbit. In general it has been the object of these devices to determine the spectra of radiations outside the spacecraft and the physical dose due to those radiations inside the spacecraft. However, on Gemini X a bremsstrahlung spectrometer was mounted inside the cabin to better define the radiations inside the craft, and as a result of electron penetration data on the Gemini hatch, a combination beta-bremsstrahlung spectrometer was flown inside the vehicle on Gemini XII. It is this latter device that will be described in detail in this report.

Data relating to electron penetration through the Gemini III hatch was obtained early in 1966 at the LTV Research Center using a Van de Graaff particle accelerator. This data indicated that electrons with energies above 1.0 MeV lost only about 0.7 MeV in the hatch and entered the spacecraft with their remaining degraded energy. It became important to determine the relative intensities of electrons and x-rays inside the spacecraft. Since LTV, under Contract NAS9-4013, provided a device to NASA for evaluation, which was capable of measuring both electrons and x-rays in a single instrument, it was decided to place that device inside Gemini XII. The flight instrument utilized an original principle devised by LTV scientists for separating and analyzing electrons and x-rays (a patent has been applied for covering this apparatus) and only those design changes necessary to conform to the physical, interfacial, and environmental requirements of flight were made. The unit was designed to operate with a NASA modified data processor unit of the type flown with the bremsstrahlung experiment on Gemini X. The major design difficulties in the program were encountered in mating the LTV unit with the data processor. The fabrication, calibration, and calibration data reduction efforts in this program were carried out under National Aeronautics and Space Administration Manned Spacecraft Center contract NAS9-5765.

The Beta-Bremsstrahlung unit, serial number 3, was successfully flown on

Gemini XII November 11-15, 1966. Data was received as planned during the flight and post flight calibration of the instrument demonstrated that the function of the unit and its data processor was identical to that prior to launch. Data was not available in a form suitable for analysis at the time of publication of this report.

## THEORY OF OPERATION

### GENERAL

The LTV Beta-Bremsstrahlung spectrometer sensor unit is a scintillation device which was designed to analyze electron and bremsstrahlung radiations in the region from approximately 0.2 to 4.0 MeV. It combines the application of a complex scintillation crystal assembly with high speed electronic circuitry to identify and separate the two radiations when the device is used in a mixed field.

### PARTICLE DETECTION PROCESSES

The basic principle of a scintillation counter employs the fact that the interaction of radiation with various materials produces excitation or ionization which is followed by the emission of light. This light is converted, usually by a photomultiplier tube, into an electronic signal. Different materials have different phosphorescent decay times which vary over several orders of magnitude. Particle identification was made possible in the Beta-Bremsstrahlung spectrometer by the use of two such materials in the configuration shown in Drawing N100-10001. The plastic scintillation material has a decay time of approximately 3 nanoseconds while that of the thallium activated cesium-iodide is 1.1 microseconds. Since electrons can enter only through the collimator shown in the drawing they must pass through the thin plastic crystal before entering the CsI. On the other hand, a gamma ray may enter from any direction and those passing through the plastic have a very low interaction probability in the material. Typical pulse shapes for electrons and gammas are shown in Fig. 1 for the curves labeled "Anode". The fast negative spike in the upper figure resulted from the electron interaction with the plastic and the remainder of the trace corresponds to energy lost in the CsI. No spike is seen for gammas in the lower figure because they interact only with the CsI. It is true, however, that some gamma interactions can occur in the plastic, plus the fact that a small number of the electrons which are produced by interactions in the CsI can escape and traverse the plastic. Due to the relative volumes of the two scintillators and the dependence of atomic number of interaction probabilities, the chance of particle confusion from this mechanism is small. To allow particle separation the pulse from



the photomultiplier anode was shaped with a shorted delay line giving the resultant signals shown in Fig. 1. The difference in these resultant signals for gammas and betas is seen to be the presence of the positive spike produced by the betas. These types of signals were amplified, as will be described below, and utilized for particle identification in the Beta-Bremsstrahlung spectrometer.

### ELECTRONICS

A general explanation of the operation of the electronics may be made by referring to Drawing N100-10900 which indicates in block form the relative association of the individual electronic circuits. The linear signal, originating at the last dynode of the photomultiplier tube, pin 7, was amplified by the linear amplifier, circuit A5. From there the signal went directly to P1 for interconnection to the analyzer-processor.

The particle identification signal originated at the anode of the photomultiplier tube and was shaped by the delay line before it entered the high speed amplifier, circuit A1. The amplified signal then went to the upper level detector, ULD, and the lower level detector, LLD, circuits A2 and A3 respectively. The outputs of these circuits then went to the logic circuit, A4, where the particle identification signals, gamma inhibit and beta enable, were produced. The particle identification signals went directly to P1 for interconnection to the analyzer-processor.

Monitoring of all the spectrometer output signals was possible through interconnections provided at P2, the AGE test connector.

A detailed discussion of the operation of these circuits plus the power supply and control circuits is given in the following paragraphs.

## ELECTRICAL DESIGN

### GENERAL DESIGN SPECIFICATIONS

The spectrometer was required to operate within the following final design specifications over a temperature range of 0° to 120° Fahrenheit from a filtered but unregulated power source of  $26 \pm 4$  volts. The linear signal was required to have nominal rise and fall time constants of 1.2  $\mu$ s and 3  $\mu$ s respectively, and a dynamic range of 7 volts. It was required to have a sensitivity of approximately 1.6 volts/MeV with a stability of  $\pm 7\%$  over the range of temperature and input voltage. The gating outputs required a rise and fall time of approximately 1  $\mu$ s when loaded with the analyzer-processor and a width of approximately 8  $\mu$ s. The amplitudes required for the logic levels were  $4.5 \pm 0.5$  volts for the inhibited condition and  $0.2 \pm 0.2$  volts for the uninhibited condition. These parameters were attained over the entire environmental conditions as evidenced by the successful completion of the qualification testing at NASA-MSU.

### PHOTOMULTIPLIER CIRCUIT (N100-10900)

The photomultiplier circuitry consisted of an RCA-4460 photomultiplier, a Pulse Engineering Corp. PE5400 photomultiplier power supply, a shorted delay line, and the necessary circuitry to set and stabilize the required phototube gain. The linear signal was derived from the last dynode current, across the effective dynode capacitance to ground. The high speed signal was derived from the anode current driving the delay line and high speed amplifier. In order to minimize effects of photocathode noise, the "Co-netic" magnetic shield surrounding the photomultiplier was elevated to photocathode potential through a high impedance filter network.

The RCA-4460 was picked due to its small size, ruggedness, and similarity to tubes used in the past in laboratory applications. The PE 5400 power supply was utilized because of its past history as reliable space hardware. The PE 5400 was designed to operate directly from a  $26 \pm 4$  volt power supply and was compatible with the sensor unit power specifications. Additional filtering was required on some of the power supply outputs and was accomplished by the addition of external capacitors.

The output voltage of the power supply, which directly determined the gain of the photomultiplier, was controlled by the network attached to pins 1 and 2 of the PE 5400 power supply. Feedback through R5 and CR1 provided the voltage control feedback from the high voltage circuit. Due to the highly unstable and non-linear gain characteristic of phototubes with temperature, it was necessary to generate an external temperature sensitive signal which would vary the high voltage applied to the phototube in a manner that would compensate for gain shifts in the photomultiplier. For example, if the voltages on the phototube were held constant, gain change of approximately 300% over the temperature range of 0°F to 120°F would result. For compensation, a correction current was fed into the feedback summing junction of the PE 5400 power supply, Pin 1, which, along with the voltage feedback network, would keep the system gain constant. A network was then designed to create a temperature correlated current which closely matched that necessary for constant system gain. Since the temperature sensitive element and the phototube did not have precise absolute values at a given temperature, it was necessary to select the network resistance values for each individual sensor unit. High stability resistors were utilized to assure that the network retained its characteristics throughout its life and expected environment. The characteristics of the phototube and the correction network were such that rather simple selection techniques were developed which stabilized the system to within the design limits,  $\pm 5\%$ . A series of adjustments were made at room temperature and the temperature extremes. Values of the various components were then picked which would give the best temperature compensation within the design limits.

The characteristic shape of the linear pulse was determined solely by the impedance seen by the last dynode. The pulse amplitude was primarily a function of the capacitance from the last dynode to ground, which consisted of C2 (N100-13900), about 30 pf of cable capacitance, and a few pf of stray capacitance. This gave a total capacitance of approximately 220 pf. The decay time of the pulse was determined by the above capacitance shunted by the effective discharge resistance across it. This consisted of R3 (N100-10900) in parallel with the input impedance of the linear amplifier. This gave a decay time constant of about 8  $\mu$ s. The rise time of the pulse was approximately

1.2  $\mu$ s, which was the combination of the 1.1  $\mu$ s CsI light decay constant and the 5  $\mu$ s RC decay constant.

The high speed pulse, used for particle identification, was derived from the anode current. This current drives simultaneously a shorted delay line and the high speed amplifier input. The characteristic pulse shapes, as seen at the amplifier input, are shown in Fig. 1. The pulse of interest, the positive spike resulting from a reflected beta interaction, had approximately a 3 ns rise time and a 10 ns decay time. It was preceded by a negative pulse corresponding to the normal signal lasting for 10 ns which was twice the time of propagation of the delay line.

#### LINEAR AMPLIFIER (NPO-13900)

At the beginning of the program the output sensitivity requirement was 1.25 volts per MeV. In order to obtain this original sensitivity, the linear amplifier was designed with a maximum gain of 10.5, a dynamic range of 5.5 volts, and a decay constant of 5  $\mu$ s. After the compatibility tests with the analyzer-processor, it was determined that proper operation required an output pulse with an 8  $\mu$ s decay constant, a 7 volt dynamic range, and an output sensitivity of approximately 1.6 volts per MeV. In order to increase the input sensitivity of the amplifier and the decay time constant of the output, the amplifier gain had to be increased. This was accomplished by increasing the inverter gain by approximately a factor of 3. Since the dynamic range of the amplifier was sufficient, no change was required to meet the new dynamic range specifications. The actual output sensitivity was adjustable through the use of an adjustment potentiometer, R5.

The circuit utilized had very good linearity and stability and a low output impedance to minimize the effect of load impedance. The instability and non-linearity characteristics were within  $\pm 0.6\%$  of full scale over the temperature range of  $-10^{\circ}\text{F}$  to  $130^{\circ}\text{F}$  and unmeasurable with the equipment utilized over the temperature range of  $-10^{\circ}\text{F}$  to  $110^{\circ}\text{F}$  (see Figure 2). This was well within the design limits of  $\pm 1\%$  full scale maximum deviation of the best straight line. The output impedance of the amplifier was matched as closely as possible to the impedance of the interconnection cable used between the sensor and analyzer-processor by the series addition of 30 ohms,

R12, in the circuitry. This was done to minimize reflection problems between the two units. The amplifier output was capacitively coupled to prevent damage if the output line were inadvertently shorted.

#### HIGH SPEED AMPLIFIER (N100-11900)

The high-speed amplifier was designed to amplify the positive output from the delay line network to such a level that amplitude detections could be performed on the pulses. The amplifier was designed with limited bandwidth to minimize accidental detection due to grass, time variant fluctuations on the signal. The amplifier itself, had a gain of approximately 75 to 80. As it was designed to amplify the reflected pulse of the delay line output, which was positive, the amplifier had to be essentially insensitive to the large negative overload pulse that preceded the positive pulse. Linearity of gain was not a requirement, but stability was. Limits of  $\pm 5\%$  gain stability over the range of  $-10^{\circ}\text{F}$  to  $130^{\circ}\text{F}$  were required for proper operation. Less than  $\pm 1.5\%$  change over this range was achieved as seen in Fig. 3.

#### HIGH SPEED LEVEL DETECTORS (N100-12900)

There were two fast detectors utilized in the sensor unit, an upper level detector designated ULD, and a lower level detector designated LLD. In each detector, there was an amplifier which served as an isolation buffer and allowed for a final gain adjustment. The detectors and amplifiers were arranged as shown in Fig. 5. As seen in Fig. 4, the detector circuits were stable to within  $\pm 1\%$ , when operated at approximately midrange on the adjustment potentiometer. It was desirable to operate the detectors near this point if possible, so a ratio was determined for the LLD and ULD, which was approximately 10. The gain of the A3 amplifier was then fixed to give this ratio of pulse amplitudes into the two detectors. The gain of the A2 amplifier was determined by the linear amplifier gain, phototube gain, and noise considerations. Of course, typical output levels were known prior to initial design. The particular tube type, crystal configuration, and physical and electrical configurations peculiar to this sensor design were used to determine the gain of the A2 amplifier. This was found to be approximately 5. With the gains determined for the high speed system and the linear amplifier, the gains of the individual spectrometers were adjusted by setting

the phototube gains. The output of the LLD and ULD discriminator circuits were fed into a pulse shaping circuit to provide the logic pulses required by the logic circuitry (N100-13900). The actual levels at which the detectors were set were determined by calibration with radioactive sources.

#### LOGIC AND OUTPUT CIRCUITS (N100-13900)

The logic and output circuitry were designed to accept the LLL and ULL outputs, and generate gamma inhibit pulses and beta enable pulses compatible with the analyzer-processor. The logic was realized utilizing military-range RTL integrated circuits. The particular elements were picked to optimize the speed and power requirements of this device. In order to minimize the number of component types utilized in the spectrometer, the entire logic was designed around dual 3-input NAND/NOR gates. Three and one half devices, seven gates, were required to fulfill the logic requirements.

One device was used as a monostable multivibrator, a technique developed at LTV prior to the initial Beta-Bremsstrahlung sensor concept. As long as precise timing throughout the temperature range was not required, it provides the functions of a monostable multivibrator with a minimum of components. Another dual gate was used, utilizing the ULL and monostable multivibrator signals, to develop the signal which was used to generate inhibits on both control outputs. The other two devices used the two previously developed signals to generate the control functions for the analyzer-processor. The outputs of the control logic gates drove output transistors to provide compatible signals for the analyzer-processor. The circuit was designed to provide signals to the analyzer-processor of proper width and sufficient amplitude to initiate the inhibit functions necessary to perform the proper analysis of the linear signal. The control signals were modified, after mating compatibility tests were performed, to eliminate a noise coupling problem. The width was increased to approximately 9  $\mu$ s and the rise and fall times were tailored to approximately 1  $\mu$ s. The output circuitry was designed such that a continuous short circuit would produce no damage to the circuitry and would produce negligible effects on power consumption.

#### LOW VOLTAGE POWER SUPPLY (N100-14900)

The operating voltage requirements for the spectrometer circuits were

4 volts  $\pm 3\%$  with  $\pm 2\%$  regulation and 6.8 and 12 volts  $\pm 8\%$  with  $\pm 3\%$  regulation over the entire range of temperature and input voltages. To obtain these requirements the 4 volts had to be within  $\pm 1\%$  and the 6.8 and 12 volts within  $\pm 5\%$  at standard conditions (26 V.D.C. input, 77°F, and operationally loaded). The ripple was not to exceed 50 millivolts.

In order to fulfill the preceding requirements, a small relatively efficient unit had to be designed. Since the 4 volt output required the highest current, an efficient means of reducing the 26 volt input had to be used. The use of a resistance series regulator would have consumed much more than the 3 watts available. The use of a transformer DC to DC converter to lower the voltage would have required too much space and design time. A switching regulator was chosen because it offers a combination of efficient regulation, simplicity and compactness. Because the 6.8 volt and 12 volt output required much less current and less voltage accuracy, zener diode regulators were found to be adequate.

In order to visualize the operation of the switching regulator, refer to Fig. 6. The switch was simply a transistor cutting on and off when commanded by the driver transistor driven by a variable-duty-factor multivibrator. The filter was of the low pass, LC type with a diode to return current during the off portion of the cycle. This essentially supplies D.C. power with an output voltage equal to the input voltage times the ratio of the on time to the switching period. Then by varying the time the switching transistor was on to the time it was off the output voltage could be varied.

The multivibrator was an astable type that commences operation upon application of voltage. The pulse width was varied by the application of current to either of its transistor bases. The differential amplifier supplied differential gain of approximately 50, proportional to the difference in the output voltage and the reference. When the output tried to increase either by an increase in input voltage or decrease in the load, the duty factor decreased and the output voltage was pulled down to approach the required output voltage. The regulator then changed the pulse widths of the multivibrator such that the output remained constant regardless of input and output variations.

The switching regulator performance was typically regulated within  $\pm 1\%$  over the entire voltage and temperature range with accurate setting of the output voltage by adjusting R2. Its efficiency was approximately 60%. The output was protected from an overvoltage of greater than 6.8 volts with no load attached by the 6.8 volt zener on the output. An LC filter at the input to the power supply isolated it and the sensor circuitry from input current spikes. The switching transistor was a high current and high voltage type so that initial capacitor charging transients on cut-on would not exceed the safe-operating area. A test involving application of 4000 cycles of a 28 volt step input caused no degradation of switching transistor performance. Output ripple was typically less than 10 millivolts at room temperature at 28 volts input. Temperature stability was achieved by a low-temperature-coefficient zener diode reference and a matched dual transistor in the differential amplifier. Switching frequency was approximately 20 KHz and the multi-vibrator would continue operation even if the output were shorted, thus, giving the output transistor about 5 seconds before it opened.

The 12 volt and 6.8 volt outputs were obtained across zener diodes. The regulation and efficiency obtained was not as good as with the series switching regulator but was adequate for the circuit requirements. The output of the 6.8 and 12 volt zeners could vary within  $\pm 5\%$  at standard conditions and regulate within  $\pm 3\%$  over the entire voltage and temperature range. Power loss in the resistor feeding the zeners was 1 watt maximum.

#### TESTING AND MONITORING

The sensor unit was provided with a test connector in order to perform tests on the unit under operating conditions. It had inputs for a linear signal, to check system linearity and analyzer-processor channel boundaries, and a high speed signal, to check the high speed circuitry and logic circuitry. All three sensor outputs could be monitored through this connector and there was a protected 4 volt power supply monitoring point. The power supply monitor had a series 1 Kohm resistor to protect the power supply and instrument from accidental shorting of this monitor point. To prevent RFI problems when the spectrometer was in use, a grounded shield cap was provided to cover the test connector. A temperature monitor was provided to the spacecraft connector to provide a signal which was a function of the sensor internal temperature.



## PACKAGE DESIGN

### DESIGN SPECIFICATIONS

To insure the success of the sensor unit in the environment of space and launch, the requirements of MAC 8433 for pressurized hardware were evoked except for humidity, rain, salt sea atmosphere, sand, dust, fungus and sinusoidal vibration as set out in the contract. Since the sensor was to be mounted on the command pilot's hatch which was rigged for explosive opening, a 150g shock test was imposed. The unit was to be less than 4.20 lbs in weight and measure 5.50 inches x 5 inches x 3 inches maximum. The unit also was to have rounded corners at edges near the astronauts in order to avoid possible damage to space-suits. The interior of the package was to be vacuum sealed to insure operation of high voltage circuitry by maintaining a dry nitrogen atmosphere inside the case on exposure to the vacuum of outerspace and the oxygen atmosphere of the capsule. All quality control of assembly was to conform to quality specification NPC-200-2 as modified by the contract.

### EXTERNAL DESIGN

In order to satisfy the external requirements, a container of the shape shown on Drawing N100-00920 was designed. The mounting configuration consisted of a back plate which was machined as an integral part of the container itself. The mounting bracket hole pattern configuration is shown on Drawing N100-00930. Adequate strength in the mounting back plate and container was maintained to insure that the unit would remain intact on the spacecraft door if it were opened in an emergency.

### INTERNAL DESIGN

The internal configuration of the package also used the back plate as the main structural member. All heavy members of the internal design were secured to the back plate or mounted as close to it as possible to reduce the torque produced at the mounting plane. Since the collimator and shielding for the photomultiplier tube constituted the majority of the weight in the package, they were mounted on the bottom plate close to the back plate and secured with a clamp to the back plate.

The major factors which influence the design of the detector head assembly (N100-10001-01) were the anticipated electron and bremsstrahlung intensities, the electron collimator and bremsstrahlung shield design, vacuum protection, and the mechanical shock and vibration environment during launch.

The crystal and collimator geometries were chosen to give, as nearly as possible, equal count rates in the electron and bremsstrahlung channels. Based on a brief experimental study of electron penetration through a Gemini hatch and NASA supplied space electron intensities it was determined that a CsI(Tl) scintillation crystal approximately 1/2-inch long and 3/4-inch diameter was optimum. If the maximum possible shielding, within weight limitations, were used, the calculations indicated that the count rates would remain within allowable limits even if the space craft were boosted into a higher orbit than the standard mission called for.

The electron collimator was then designed to have a maximum acceptance cone angle compatible with this crystal size. Tantalum was chosen for the collimator and shield material because of its high density, high strength, and machinability; thus, giving the maximum shielding to weight ratio and allowing the shield to be an integral part of the mechanical structure.

The collimator design also included an aluminum spacer between the tantalum apertures to reduce the scattering of electrons from the collimator walls. Each aperture was made thick enough to absorb electrons to approximately 6 MeV, the maximum energy which could introduce significant distortions into the pulse height spectra.

The photomultiplier was guarded against shock and vibration by the use of silicone rubber gaskets at each end of the tube assembly, one compressing against the scintillation crystal and the other against the base of the photomultiplier tube. Thermal expansion problems were eliminated in the detector head assembly by these shock absorbing gaskets.

The "Co-netic" shield (N100-10010-03) around the photomultiplier tube served a dual purpose: it shielded the tube against the earth's and local magnetic fields and, since it was maintained at the potential of the photocathode of the photomultiplier tube, it acted as an electrostatic shield to reduce field effect noise at the photocathode.

To insure continued operation in the vacuum of space during extra-vehicular activity the unit had to be sealed at cover removal points, input connectors, and collimator assembly. The vacuum seal at the cover removal points were formed by gaskets of silicon rubber compressed by the mating surfaces. The input connectors were hermetically sealed types and were sealed by "O" rings between connector bodies and case. To achieve a vacuum seal at the detector head the electron window (N100-10006-01) was machined as an integral part of the washer which pressed against the O-ring. This gave the window strength and did not require the bonding of a foil to the sealing washer.

The printed circuit boards were made accessible to adjustment and service. Since the high speed amplifier (N100-11000-01), level detectors (N100-12000-01) and linear amplifier and logic (N100-13000-01) were the main active boards and probably required the most adjustment, they were mounted as plug in boards and used miniature RF connectors where required. The boards were plugged into connectors at the bottom and were secured to the sides by vibration absorbing card slides. In addition to the slides, pressure was applied to both the top and bottom of boards by rubber pads to insure vibration isolation and adequate structural strength. This method of mounting reduced the possibility of board resonances.

The high voltage control board (N100-15000-01) and HV power supply were mounted on bases in the top section to allow access to the board with the cover removed. The harness wiring (N100-10300-01) to the photomultiplier tube and to the wiring below (N100-10200-01) was made of sufficient length to allow the board to be lifted out of case for maintenance and case removal. The low voltage power supply (N100-14000-01) was installed on bosses on the bottom cover and wired into the N100-10200-01 harness. To gain access to this power supply it was necessary to remove the bottom cover.

All boards were layed out on artwork per specification MSFC-STD-154. Components were mounted on the board with lead spacing to allow conformity to soldering specification NPC-200-4. The plug-in boards as well as the upper low voltage power supply board were made of .063 inch thickness glass epoxy board per Mil-P-13949. The lower low voltage power supply board and the high voltage power supply control board were made of .093 inch thickness glass

epoxy board per the same specification. To insure added vibration strength and component protection a conformal coating of Isotachast 8 was used and applied per Garland Division of LTV ElectroSystems process specification 404-00060. Each of the three plug-in boards were rhodium plated in the connector area to reduce insertion wear. The unit was designed to be one complete operating package outside of the case and could be checked out for proper operation in this configuration.

The wiring between connectors and boards was accomplished per LTV Aerospace Missiles and Space Division fabrication specification 308-11-2. All wires were per Mil-W-16378 type E and cables per MIL-C-17. The wiring to the high voltage power supply from the photomultiplier tube used Mil-W-16378 type E wire covered by teflon tubing on wires exceeding 600V potential to prevent possible voltage breakdown of wires in harness. The entire top of the high voltage power supply was conformally coated to add strength and reduce possibility of high voltage breakdown.

## ANALYSIS OF DATA

Calibration data was obtained for both the flight unit (S/N 3) and the back-up unit (S/N 2). The data reduction matrices were determined only for the flight unit, however, since the back-up unit was not required for flight. This section gives a discussion of the manner in which the calibration data was taken, the method by which it was reduced, and a suggested technique for the reduction of the actual space pulse height distributions.

### DATA REDUCTION EQUATIONS

Because the exclusion of electrons from the bremsstrahlung channels (and vice versa) was not absolute it is impossible to make an analysis of one spectrum without a consideration of the other. A complete data reduction technique is discussed in this section which employs matrix algebra. The definition of the various matrices is given first, then the construction and solution of the equations, and, finally, the method by which each matrix was obtained. We should define at this point the relevant terms and matrices.

$E$	=	incident particle energy in MeV
$E'$	=	pulse height given in MeV
$R_\gamma$	=	normalized gamma resolution matrix
$R_\beta$	=	normalized beta resolution matrix
$C_\gamma$	=	normalized matrix of gamma cross-talk in the electron channels
$C_\beta$	=	normalized matrix of electron cross-talk in the gamma channels
$\epsilon_\gamma$	=	gamma efficiency matrix
$\epsilon_\beta$	=	beta efficiency matrix
$f_\gamma$	=	fraction of gamma cross-talk in the beta channels
$f_\beta$	=	fraction of beta cross-talk in the gamma channels
$N_\gamma$	=	gamma pulse height spectrum
$N_\beta$	=	beta pulse height spectrum
$S_\gamma$	=	true gamma spectrum
$S_\beta$	=	true beta spectrum

The equations relating these terms are as follows:

$$N_\gamma = R_\gamma \epsilon_\gamma S_\gamma + C_\beta \epsilon_\beta f_\beta S_\beta \quad (1)$$

$$N_{\beta} = R_{\beta} \epsilon_{\beta} S_{\beta} + C_{\gamma} \epsilon_{\gamma} f_{\gamma} S_{\gamma} \quad (2)$$

These represent a set of simultaneous, linear, matrix equations which may be solved in a manner similar to a set of simultaneous, linear, algebraic equations. Perhaps the simplest solution is by direct matrix inversion. We first write the set as a single matrix equation.

$$\begin{pmatrix} N_{\gamma} \\ N_{\beta} \end{pmatrix} = \begin{pmatrix} R_{\gamma} \epsilon_{\gamma} & C_{\beta} \epsilon_{\beta} f_{\beta} \\ C_{\gamma} \epsilon_{\gamma} f_{\gamma} & R_{\beta} \epsilon_{\beta} \end{pmatrix} \begin{pmatrix} S_{\gamma} \\ S_{\beta} \end{pmatrix} \quad (3)$$

The solution of which is

$$\begin{pmatrix} S_{\gamma} \\ S_{\beta} \end{pmatrix} = \begin{pmatrix} R_{\gamma} \epsilon_{\gamma} & C_{\beta} \epsilon_{\beta} f_{\beta} \\ C_{\gamma} \epsilon_{\gamma} f_{\gamma} & R_{\beta} \epsilon_{\beta} \end{pmatrix}^{-1} \begin{pmatrix} N_{\gamma} \\ N_{\beta} \end{pmatrix} \quad (4)$$

which for this case involves the inversion of one forty by forty matrix.

In the event it is impractical to invert a forty by forty matrix an alternate solution, which involves the inversion of several twenty by twenty matrices, may be obtained by the solution of Equations (1) and (2) using the elimination method. Care must be taken with this method when working with  $R_{\beta}$  and  $C_{\beta}$ , since each has at least one zero row. Either of these techniques should yield satisfactory results. The resulting functions for both electrons and bremsstrahlung will be the differential spectra in particles or photons per MeV per square centimeter per second at the detector.

#### EXPERIMENTAL DISTRIBUTIONS

In any data reduction technique, statistical fluctuations are amplified when one attempts to remove the effect of response functions from data. Further, data reduction is made more complex when unequal data acquisition channel widths are employed. The data anticipated from the beta-bremsstrahlung spectrometer will suffer from both these difficulties; however, a curve fitting technique may be employed to effect a solution. Let us denote  $C_i$  as the counts received during a given period of time  $T$  in channel  $i$  of width

$W_i$ , then

$$N_i = \frac{C_i}{W_i T} \quad (5)$$

denotes the integral of the pulse height spectrum over the  $i^{\text{th}}$  channel, or

$$N_i = \int_i N(V) dV \quad (6)$$

where  $V$  is the voltage of the pulse. It then remains to determine an analytical expression for  $N(V)$ .

Although, at the time of the preparation of this report, no actual data was available, the brief experimental investigation at LLV of electron penetration through a Gemini hatch and other electron penetration and bremsstrahlung studies at LLV have indicated that the shape of the pulse height distributions should be near exponential. If, in fact, the data demonstrates this characteristic a fitting function of the following form may be employed:

$$N(V) = e^{-(aV^2 + bV + c)} \quad (7)$$

where

$a$ ,  $b$ , and  $c$  are constants. The function may then be written in the form

$$\ln N(V) = -(aV^2 + bV + c) \quad (8)$$

A least squares fit may be used to determine the constants if the data points are weighted according to the statistical fluctuations. Since the fit is made to  $\ln N_i$ , the proper weighting function  $U_i$  may be shown to be

$$U_i = \left( C_i \ln \frac{C_i}{W_i T} \right)^{-1} \quad (9)$$

Since the raw data is actually the integral of  $N(V) dV$  over the channel, the fit must first be made to the  $N_i$ 's assuming they lie at the midpoint of the channels. Then a first correction may be obtained by integrating the function

over each channel, subtracting the difference from the original  $N_i$ 's and repeating the fit with the new  $N_i$ 's until convergence occurs.

The resulting spectrum must be converted at this point to a pseudo-energy scale before being operated on by the matrix. This scale is defined in terms of the pulse height voltage of the center of photo-peak of gamma rays in the CsI(Tl) crystal. The absolute value of the conversion constant was determined using a thorium-226 gamma source in a manner described in the Final Calibration section at the end of this report. The conversion relationship was found to be

$$V = 1.53 \text{ (volts/MeV)}E' \quad (10)$$

where we shall use  $E'$  as the pseudo-energy referring to pulse amplitude. If any variation in this conversion coefficient is found at post-flight calibration or because of temperature effects, it may be inserted into the program later. We may then write the final analytical pulse height spectrum as follows:

$$N(E') = e^{-(AE'^2 + BE' + C)} \quad (11)$$

where A, B, and C are the constants for the function in terms of  $E'$ .

This function must then be divided into twenty increments to match the resolution matrices discussed in the following sections. This involves integrating  $N(E')dE'$  over each of the 200 keV intervals with the first beginning at 100 keV.

#### BETA RESPONSE MATRIX $R_\beta$

The response of the spectrometer was measured for eight electron energies between 0.4 and 2.5 MeV. The information obtained was used to determine not only the response matrix  $R_\beta$  but also the efficiency matrix  $\epsilon_\beta$ , the normalized cross-talk response matrix  $C_\beta$ , and the cross-talk efficiency  $f_\beta$ . The determination of the last three matrices will be discussed later. The spectrometer was placed in an evacuated chamber at the end of the drift tube of the LTV Research Center's 3 MeV Van de Graaff Accelerator. The experimental arrangement is shown in Fig. 7. Approximately six feet in front of the spectrometer, the



beam passed through a thin aluminum foil 0.0025 inches thick which scattered the beam and caused a homogeneous flux of electrons to fall on the spectrometer. The homogeneity of the flux was monitored, prior to the data taking, with a lithium ion drift (LID) solid state detector and was shown to be within the required  $\pm 10\%$  maximum deviations, in accordance with the Quality Control Bulletin (QCB-CP-001) "Calibration of the LTV Beta-Bremsstrahlung Spectrometer for Gemini-12". The same LID detector was then mounted on one side of the beam tube slightly in front of the spectrometer and was used as the beam flux and energy monitor. The LID detector was calibrated for electron energy using the internal conversion electrons from two sources: Cesium-137 at .625 MeV and bismuth-207 at .482 and .972 MeV. The accelerator electron energy was then determined from this calibration.

Response functions were measured at several incident angles; however, the deviations in the shape of the response functions were found to be so small, even near cut-off, that only one matrix was required. The functions were obtained at eight energies between 0.4 and 2.5 MeV by accumulating data directly from the linear output of the Beta-Bremsstrahlung spectrometer sensor unit in a 256 channel pulse height analyzer. The analyzer was gated by the sensor particle identification outputs so that the electrons were stored in one half of the memory and the actual bremsstrahlung plus the cross-talk in the other. Typical electron pulse height distributions are shown in Figs. 8 and 9.

To obtain the required distributions for the matrix it was necessary to interpolate between and extrapolate from these distributions. To do this most accurately the curves were normalized to the same peak position and integral and cross-plots were made at steps equal to 0.05 of the peak value. From these cross-plots new pulse height distributions were determined at 200 keV steps from 200 keV to 4.0 MeV. These spectra were integrated over 200 keV intervals beginning at 100 keV and ending at 4.1 MeV. These integrals plus the value from 0 to 100 keV were then normalized to one. The results are shown in the matrix for  $R_{\beta}$  given in Table 1.

BETA EFFICIENCY MATRIX  $\epsilon_{\beta}$

The electron efficiencies  $\epsilon_{\beta}(\theta)$  were measured as a function of incident

electron angle  $\theta$  and electron energy  $E$ . A typical curve at 2 MeV is shown in Fig. 10 and compared with the function calculated from pure geometrical considerations. The pulse height distributions were integrated over channel and the resulting number was corrected for analyzer dead time. The flux was determined by the count rate of the LID detector when corrected for the geometry of the collimator and for backscatter from the detector's silicon wafer. With this information the  $\epsilon_{\beta}(\theta)$  functions were obtained as counts per electron per square centimeter. With this data, if angular distributions of electrons which penetrate the Gemini spacecraft walls are known, one may make an integration over  $\theta$  to determine the actual flux of electrons at the collimator. However, electron scattering experiments (some of which were carried out at LTV) have indicated that the distribution is near isotropic. Using this assumption an electron efficiency function  $\epsilon_{\beta}$  was obtained from the angular efficiency functions  $\epsilon_{\beta}(\theta)$  follows:

$$\epsilon_{\beta} = \frac{\int_{\Omega} \epsilon_{\beta}(\theta) d\Omega}{\int_{\Omega} d\Omega} \quad (12)$$

where  $\Omega$  denotes the element of solid angle. This reduces to

$$\epsilon_{\beta} = \frac{1}{2} \int_0^{2\pi} \epsilon_{\beta}(\theta) \sin\theta d\theta \quad (13)$$

This integral was evaluated numerically to obtain  $\epsilon_{\beta}$  which is a function of energy. This function is shown in Fig. 11 and is tabulated in Table 2 where the values represent the average values over the 200 keV increments. These values are then the elements of the diagonal matrix  $\epsilon_{\beta}$ .

#### BETA CROSS-TALK RESPONSE MATRIX $C_{\beta}$

As mentioned above, the data to determine the amount of electron cross-talk received in the bremsstrahlung channels was taken during the electron response function measurements. The data received in the bremsstrahlung channels included not only cross-talk but also the actual electron-produced bremsstrahlung counts. The latter effect was determined by accumulating data with the detector at  $90^{\circ}$  to the beam and the proper amount was then removed

from the false electron counts. In a manner identical to that discussed for the  $R_{\beta}$  matrix, the normalizations and cross-plots were made and the elements for the matrix  $C_{\beta}$  were determined. These are given in Table 3.

#### BETA CROSS-TALK EFFICIENCY MATRIX $f_{\beta}$

The magnitude of the cross-talk was determined relative to the number of electrons detected. After the removal of the bremsstrahlung background, the integrals of the cross-talk spectra were divided by those of the electron spectra. These values are plotted in Fig. 12. The average values of this curve over 200 keV increments are given in Table 4. These values form the elements of the diagonal matrix  $f_{\beta}$ .

#### GAMMA RESPONSE MATRIX $R_{\gamma}$

The gamma response functions and efficiencies were measured for the Beta-Bremsstrahlung sensor using a series of accurately calibrated gamma ray sources, listed in Table 5. The spectrometer was mounted on a rotating mill table with a source located from 25 to 100 centimeters from the center of the crystal. Response functions for most of the sources were recorded at 26 orientations using a 256 channel pulse height analyzer. The values of the orientation indices  $\theta$  and  $\phi$  are defined by Fig. 13. The response functions for the sources are shown in Figs 14 through 19. For those sources with two or more lines, the responses from the lower lines were removed on the basis of a knowledge of the shape of the lower response functions. For example, the 511 keV line in sodium-22 was removed from the 1.28 MeV distribution by normalizing the 511 keV shape to the 662 keV distribution of Cesium-137 and subtracting the resulting shape from the total spectrum. The data taken in this manner at the various angles showed that the shape of the distributions was independent of angle. This allowed the use of only one response matrix at all angles. The set of pulse height distributions were then normalized to the same integral and photo-peak position. Finally, in a manner identical to that used for the electron response matrix, the gamma response matrix  $R_{\gamma}$  was obtained and is given in Table 6.

#### GAMMA EFFICIENCY MATRIX $\epsilon_{\gamma}$

The efficiency function for gamma rays  $\epsilon_{\gamma}$  was more complex in construction

than that for electrons, since the efficiency varies with angle and the bremsstrahlung intensity is not expected to be isotropic over all angles. The values of the angular efficiency function  $\epsilon_{\gamma}(\theta, \phi)$  were obtained at  $\theta = 0$  and  $180^{\circ}$ , plus several representative directions at  $\theta = 45^{\circ}, 90^{\circ},$  and  $135^{\circ}$ , for most of the calibration sources by first integrating over the pulse height spectra and correcting for analyzer dead time. These spectra were obtained as discussed in the  $R_{\gamma}$  section. The values at the remaining angles were obtained by simply scaling the pulse height distributions above a certain discriminator level and comparing these values with those taken at the representative angles. The flux was then calculated at the crystal for each source, based on the geometry and source strength given in Table 5. This gave  $\epsilon_{\gamma}(\theta, \phi)$  in counts per gamma per square centimeter.

The calibration of the sources was determined at LTV as a part of this contract using a sodium-iodide, anticoincidence spectrometer which has been used several years for making absolute bremsstrahlung measurements under contract for NASA-Headquarters. A new calibration of the spectrometer was made for this work using a series of low level calibration sources with a quoted accuracy of  $\pm 2\%$ . These sources were obtained from the Amersham Corporation in England.

For reference the curves for  $\epsilon_{\gamma}(0^{\circ}, 0^{\circ})$  and  $\epsilon_{\gamma}(90^{\circ}, 0^{\circ})$  are shown in Fig. 20. The average values over 200 keV increments for these  $\epsilon_{\gamma}(\theta, \phi)$  plus those for  $\epsilon_{\gamma}(180^{\circ}, 0^{\circ})$  are given in Table 7. For all angles, except at  $\theta = 0^{\circ}$  and  $180^{\circ}$ , the shape of the  $\epsilon_{\gamma}(\theta, \phi)$  functions were identical. It was, thus, possible to obtain these functions from  $\epsilon_{\gamma}(90^{\circ}, 0^{\circ})$  by a simple multiplication as indicated by the following equation:

$$\epsilon_{\gamma}(\theta, \phi) = N_{\theta\phi} \epsilon_{\gamma}(90^{\circ}, 0^{\circ})$$

The values of  $N_{\theta\phi}$  are given in Table 8. The equation relating the functions to an overall gamma efficiency matrix  $\epsilon_{\gamma}$  may be written as follows:

$$\epsilon_{\gamma} = \frac{1}{26} \sum_{\theta\phi} \epsilon_{\gamma}(\theta, \phi),$$

where we have ascribed equal area weighting to the  $\epsilon_{\gamma}(\theta, \phi)$  functions, since they are very evenly distributed around the crystal.  $P_{\theta\phi}$  is a function which

describes the probability of receiving radiation from the direction  $\theta\phi$ . The  $P_{\theta\phi}$  functions must be normalized, i.e.,

$$\sum_{\theta\phi} P_{\theta\phi} = I$$

where  $I$  is the identity matrix. The values of the  $P_{\theta\phi}$  may be determined approximately by a consideration of the spacecraft material composition and configuration. One first estimates a source function over the area covered by each  $\epsilon_{\gamma}(\theta\phi)$ . Then this is attenuated by the average mass per unit area of the spacecraft between the source and detector. The resulting spectra are then normalized to give the  $P_{\theta\phi}$  values. The derivation of the  $P_{\theta\phi}$  functions were not a part of this program; however, the information required for their determination should be available at NASA-MSC. To make a rapid but less accurate calculation of the intensity one may assume an isotropic source and attenuation function and insert the constants.

#### GAMMA CROSS-TALK RESPONSE MATRIX $C_{\gamma}$

The information required to determine the pulse height distributions of false gamma counts received in the electron channels was obtained simultaneously with response function data for the gamma response matrix. Since no background removal was required, the spectra were plotted and a smooth curve was drawn through the data to remove statistical fluctuations. In a manner identical to that used for the determination of  $R_{\beta}$  the curves were normalized, cross-plots were made and the matrix elements calculated by averaging over 200 keV intervals. The matrix for  $C_{\gamma}$  is given in Table 9.

#### GAMMA CROSS-TALK EFFICIENCY MATRIX $f_{\gamma}$

The magnitude of the cross-talk was determined relative to the number of photons detected. The integrals of the cross-talk spectra were divided by those of the gamma pulse height spectra. These values are plotted in Fig. 21. The average values of this curve over 200 keV increments, which form the elements of the diamond matrix  $f_{\gamma}$ , are given in Table 10.

#### TEST SPECTRA

In order to demonstrate the effectiveness of the analysis technique

described above for converting pulse height information into energy spectra, two known spectral distributions of electrons and bremsstrahlung were measured with the ITV Beta-Bremsstrahlung spectrometer and comparisons were made between the known values and those obtained from the spectrometer. Since the computer program for performing the analysis of data was not included under this contracted effort, the comparison of test spectra to measured spectra was made indirectly. This was done analytically by distorting the known spectra with the measured response and efficiency functions of the spectrometer and plotting the resulting curves on a graph with the measured spectra. The following paragraphs detail this procedure.

#### Beta Spectrum

The beta spectra from a thin source of  $\text{Sr}^{90}$  -  $\text{Y}^{90}$  were measured with the Beta-Bremsstrahlung spectrometer. The results of this measurement are shown in Fig. 22. The spectra from the same source were measured with a large anthracene crystal type spectrometer. The object of this measurement was to obtain as closely as possible the true shape of the  $\text{Sr}^{90}$  -  $\text{Y}^{90}$  spectra. By using an anthracene crystal the amount of electron backscatter was minimized and this spectrometer's response was practically all Gaussian. Thus, the anthracene measured  $\text{Sr}^{90}$  -  $\text{Y}^{90}$  spectra had little distortion except that near the end point, which is due to the spectrometer's finite resolution. These "true"  $\text{Sr}^{90}$  -  $\text{Y}^{90}$  spectra were then multiplied by the electron efficiency diagonal matrix  $\epsilon_{\beta}$  and the electron response matrix  $R_{\beta}$ . These results were compared with the shape of the measurement obtained with the Beta-Bremsstrahlung spectrometer. The comparison is shown in Fig. 22.

The relative magnitude of the two distributions shown was determined by a normalization of their total areas. The agreement is within the experimental uncertainties involved in the two determinations except in the last few energy lines. Here the "true" distorted or smeared distribution takes on progressively higher values than the beta-gamma measured distribution. This is expected though since the "true" smeared distribution also contained the anthracene spectrometer resolution. A correction for this effect, i.e., the removal of the resolution, would reduce the last bin by approximately 50% and the previous bins by progressively lesser amounts. This would bring these

points in line with the agreement observed at the other points.

### Bremsstrahlung Spectrum

The bremsstrahlung or x-ray spectrum resulting from a 2 MeV beam of electrons striking a thick aluminum target was measured with the Beta-Bremsstrahlung spectrometer. The angle of observation was  $30^\circ$  from the direction of the incident beam. The results of this measurement are shown in Fig. 23. The true spectrum emitted under these conditions was previously measured in our laboratory utilizing a 2 inch by 6 inch NaI crystal and annulus arrangement which exhibited a high photopeak efficiency at 2 MeV. This true spectrum was multiplied by the photon efficiency diagonal matrix  $\epsilon_\gamma$  and the photon response matrix  $R_\gamma$ . The result of these multiplications was compared with the spectrum measured with the Beta-Bremsstrahlung spectrometer. The comparison is shown in Fig. 23 and is on an absolute basis as indicated by the ordinate values. On the basis of the many experimental uncertainties which are involved in obtaining these absolute x-ray yields the agreement is well within the expected experimental error.

### FINAL SYSTEM CALIBRATION

The final adjustment in calibration of the sensor unit was the exact setting of the output linear pulse amplitude relative to the photo-peak of a gamma ray pulse height distribution. The source used was thorium-226 which has a gamma energy of 2.615 MeV. A spectrum was taken, printed out, and plotted. The spectrum was then hand stripped to determine the proper channel for the 2.615 MeV peak. A pulser was then fed into the spectrometer test input and the amplitude adjusted until the output was in the channel corresponding to 2.615 MeV. The gain of the linear amplifier was then adjusted until the amplitude of a 2.615 MeV pulse was 4.00 volts giving a calibration of 1.53 volts per MeV.

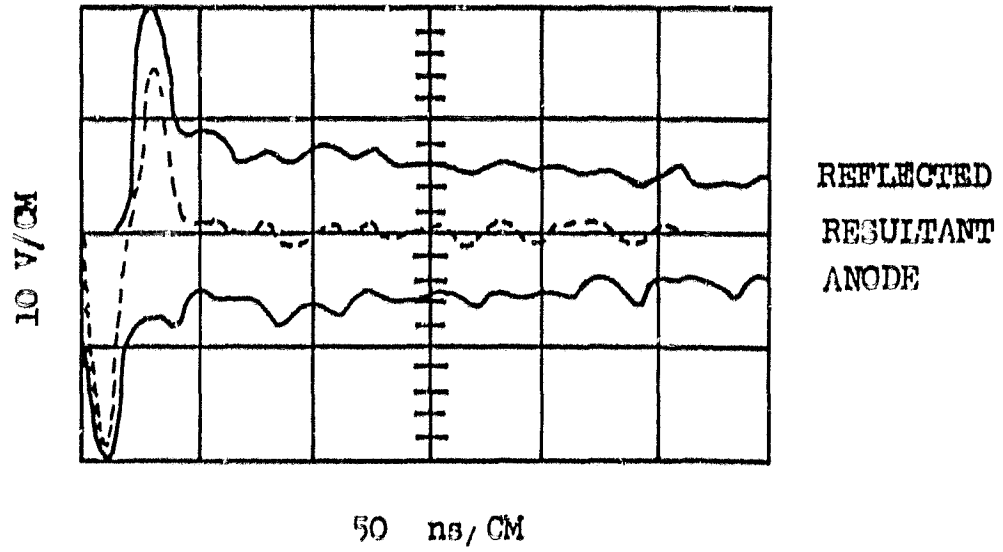
With the outputs of the analyzer-processor connected to the NASA AGE, the channel boundaries were determined by adjusting the amplitude of a calibrated pulser until equal count rates were accumulated in adjacent channels. This pulser amplitude was determined relative to the thorium-226 calibration and provided the lower and upper channel boundaries. A list of channel

boundaries and widths which were derived from the above tests are shown in Table 11. The boundaries are given in volts with a calibration basis of 4.00 volts for the 2.615 MeV thorium-226 gamma peak as determined above.



BETA PULSE

(RESULTING FROM AN INTERACTION  
IN BOTH PHOSPHORS)



GAMMA PULSE

(RESULTING FROM AN INTERACTION  
IN THE CsI(Tl) ONLY)

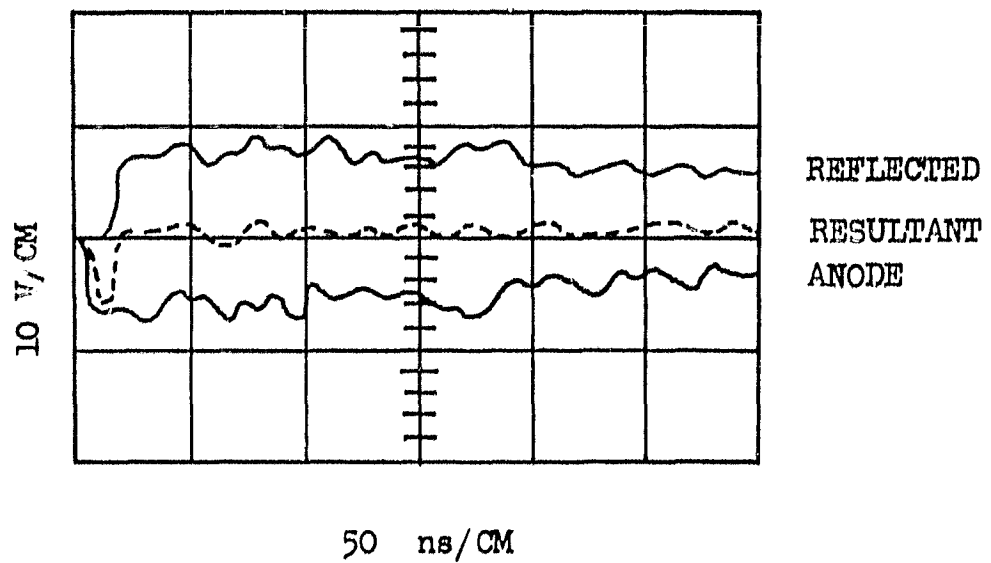


FIGURE 1 SIGNALS FROM CRYSTAL ASSEMBLY

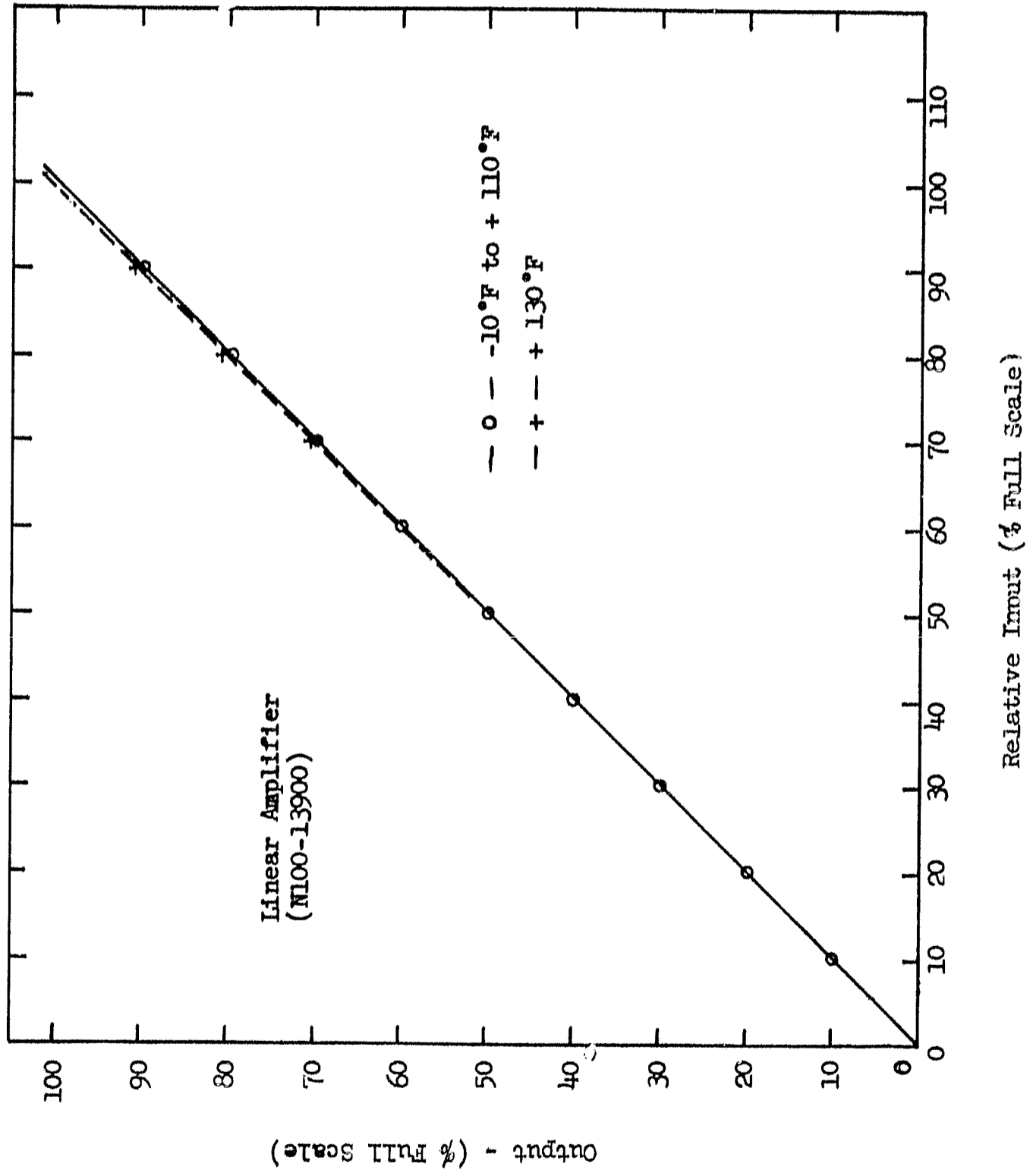
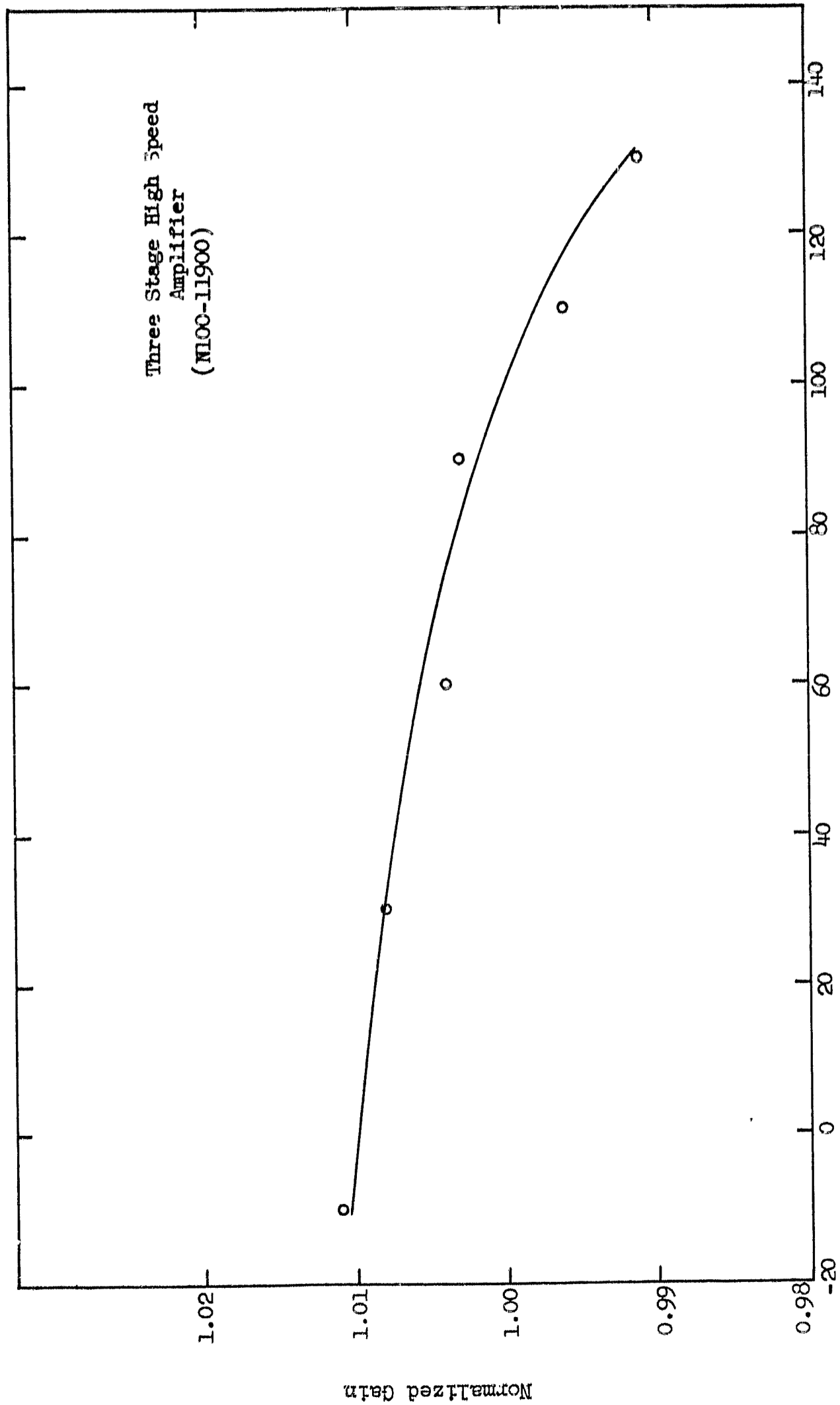


FIGURE 2 LINEAR AMPLIFIER GAIN - TEMPERATURE CHARACTERISTICS



Temperature (Degrees Fahrenheit)

FIGURE 3 HIGH SPEED AMPLIFIER GAIN - TEMPERATURE CHARACTERISTICS

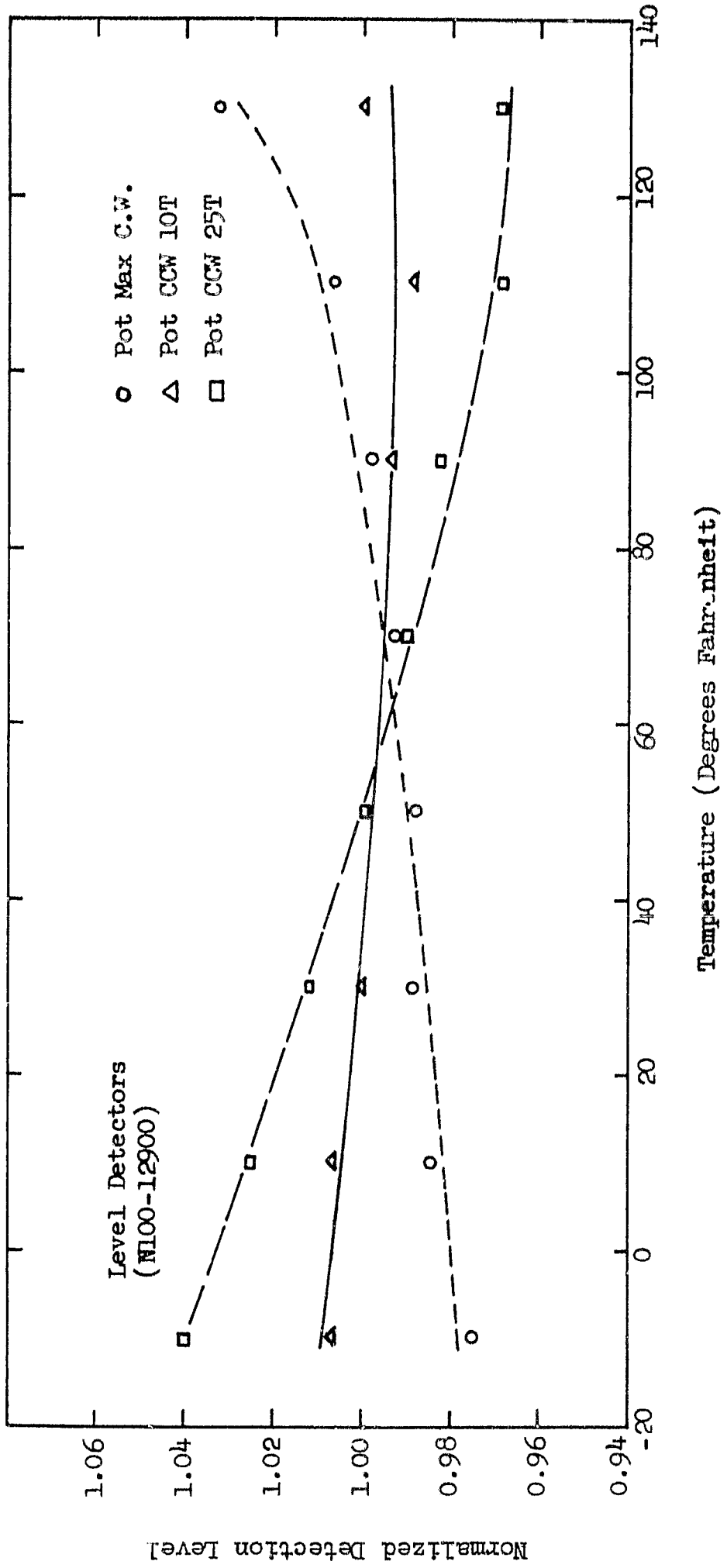


FIGURE 4 LEVEL DETECTOR TEMPERATURE CHARACTERISTICS

Input from  
High Speed  
Amplifier

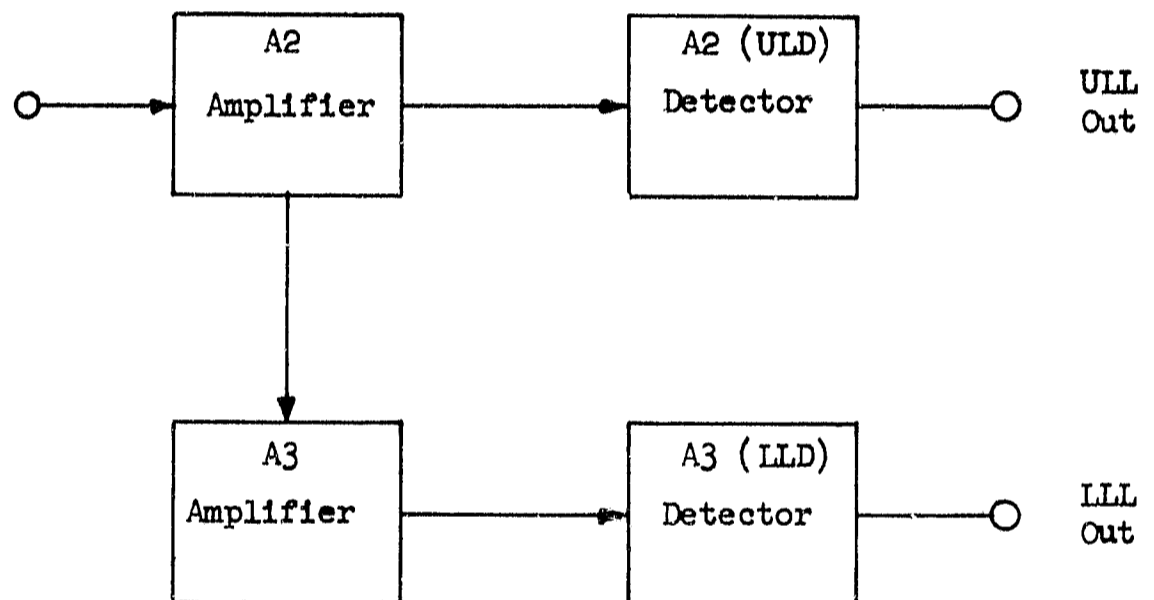


FIGURE 5 LEVEL DETECTOR BLOCK DIAGRAM

Unregulated  
DC Input

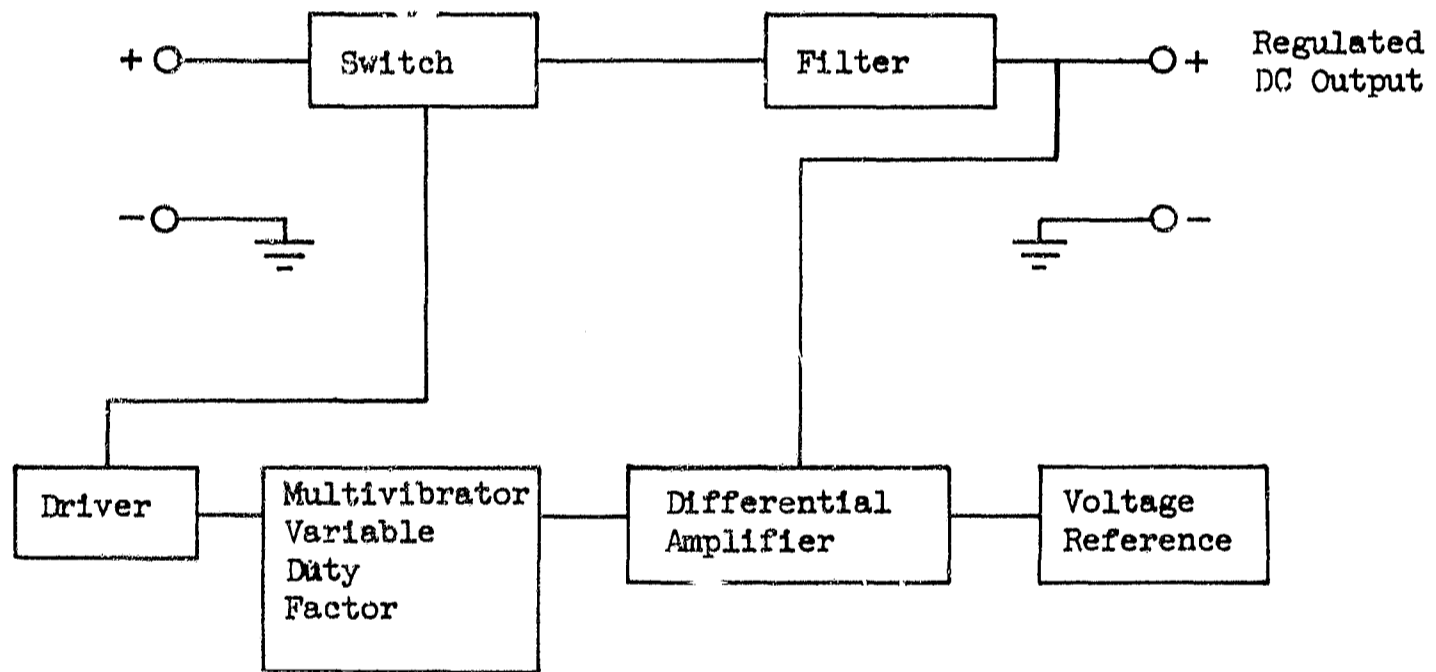


FIGURE 6 SWITCHING REGULATOR FUNCTIONAL DIAGRAM

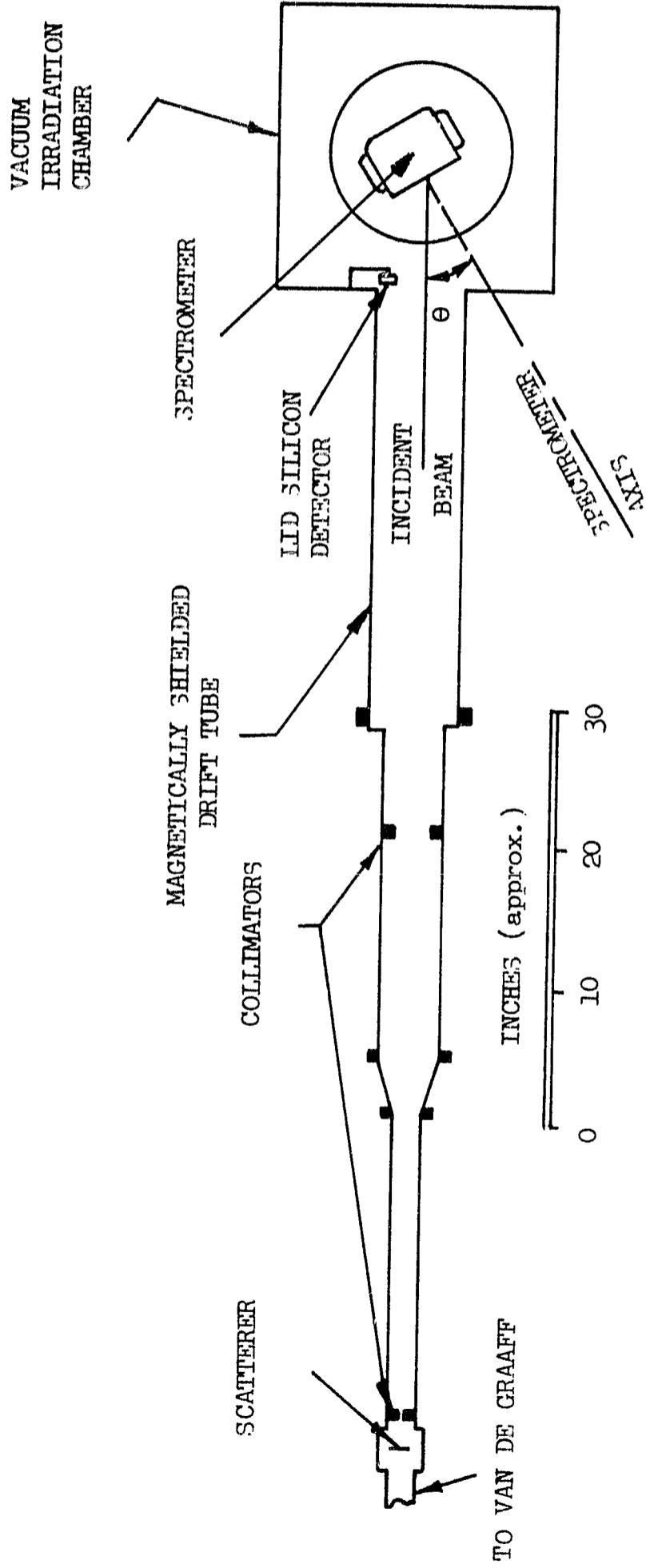


FIGURE 7 EXPERIMENTAL ARRANGEMENT FOR ELECTRON CALIBRATION

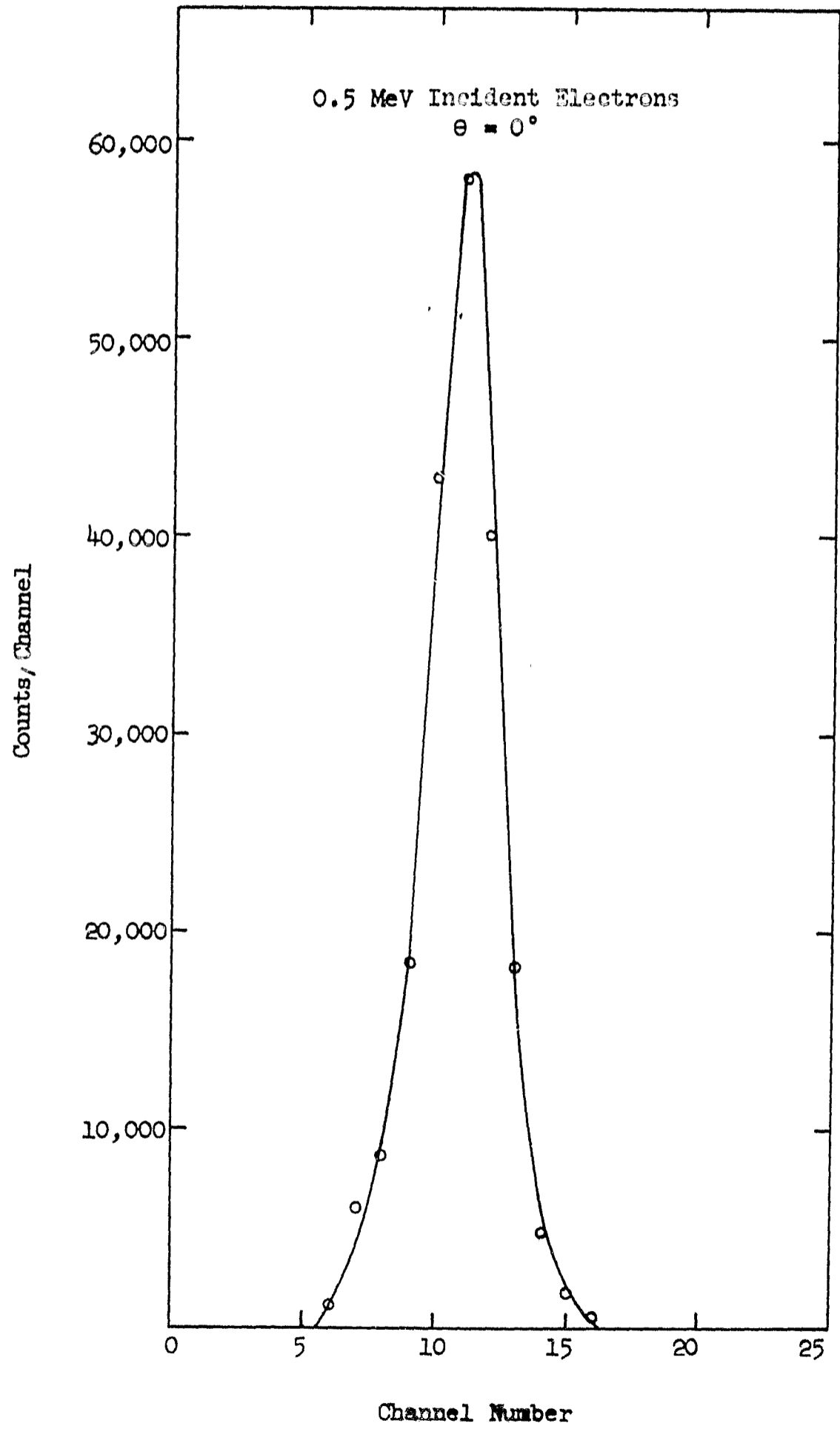


FIGURE 8 ELECTRON PULSE HEIGHT DISTRIBUTION



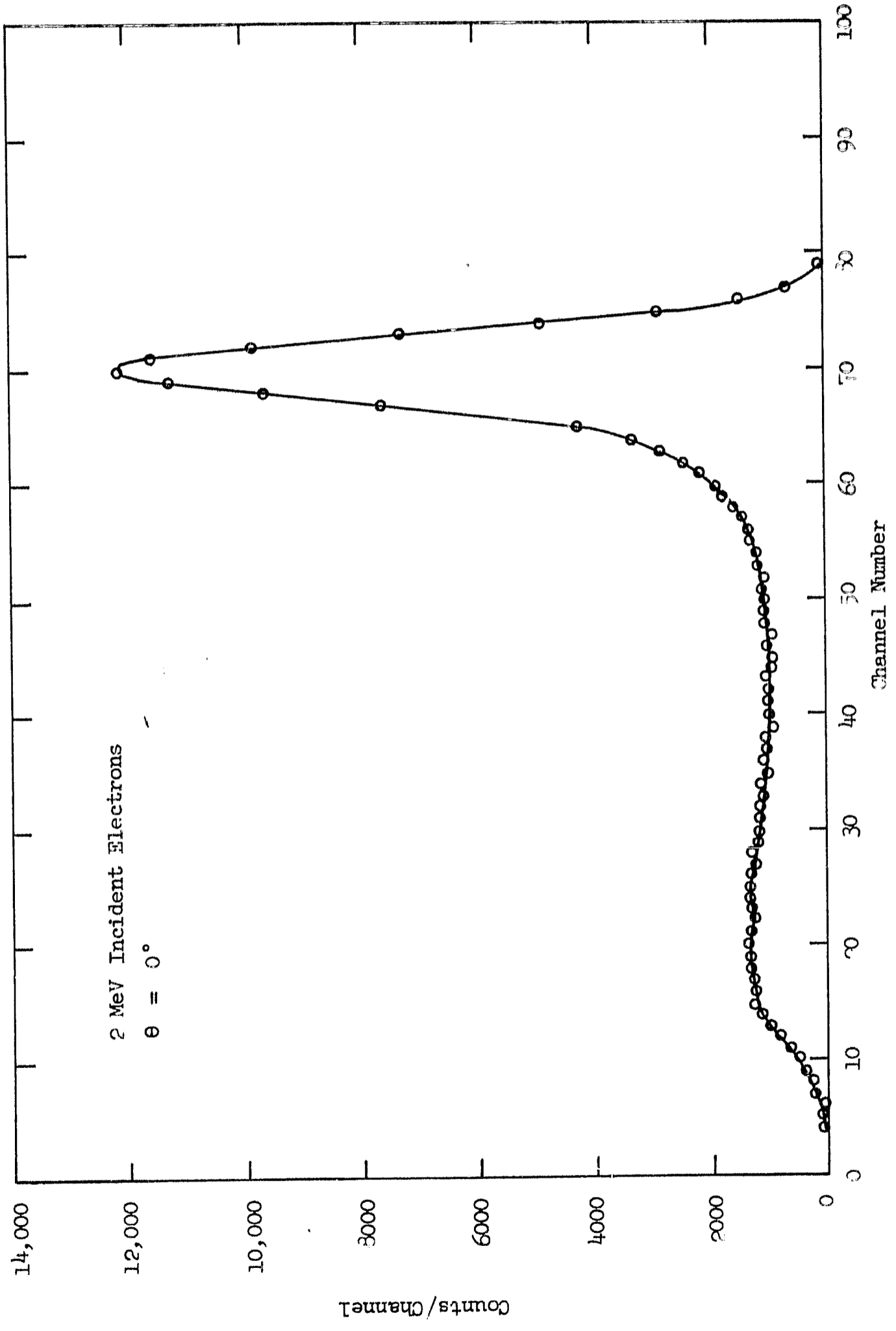
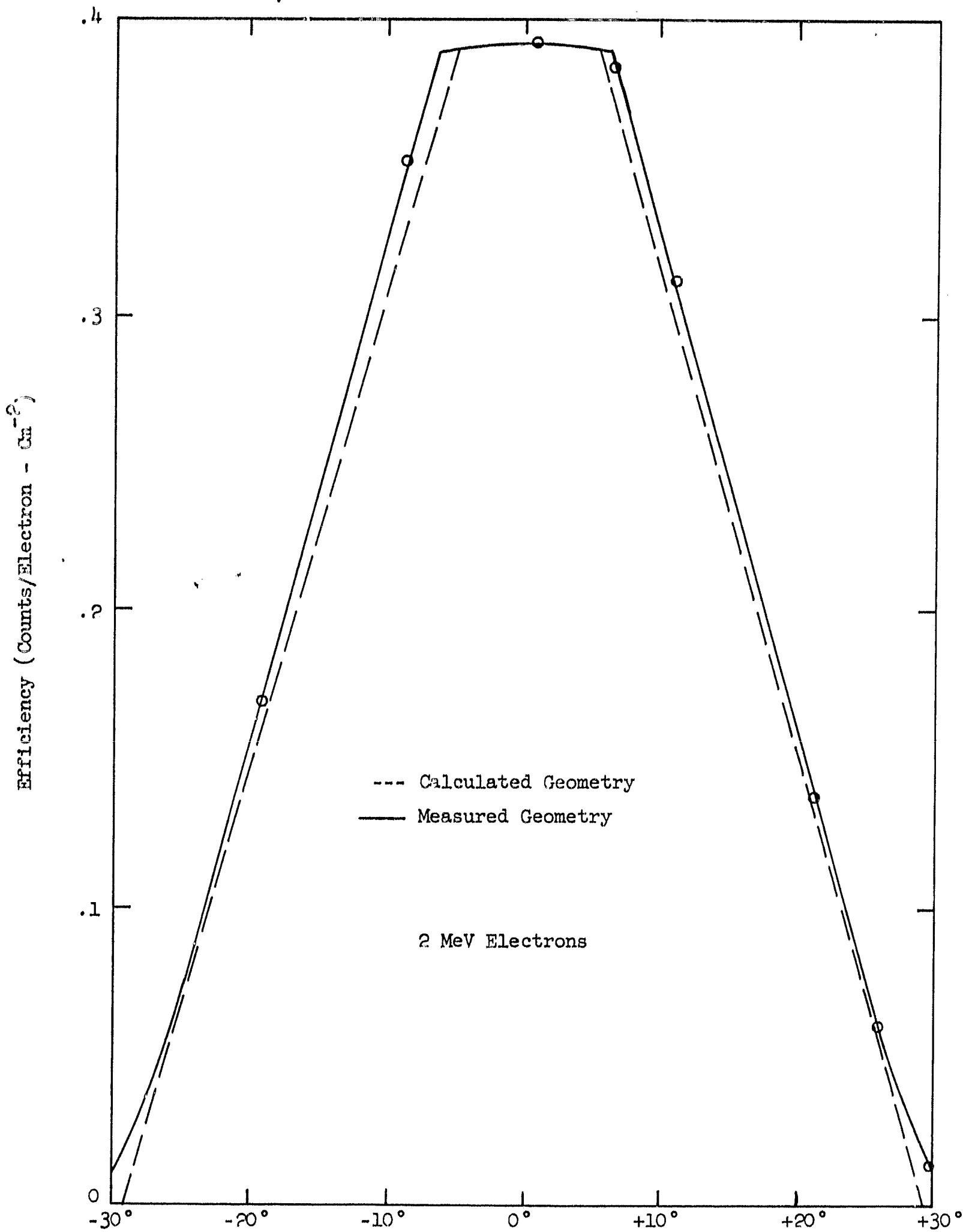


FIGURE 9 ELECTRON PULSE HEIGHT DISTRIBUTION



θ Detector-Beam Angle (Degrees)  
 FIGURE 10 COLLIMATOR EFFICIENCY  $\epsilon_{\beta}(\theta)$

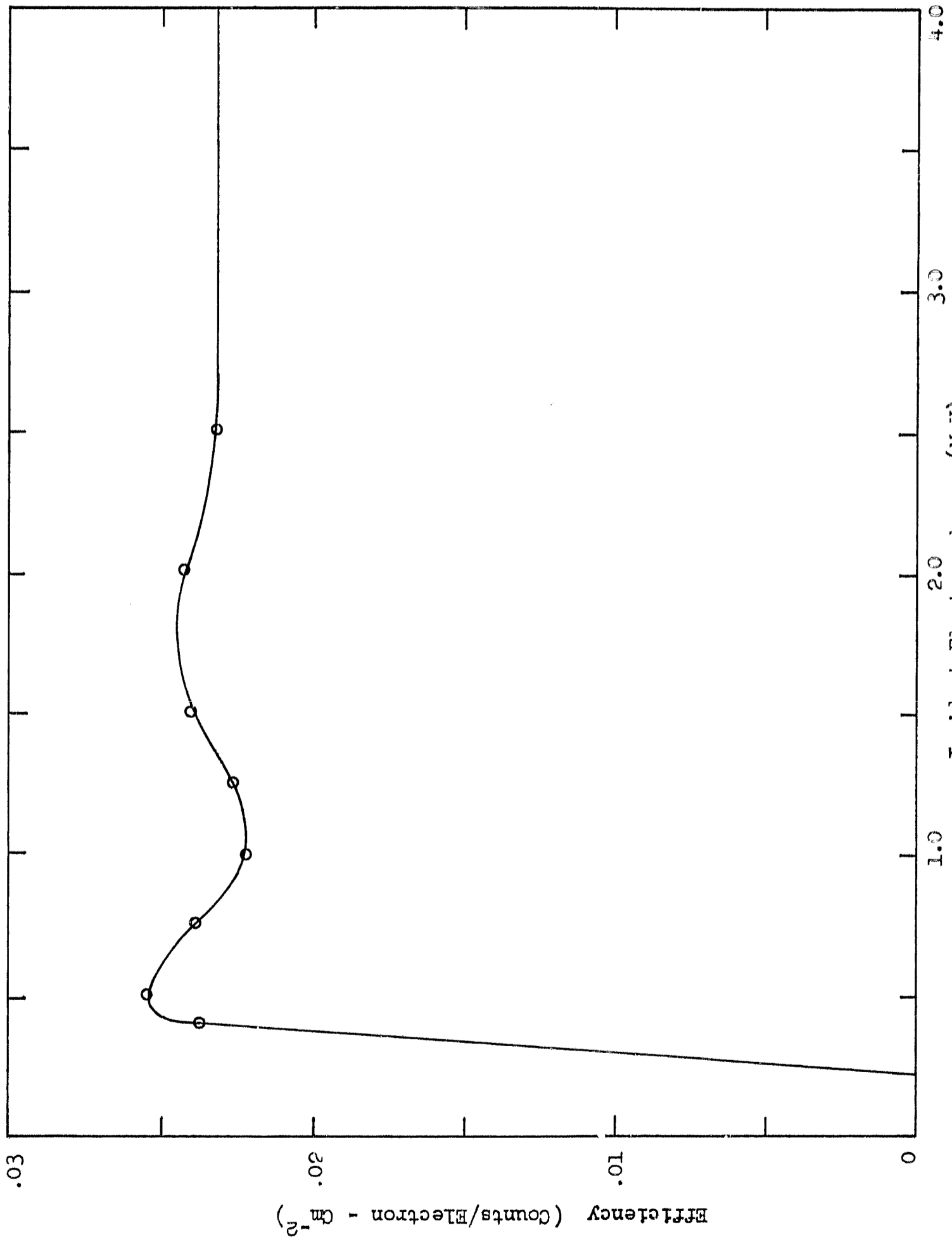


FIGURE 11 CMMIDIRECTIONAL ELECTRON EFFICIENCY  $\epsilon_{\beta}$

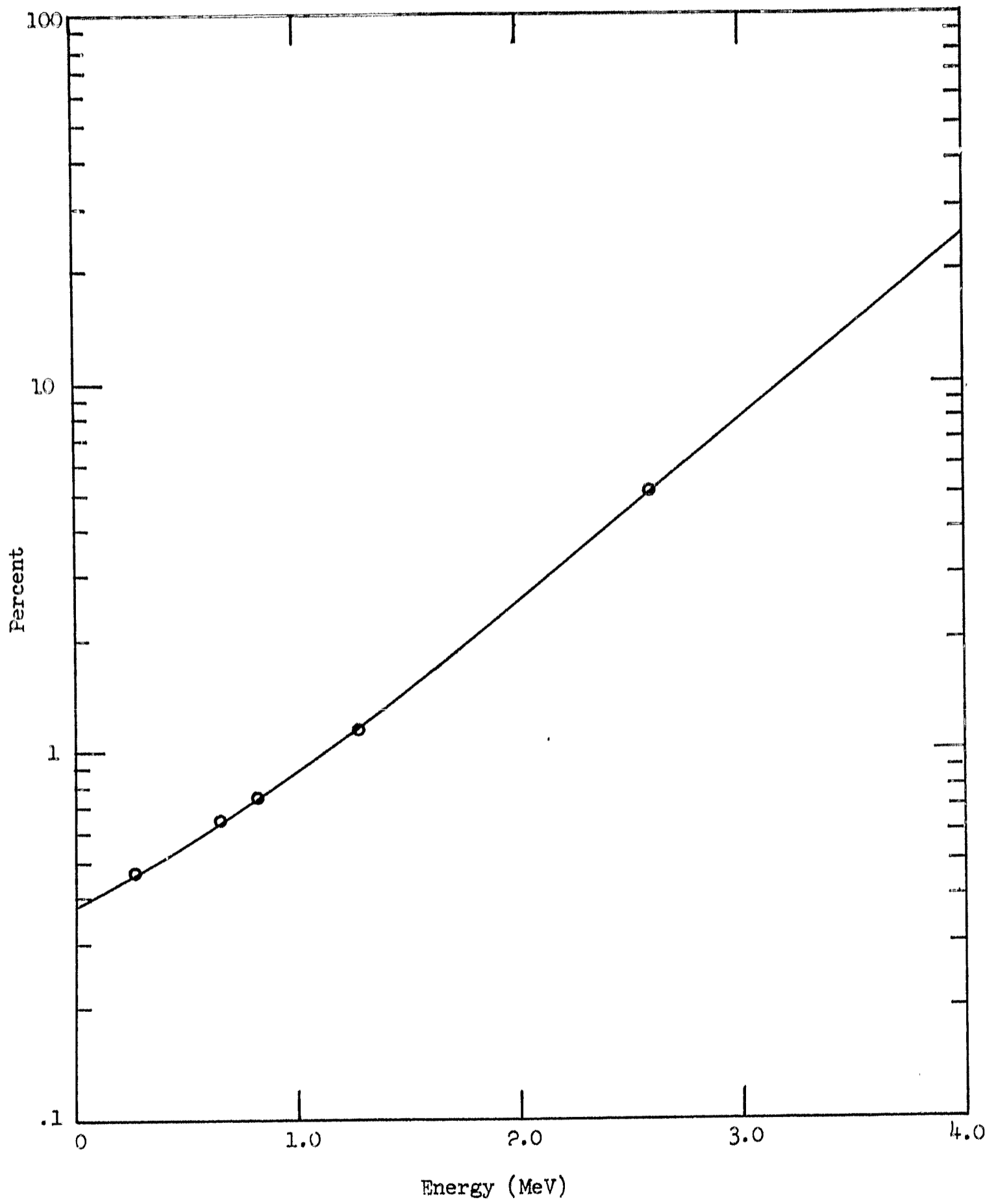


FIGURE 12 FALSE PHOTON COUNTS IN ELECTRON CHANNELS  $f_{\gamma}$

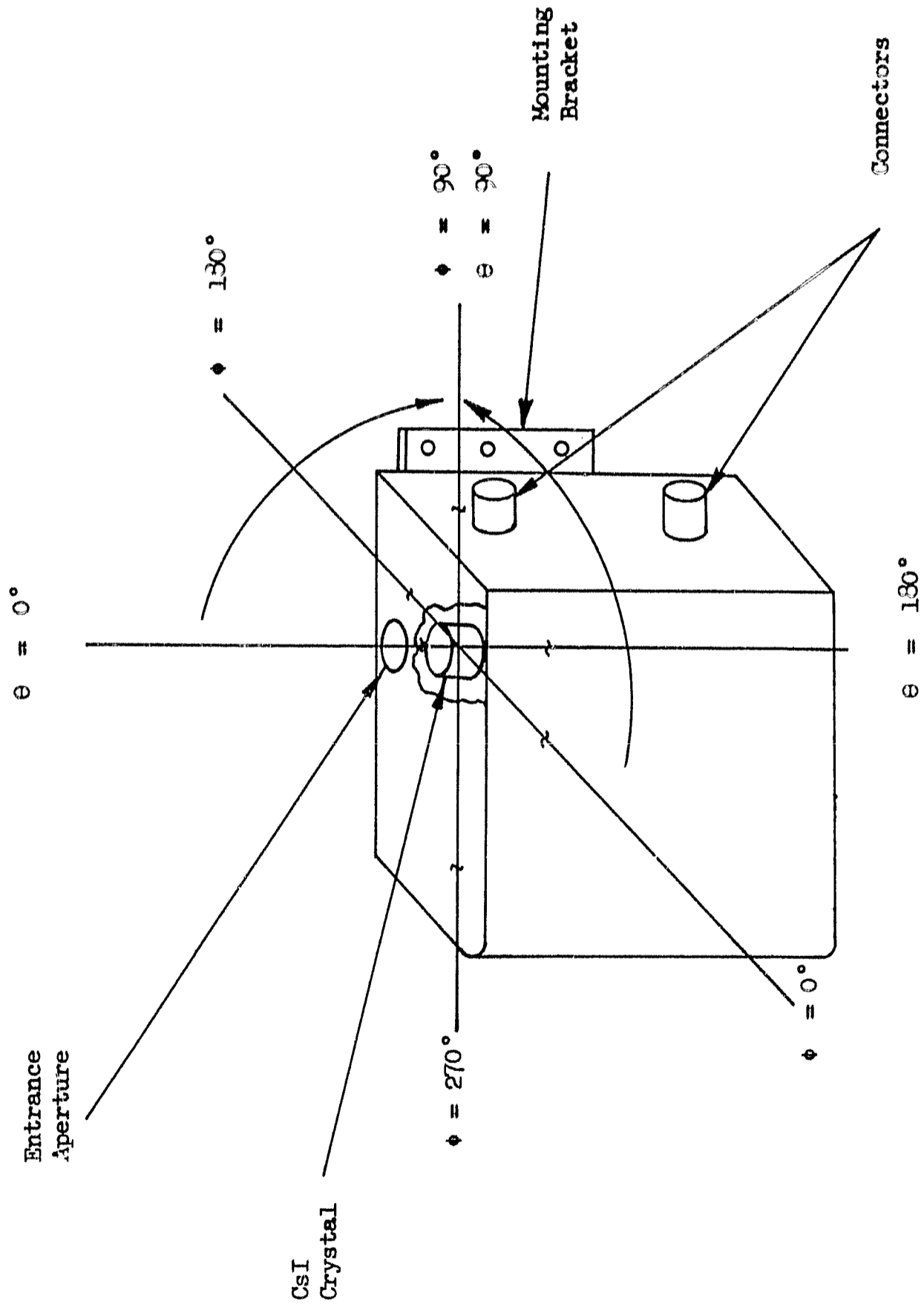


FIGURE 13 GAMMA CALIBRATION GEOMETRY

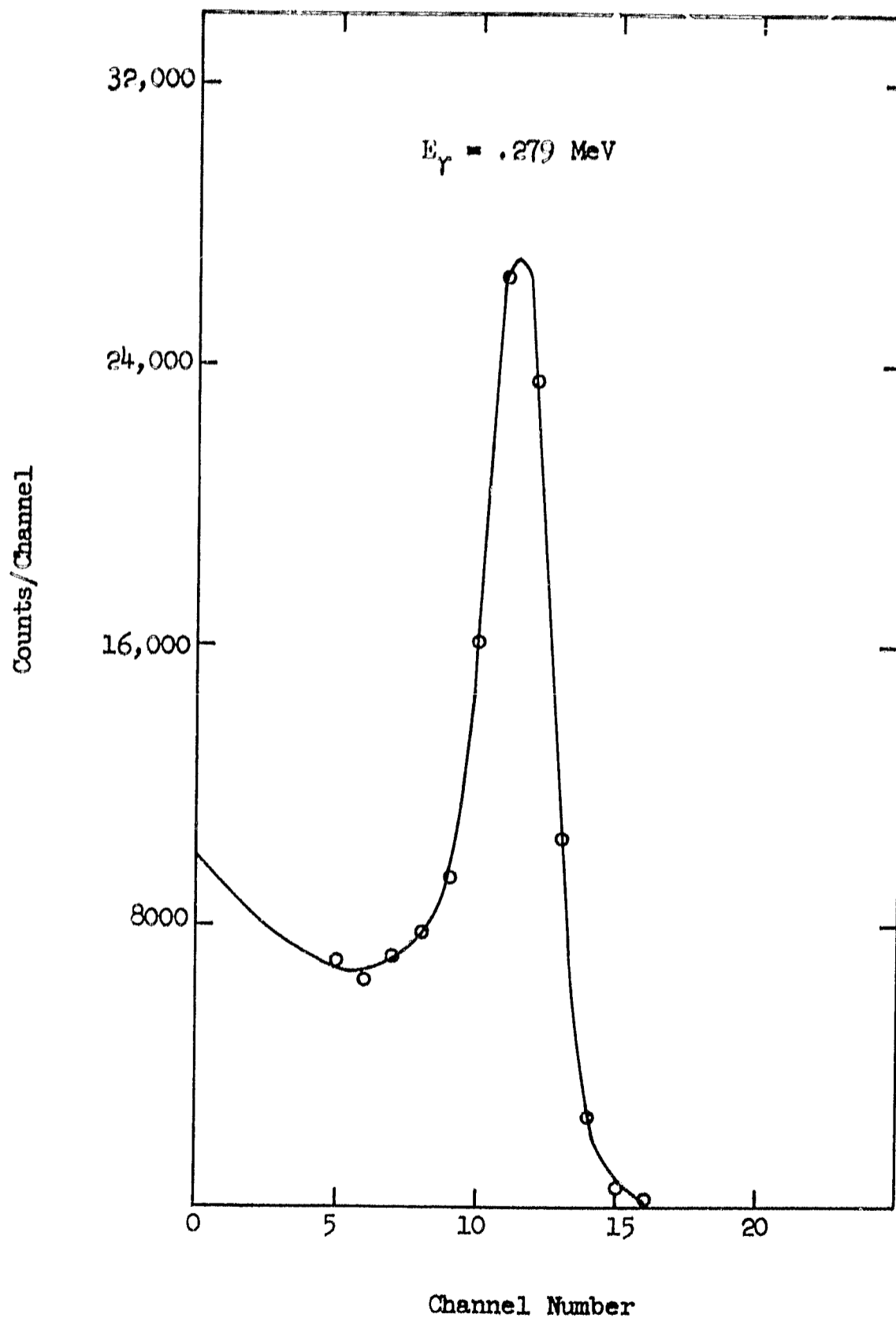


FIGURE 14 Hg-203 PULSE HEIGHT SPECTRUM

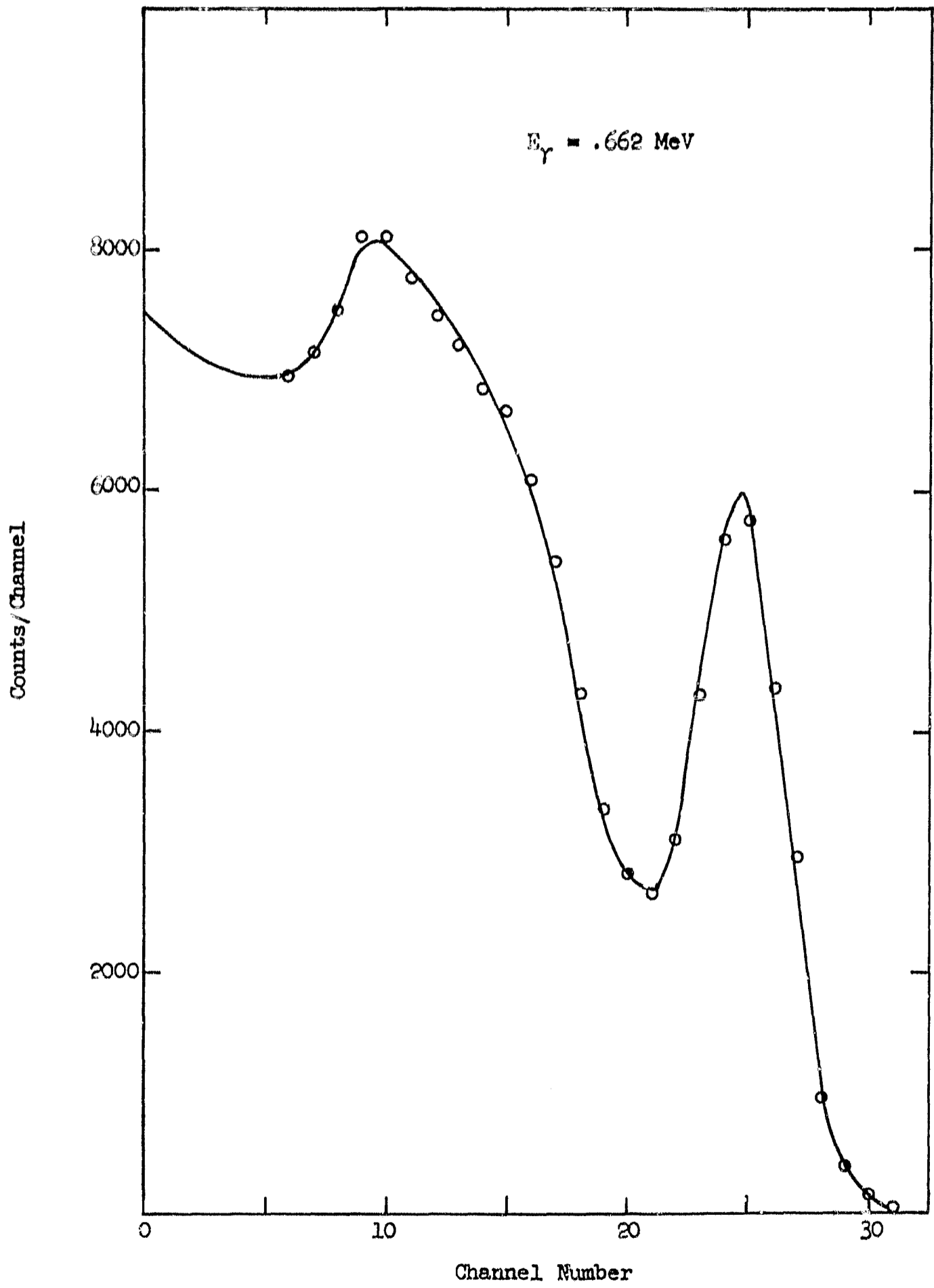


FIGURE 15 Cs-137 PULSE HEIGHT SPECTRUM

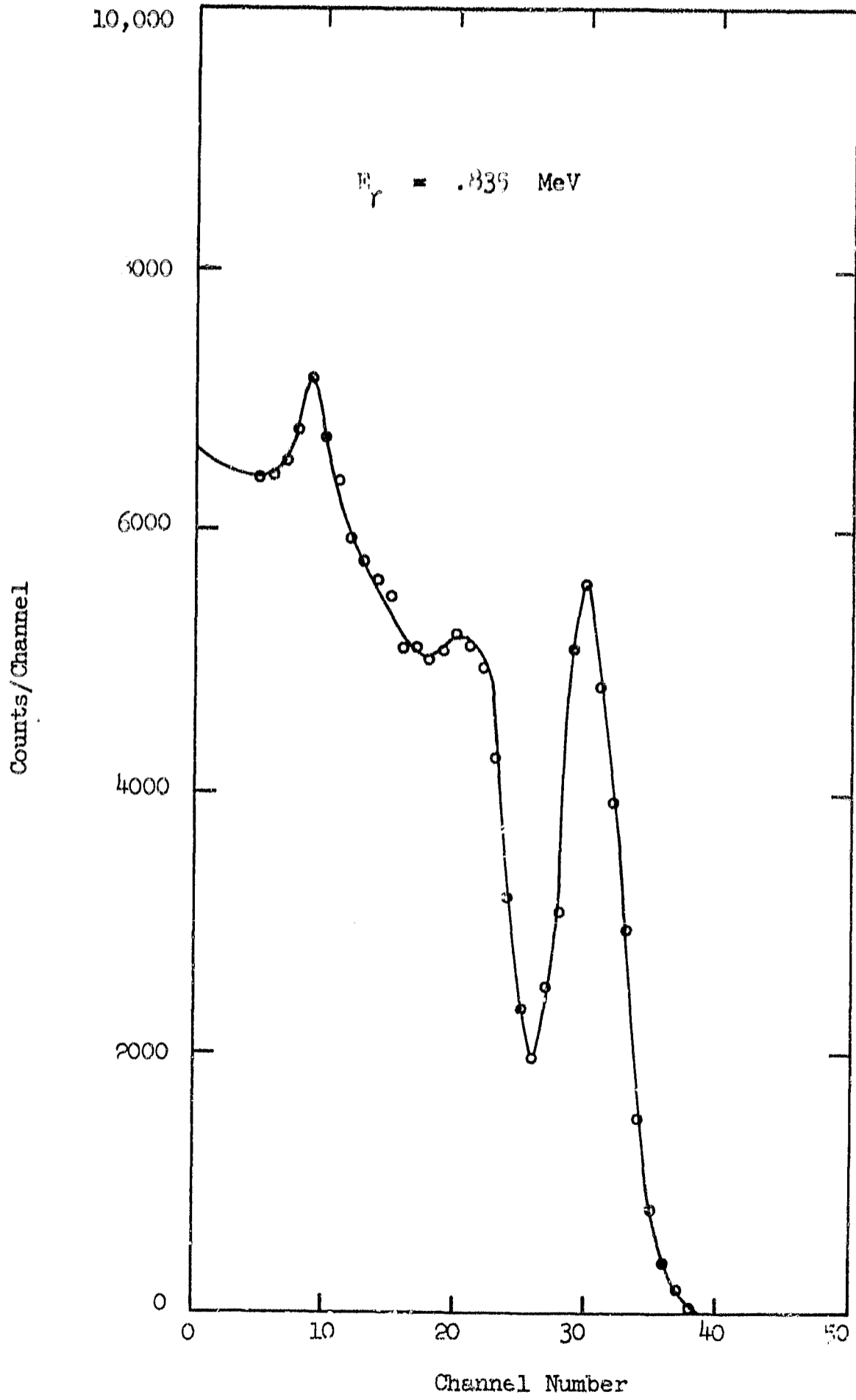


FIGURE 16 Mn-54 PULSE HEIGHT SPECTRUM



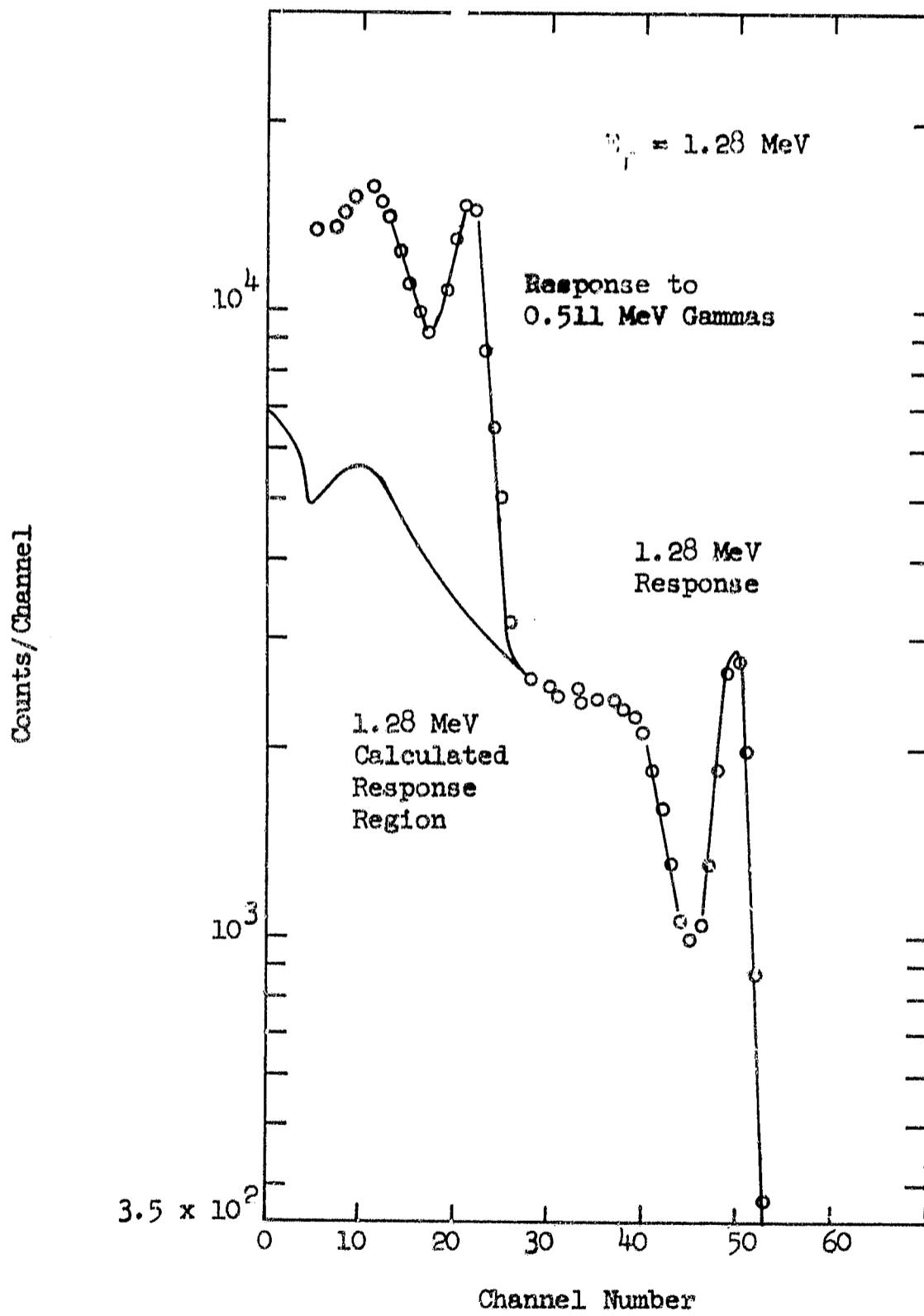


FIGURE 17 Na-22 PULSE HEIGHT SPECTRUM

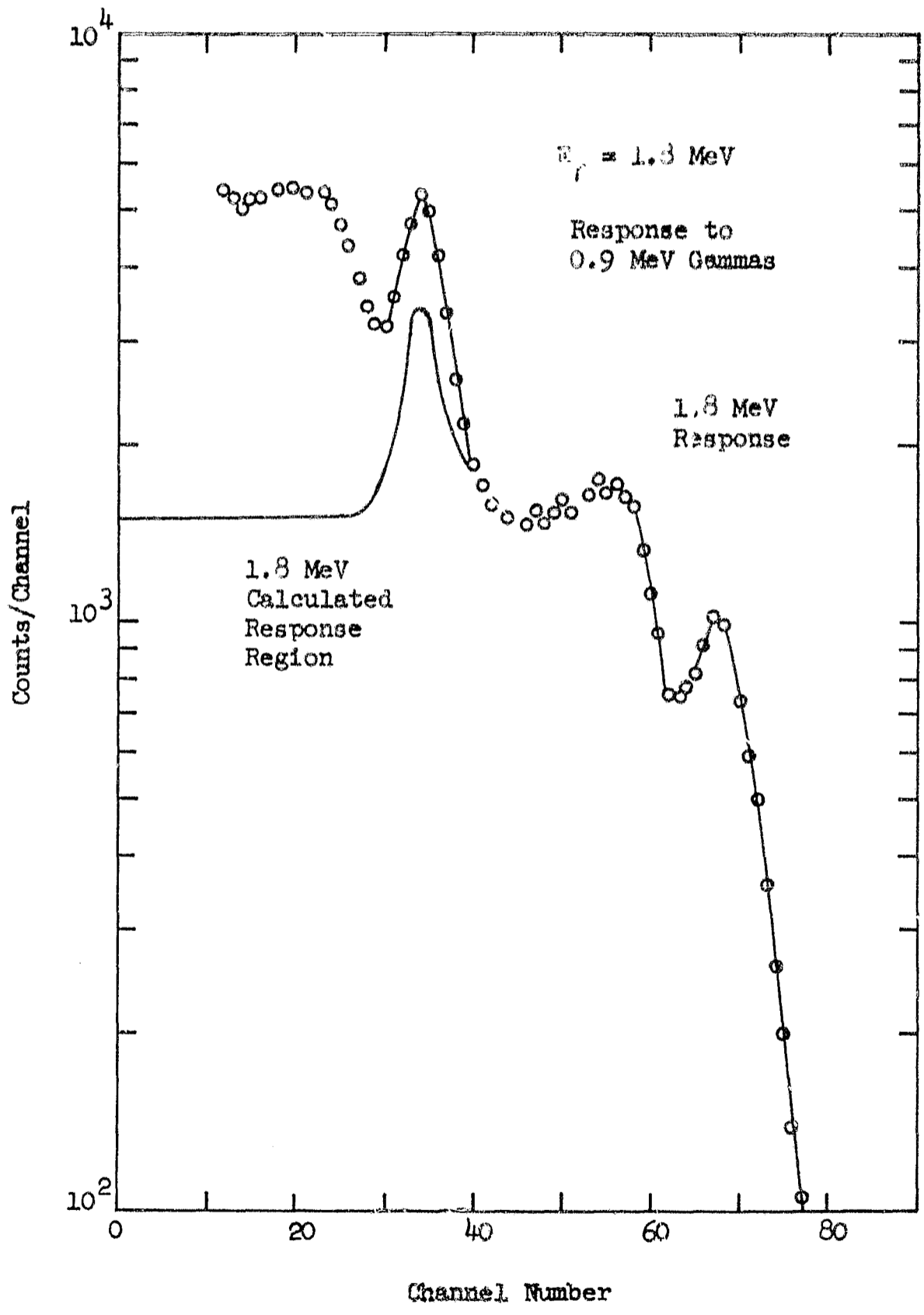


FIGURE 18 Y-88 PULSE HEIGHT SPECTRUM

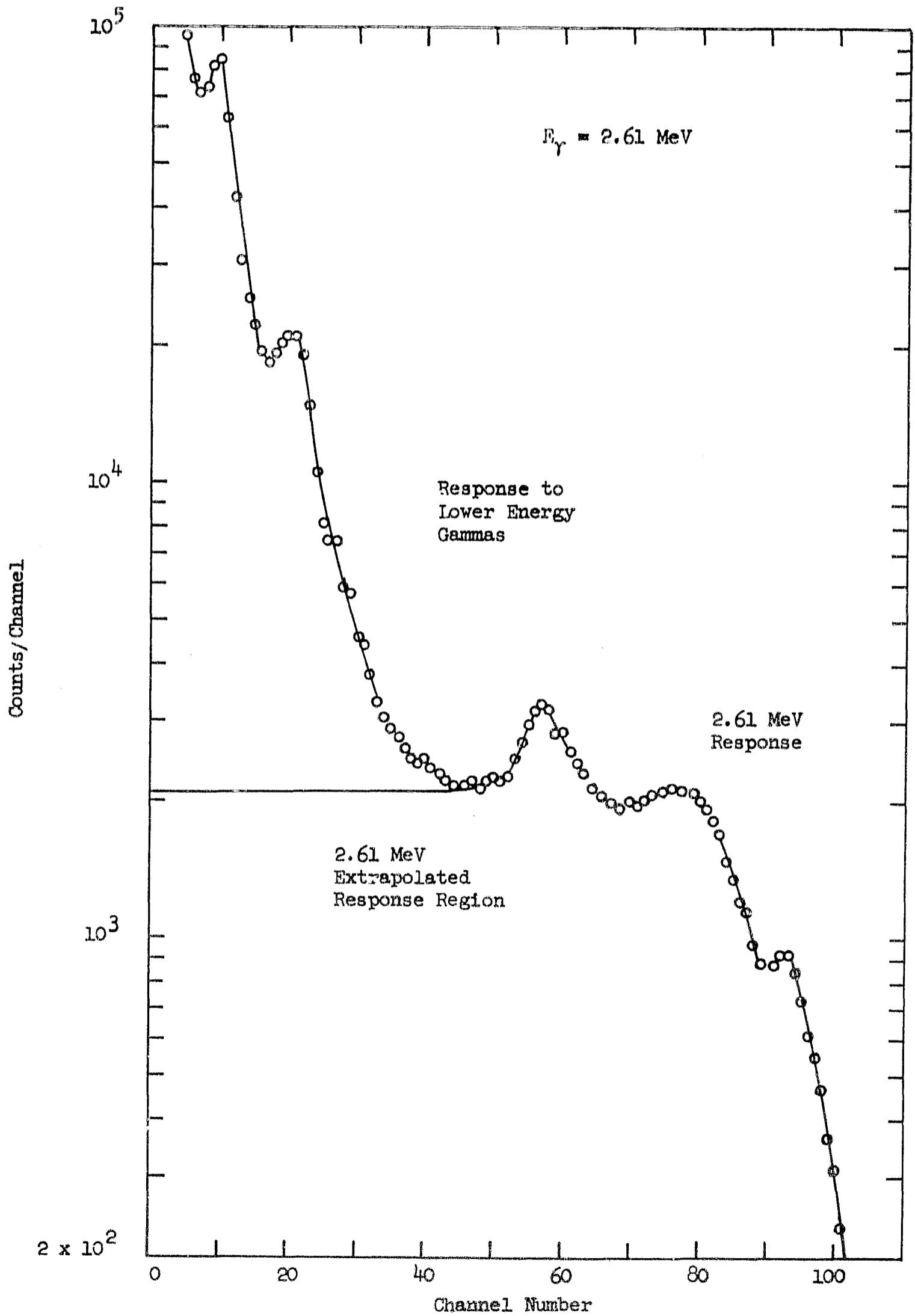
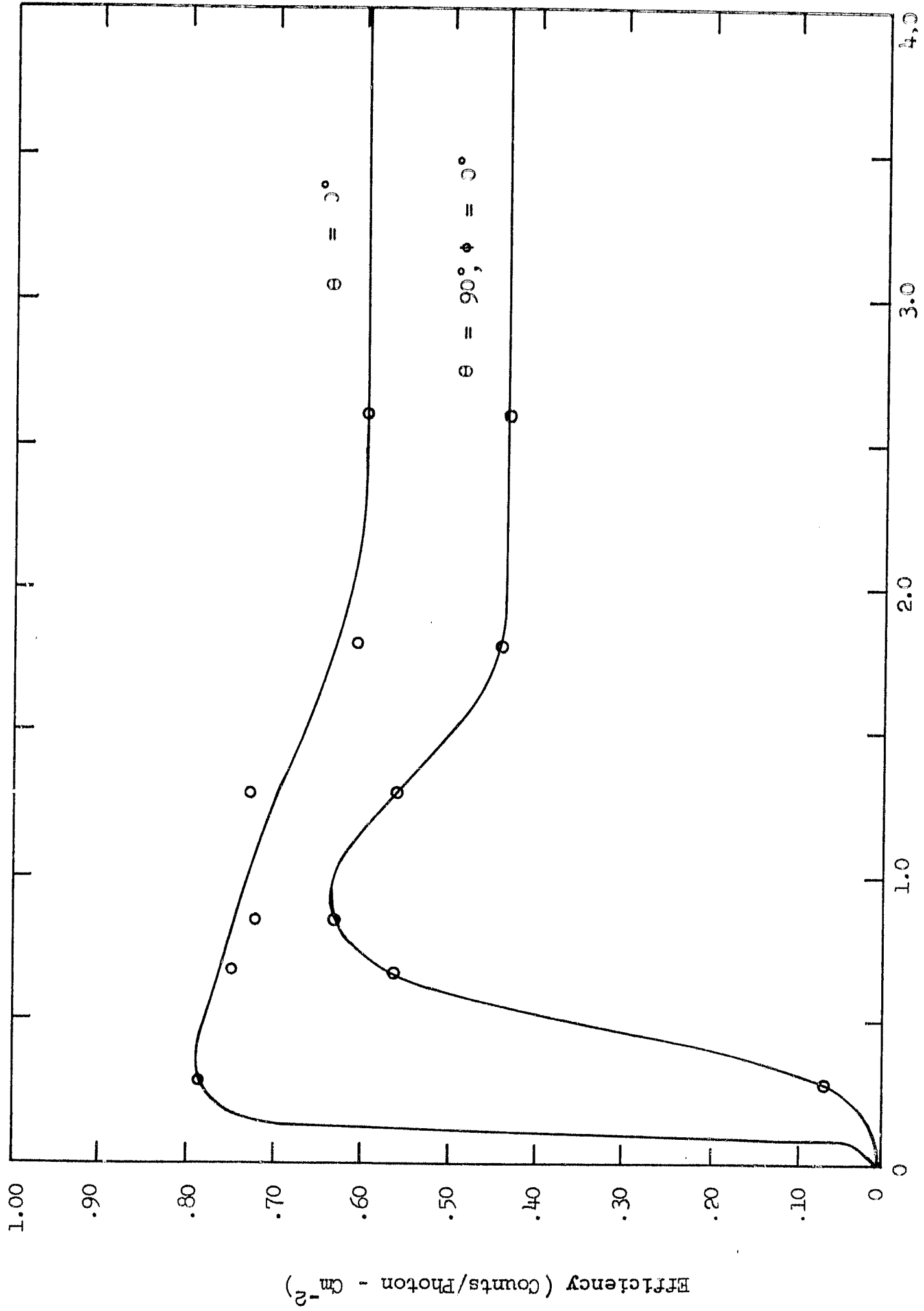


FIGURE 19 Th-226 PULSE HEIGHT SPECTRUM



Incident Photon Energy (MeV)  
 FIGURE 20 GAMMA EFFICIENCY  $\epsilon_\gamma$

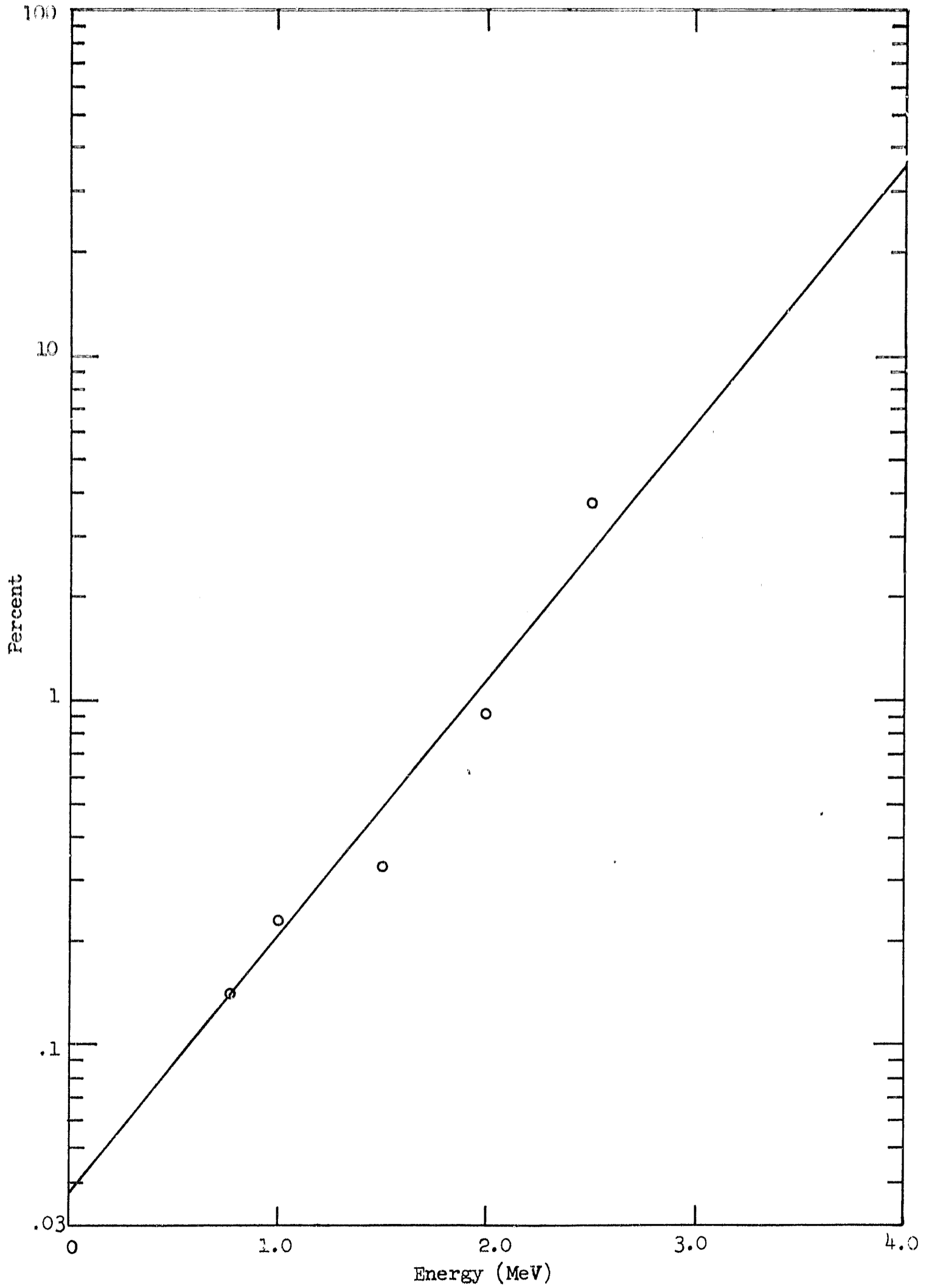


FIGURE 21 FALSE ELECTRON COUNTS IN GAMMA CHANNELS  $f_{\beta}$

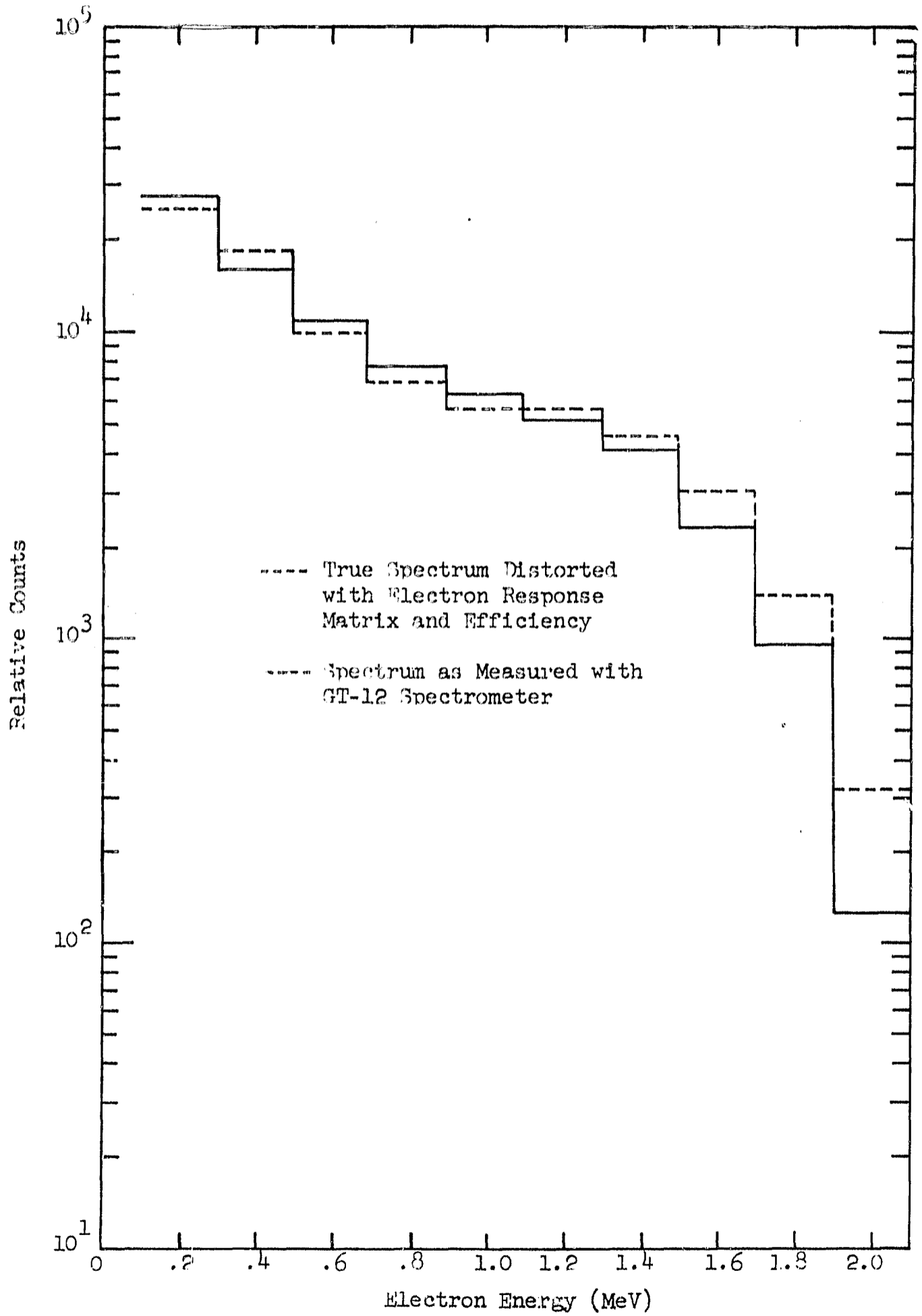


FIGURE 22 Sr-90 BETA PULSE HEIGHT SPECTRUM

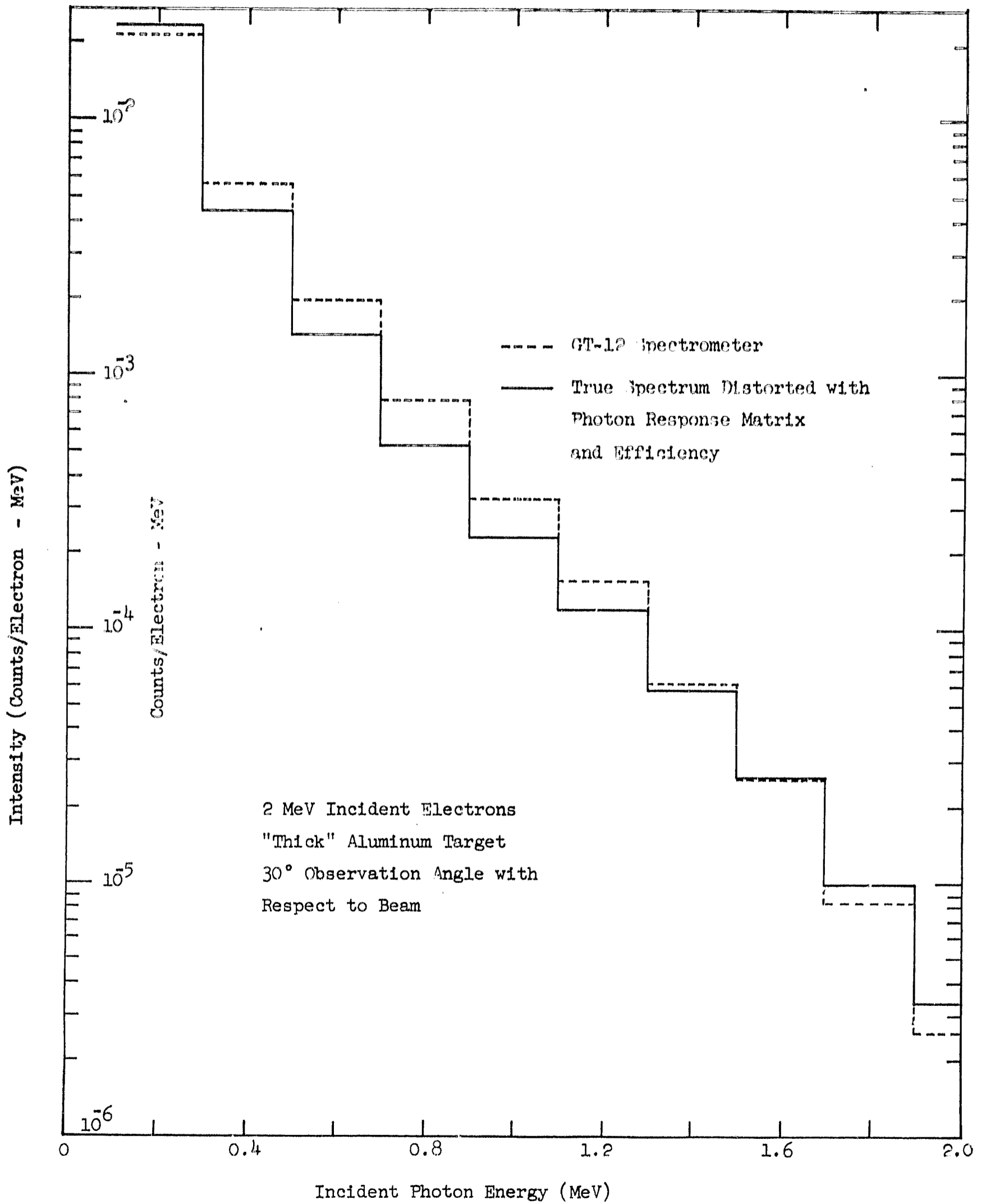


FIGURE 23 BREMSSTRAHLUNG PULSE HEIGHT SPECTRUM

TABLE 1

BETA RESPONSE MATRIX -  $R_{\beta}$ 

<u>E</u> <u>Incident</u> <u>Energy</u> <u>(MeV)</u>	<u>E' - Pulse Height(MeV)</u>				
	<u>0.2</u>	<u>0.4</u>	<u>0.6</u>	<u>0.8</u>	<u>1.0</u>
0.2	0	0	0	0	0
0.4	8.43(-1)	1.13(-2)	0	0	0
0.6	1.27(-1)	8.00(-1)	6.13(-2)	0	0
0.8	4.13(-2)	3.58(-1)	5.14(-1)	8.24(-2)	0
1.0	3.95(-2)	1.72(-1)	1.57(-1)	4.37(-1)	1.91(-1)
1.2	3.35(-2)	1.38(-1)	1.10(-1)	1.11(-1)	3.26(-1)
1.4	1.83(-2)	9.46(-2)	9.48(-2)	6.54(-2)	8.42(-2)
1.6	1.38(-2)	8.35(-2)	7.56(-2)	6.53(-2)	5.89(-2)
1.8	1.25(-2)	6.10(-2)	7.63(-2)	6.33(-2)	5.36(-2)
2.0	1.14(-2)	4.35(-2)	6.33(-2)	5.88(-2)	5.24(-2)
2.2	1.08(-2)	3.23(-2)	5.22(-2)	5.78(-2)	5.48(-2)
2.4	6.42(-3)	3.09(-2)	4.83(-2)	5.16(-2)	4.94(-2)
2.6	5.94(-3)	2.48(-3)	4.01(-2)	4.40(-2)	4.38(-2)
2.8	4.58(-3)	2.14(-2)	3.66(-2)	4.00(-2)	4.00(-2)
3.0	3.64(-3)	1.85(-2)	3.00(-2)	3.57(-2)	3.81(-2)
3.2	3.08(-3)	1.48(-2)	2.73(-2)	3.30(-2)	3.58(-2)
3.4	2.92(-3)	7.84(-3)	2.36(-2)	2.78(-2)	3.06(-2)
3.6	2.47(-3)	1.20(-2)	2.38(-2)	2.87(-2)	3.10(-2)
3.8	2.01(-3)	1.12(-2)	2.22(-2)	2.70(-2)	2.97(-2)
4.0	1.77(-3)	9.21(-3)	2.03(-2)	2.58(-2)	2.88(-2)



TABLE 1  
BETA RESPONSE MATRIX -  $R_{\beta}$  (Con't)

<u>E</u> Incident Energy (MeV)	<u>E' - Pulse Height (MeV)</u>				
	<u>1.2</u>	<u>1.4</u>	<u>1.6</u>	<u>1.8</u>	<u>2.0</u>
.2	0	0	0	0	0
.4	0	0	0	0	0
.6	0	0	0	0	0
.8	0	0	0	0	0
1.0	0	0	0	0	0
1.2	2.30(-1)	0	0	0	0
1.4	3.39(-1)	3.02(-1)	0	0	0
1.6	3.43(-2)	3.11(-1)	2.80(-1)	4.23(-3)	0
1.8	5.50(-2)	8.91(-2)	3.53(-1)	2.67(-1)	0
2.0	4.85(-2)	5.37(-2)	8.31(-2)	3.16(-1)	2.67(-1)
2.2	5.33(-2)	5.64(-2)	9.08(-2)	2.89(-1)	2.93(-1)
2.4	4.89(-2)	5.12(-2)	5.34(-2)	6.09(-2)	9.73(-2)
2.6	4.46(-2)	4.94(-2)	5.25(-2)	5.27(-2)	6.28(-2)
2.8	4.07(-2)	4.49(-2)	5.36(-2)	5.52(-2)	5.35(-2)
3.0	3.83(-2)	3.96(-2)	4.82(-2)	5.64(-2)	5.51(-2)
3.2	3.67(-2)	3.75(-2)	4.11(-2)	4.96(-2)	5.85(-2)
3.4	3.32(-2)	3.54(-2)	3.85(-2)	4.57(-2)	5.63(-2)
3.6	3.17(-2)	3.25(-2)	3.46(-2)	3.94(-2)	5.31(-2)
3.8	3.06(-2)	3.11(-2)	3.24(-2)	3.51(-2)	4.18(-2)
4.0	3.02(-2)	3.04(-2)	3.05(-2)	3.18(-2)	3.54(-2)

TABLE 1  
BETA RESPONSE MATRIX -  $R_{\beta}$  (Con't)

<u>E</u> Incident Energy (MeV)	<u>E' - Pulse Height (MeV)</u>				
	<u>2.2</u>	<u>2.4</u>	<u>2.6</u>	<u>2.8</u>	<u>3.0</u>
.2	0	0	0	0	0
.4	0	0	0	0	0
.6	0	0	0	0	0
.8	0	0	0	0	0
1.0	0	0	0	0	0
1.2	0	0	0	0	0
1.4	0	0	0	0	0
1.6	0	0	0	0	0
1.8	0	0	0	0	0
2.0	2.27(-3)	0	0	0	0
2.2	9.23(-3)	0	0	0	0
2.4	2.57(-1)	2.36(-1)	1.12(-3)	0	0
2.6	1.05(-1)	2.56(-1)	2.10(-1)	8.35(-3)	0
2.8	6.73(-2)	1.06(-1)	2.33(-1)	1.92(-1)	1.15(-2)
3.0	5.37(-2)	6.98(-2)	1.05(-1)	2.11(-1)	1.81(-1)
3.2	5.49(-2)	5.87(-2)	7.54(-2)	1.06(-1)	1.94(-1)
3.4	6.05(-2)	5.49(-2)	5.87(-2)	7.57(-2)	1.01(-1)
3.6	6.21(-2)	5.89(-2)	5.03(-2)	6.06(-2)	7.52(-2)
3.8	5.61(-2)	6.29(-2)	5.55(-2)	4.80(-2)	5.95(-2)
4.0	4.78(-2)	6.14(-2)	6.07(-2)	5.10(-2)	4.77(-2)

TABLE 1

BETA RESPONSE MATRIX  $R_{\beta}$  (Con't)

<u>E</u> <u>Incident</u> <u>Energy</u> <u>(MeV)</u>	<u>E' - Pulse Height (MeV)</u>				
	<u>3.2</u>	<u>3.4</u>	<u>3.6</u>	<u>3.8</u>	<u>4.0</u>
.2	0	0	0	0	0
.4	0	0	0	0	0
.6	0	0	0	0	0
.8	0	0	0	0	0
1.0	0	0	0	0	0
1.2	0	0	0	0	0
1.4	0	0	0	0	0
1.6	0	0	0	0	0
1.8	0	0	0	0	0
2.0	0	0	0	0	0
2.2	0	0	0	0	0
2.4	0	0	0	0	0
2.6	0	0	0	0	0
2.8	0	0	0	0	0
3.0	1.93(-2)	0	0	0	0
3.2	1.57(-1)	1.67(-2)	0	0	0
3.4	1.74(-1)	1.49(-1)	2.45(-2)	0	0
3.6	9.34(-2)	1.52(-1)	1.34(-1)	2.46(-2)	0
3.8	7.15(-2)	8.65(-2)	1.29(-1)	1.26(-1)	4.17(-2)
4.0	6.18(-2)	6.86(-2)	7.80(-2)	1.14(-1)	1.23(-1)

TABLE 2

BETA EFFICIENCY MATRIX -  $\epsilon_{\beta}$ 

<u>E (MeV)</u>	<u><math>\epsilon_{\beta}</math> (Counts/Electron - <math>\text{cm}^{-2}</math>)</u>
0.2	0
0.4	2.37(-2)
0.6	2.50(-2)
0.8	2.34(-2)
1.0	2.22(-2)
1.2	2.24(-2)
1.4	2.34(-2)
1.6	2.43(-2)
1.8	2.45(-2)
2.0	2.43(-2)
2.2	2.38(-2)
2.4	2.34(-2)
2.6	2.32(-2)
2.8	2.32(-2)
3.0	2.32(-2)
3.2	2.32(-2)
3.4	2.32(-2)
3.6	2.32(-2)
3.8	2.32(-2)
4.0	2.32(-2)

TABLE 3

BETA CROSS-TALK RESPONSE MATRIX  $C_{\beta}$ 

<u>E</u> Incident Energy (MeV)	<u>E' - Pulse Height (MeV)</u>				
	<u>0.2</u>	<u>0.4</u>	<u>0.6</u>	<u>0.8</u>	<u>1.0</u>
0.2	0	0	0	0	0
0.4	0	9.65(-1)	3.50(-2)	0	0
0.6	0	1.27(-1)	7.65(-1)	1.01(-1)	0
0.8	8.47(-2)	3.04(-1)	3.63(-1)	2.12(-1)	3.25(-2)
1.0	1.55(-2)	7.94(-2)	2.06(-1)	4.36(-1)	2.33(-1)
1.2	7.62(-3)	1.08(-2)	1.83(-2)	5.58(-2)	3.31(-1)
1.4	8.39(-3)	1.06(-2)	1.32(-2)	1.76(-2)	4.25(-2)
1.6	9.35(-3)	1.23(-2)	1.73(-2)	2.52(-2)	3.84(-2)
1.8	9.20(-3)	1.06(-2)	1.35(-2)	1.93(-2)	2.99(-2)
2.0	7.20(-3)	7.92(-3)	9.14(-3)	1.12(-2)	1.47(-2)
2.2	5.91(-3)	7.59(-3)	9.55(-3)	1.15(-2)	1.39(-2)
2.4	3.86(-3)	7.78(-3)	1.22(-2)	1.66(-2)	2.07(-2)
2.6	2.20(-3)	7.75(-3)	1.40(-2)	2.02(-2)	2.58(-2)
2.8	1.33(-3)	6.37(-3)	1.17(-2)	1.70(-2)	2.20(-2)
3.0	1.07(-3)	5.18(-3)	9.72(-3)	1.44(-2)	1.88(-2)
3.2	8.07(-4)	4.31(-3)	8.39(-3)	1.25(-2)	1.65(-2)
3.4	5.36(-4)	3.67(-3)	7.31(-3)	1.08(-2)	1.45(-2)
3.6	3.82(-4)	3.00(-3)	5.99(-3)	9.23(-3)	1.23(-2)
3.8	2.94(-4)	2.56(-3)	5.52(-3)	8.56(-3)	1.13(-2)
4.0	2.35(-4)	2.18(-3)	4.58(-3)	7.06(-3)	9.55(-3)

TABLE 3

BETA CROSS-TALK RESPONSE MATRIX  $C_{\beta}$  (Con't)

E Incident Energy (MeV)	E' - Pulse Height (MeV)				
	<u>1.2</u>	<u>1.4</u>	<u>1.6</u>	<u>1.8</u>	<u>2.0</u>
0.2	0	0	0	0	0
0.4	0	0	0	0	0
0.6	0	0	0	0	0
0.8	0	0	0	0	0
1.0	2.59(-2)	0	0	0	0
1.2	5.02(-1)	6.10(-2)	6.76(-3)	0	0
1.4	3.52(-1)	4.81(-1)	5.81(-2)	8.89(-3)	0
1.6	6.56(-2)	3.21(-1)	4.44(-1)	3.21(-2)	1.61(-2)
1.8	4.87(-2)	3.78(-2)	4.05(-1)	3.34(-1)	1.85(-2)
2.0	2.11(-2)	3.48(-2)	6.76(-2)	3.76(-1)	4.23(-1)
2.2	1.72(-2)	2.36(-2)	3.60(-2)	6.69(-2)	4.05(-1)
2.4	2.38(-2)	2.58(-2)	2.98(-2)	3.85(-2)	6.46(-2)
2.6	3.07(-2)	3.43(-2)	3.63(-2)	3.76(-2)	4.20(-2)
2.8	2.63(-2)	3.03(-2)	3.29(-2)	3.40(-2)	3.52(-2)
3.0	2.27(-2)	2.61(-2)	2.89(-2)	3.06(-2)	3.15(-2)
3.2	2.01(-2)	2.34(-2)	2.65(-2)	2.86(-2)	2.97(-2)
3.4	1.81(-2)	2.13(-2)	2.40(-2)	2.61(-2)	2.75(-2)
3.6	1.53(-2)	1.81(-2)	2.06(-2)	2.28(-2)	2.43(-2)
3.8	1.39(-2)	1.66(-2)	1.91(-2)	2.13(-2)	2.30(-2)
4.0	1.19(-2)	1.43(-2)	1.66(-2)	1.85(-2)	2.02(-2)

TABLE 3

BETA CROSS-TALK RESPONSE MATRIX  $C_{\beta}$  (Con't)

<u>E</u> Incident Energy (MeV)	<u>E' - Pulse Height (MeV)</u>				
	<u>2.2</u>	<u>2.4</u>	<u>2.6</u>	<u>2.8</u>	<u>3.0</u>
0.2	0	0	0	0	0
0.4	0	0	0	0	0
0.6	0	0	0	0	0
0.8	0	0	0	0	0
1.0	0	0	0	0	0
1.2	0	0	0	0	0
1.4	0	0	0	0	0
1.6	1.01( 2)	0	0	0	0
1.8	1.02(-2)	4.42(-3)	0	0	0
2.0	1.38(-2)	4.30(-3)	1.13(-3)	0	0
2.2	3.75(-1)	1.46(-2)	4.49(-3)	2.22(-3)	7.45(-4)
2.4	3.38(-1)	3.75(-1)	3.63(-2)	2.32(-3)	1.23(-3)
2.6	7.16(-2)	3.11(-1)	3.13(-1)	4.86(-2)	1.79(-3)
2.8	4.00(-2)	7.35(-2)	2.85(-1)	3.10(-1)	6.95(-2)
3.0	3.32(-2)	3.83(-2)	8.32(-2)	2.86(-1)	2.88(-1)
3.2	3.04(-2)	3.27(-2)	3.91(-2)	9.52(-2)	2.87(-1)
3.4	2.83(-2)	2.91(-2)	3.15(-2)	3.72(-2)	8.38(-2)
3.6	2.53(-2)	2.58(-2)	2.67(-2)	2.94(-2)	3.53(-2)
3.8	2.42(-2)	2.49(-2)	2.53(-2)	2.64(-2)	2.90(-2)
4.0	2.15(-2)	2.25(-2)	2.30(-2)	2.34(-2)	2.46(-2)

TABLE 3

BETA CROSS-TALK RESPONSE MATRIX  $C_{\beta}$  (Con't)

<u>E</u> Incident Energy (MeV)	<u>E' - Pulse Height (MeV)</u>				
	<u>3.2</u>	<u>3.4</u>	<u>3.6</u>	<u>3.8</u>	<u>4.0</u>
0.2	0	0	0	0	0
0.4	0	0	0	0	0
0.6	0	0	0	0	0
0.8	0	0	0	0	0
1.0	0	0	0	0	0
1.2	0	0	0	0	0
1.4	0	0	0	0	0
1.6	0	0	0	0	0
1.8	0	0	0	0	0
2.0	0	0	0	0	0
2.2	0	0	0	0	0
2.4	4.55(-4)	0	0	0	0
2.6	9.72(-4)	4.00(-4)	0	0	0
2.8	2.06(-3)	1.01(-3)	7.13(-4)	1.54(-4)	0
3.0	7.62(-2)	2.97(-3)	1.02(-3)	7.19(-4)	2.62(-4)
3.2	2.68(-1)	6.85(-2)	4.44(-3)	1.04(-3)	7.42(-4)
3.4	2.71(-1)	2.71(-1)	8.28(-2)	6.80(-3)	1.13(-3)
3.6	9.05(-2)	2.96(-1)	2.47(-1)	8.00(-2)	8.23(-3)
3.8	3.57(-2)	9.03(-2)	2.46(-1)	2.56(-1)	1.01(-1)
4.0	2.72(-2)	3.45(-2)	9.14(-2)	2.26(-1)	2.55(-1)



TABLE 4  
BETA CROSS-TALK EFFICIENCY MATRIX -  $f_{\beta}$

<u>E (MeV)</u>	$f_{\beta}$
.2	.00052
.4	.00075
.6	.00105
.8	.00148
1.0	.00205
1.2	.00295
1.4	.0041
1.6	.0058
1.8	.0082
2.0	.0115
2.2	.0161
2.4	.0225
2.6	.032
2.8	.045
3.0	.064
3.2	.089
3.4	.124
3.6	.178
3.8	.245
4.0	.349

TABLE 5

GAMMA RADIATION SOURCES						
<u>Source</u>	<u>Half Life</u>	<u>Config.</u>	<u>Strength</u>	<u>Energy (MeV)</u>	<u>Source Strength (r/Sec)</u>	<u>Date 1200 Hrs. CST</u>
Na <sup>22</sup>	2.58 Yrs.	Needle	4.0 mc	1.28	1.15 (8)	8/31/66
Na <sup>22</sup>		Bottle	0.1 mc	1.28	3.54 (6)	9/8/66
Cs <sup>137</sup>	30.2 Yrs.	Bottle	0.1 mc	0.662	3.21 (6)	9/9/66
Cs <sup>137</sup>		Needle	3.7 mc	0.662	1.23 (8)	9/1/66
Co <sup>60</sup>	5.28 Yrs.	Bottle	0.1 mc	1.17-1.33	83.51 $\mu$ c	4/1/66*
Co <sup>60</sup>		Needle	0.5 mc	1.17	1.42 (7)	9/1/66
				1.33	1.42 (7)	
Co <sup>60</sup>		Needle	4.0 mc	1.17	1.39 (8)	9/1/66
				1.33	1.39 (8)	
Hg <sup>203</sup>	46.7 Dys	Needle	0.5 mc	0.279	9.28 (6)	9/1/66
Hg <sup>203</sup>		Needle	4.0 mc	0.279	5.29 (7)	9/1/66
Mn <sup>54</sup>	301. Dys	Needle	0.5 mc	0.835	1.80 (7)	9/1/66
Mn <sup>54</sup>		Needle	4.0 mc	0.835	1.02 (8)	9/1/66
Y <sup>88</sup>	105 Dys	Needle	2.99 mc	0.9	7.71 (7)	9/9/66
				1.8	8.86 (7)	
				2.76	5.27 (5)	

\* 1200 Hrs. GMT

TABLE 6

GAMMA RESPONSE MATRIX-  $R_{\gamma}$ 

<u>E</u> Incident Energy (MeV)	<u>E' - Pulse Height(MeV)</u>				
	<u>0.2</u>	<u>0.4</u>	<u>0.6</u>	<u>0.8</u>	<u>1.0</u>
0.2	3.86(-1)	0	0	0	0
0.4	2.54(-1)	3.35(-1)	5.38(-3)	0	0
0.6	2.90(-1)	1.87(-1)	2.14(-1)	8.43(-3)	0
0.8	2.45(-1)	1.94(-1)	1.34(-1)	1.34(-1)	1.21(-2)
1.0	2.16(-1)	1.60(-1)	1.10(-1)	8.68(-2)	8.31(-2)
1.2	2.00(-1)	1.76(-1)	1.10(-1)	8.98(-2)	7.95(-2)
1.4	1.65(-1)	1.23(-1)	1.12(-1)	9.25(-2)	7.77(-2)
1.6	1.27(-1)	1.20(-1)	1.20(-1)	1.30(-1)	1.02(-1)
1.8	9.68(-2)	9.61(-2)	9.61(-2)	1.31(-1)	1.40(-1)
2.0	8.71(-2)	8.58(-2)	8.58(-2)	9.04(-2)	1.50(-1)
2.2	7.82(-2)	7.69(-2)	7.69(-2)	7.80(-2)	1.11(-1)
2.4	7.44(-2)	7.44(-2)	7.44(-2)	7.44(-2)	7.85(-2)
2.6	7.02(-2)	7.16(-2)	7.16(-2)	7.16(-2)	7.16(-2)
2.8	6.51(-2)	6.90(-2)	7.04(-2)	6.97(-2)	6.84(-2)
3.0	6.18(-2)	6.75(-2)	6.84(-2)	6.80(-2)	6.73(-2)
3.2	5.87(-2)	6.34(-2)	6.53(-2)	6.46(-2)	6.59(-2)
3.4	5.74(-2)	6.27(-2)	6.46(-2)	6.39(-2)	6.46(-2)
3.6	5.90(-2)	6.06(-2)	6.13(-2)	5.96(-2)	5.96(-2)
3.8	4.83(-2)	5.54(-2)	5.90(-2)	6.03(-2)	5.96(-2)
4.0	4.70(-2)	5.48(-2)	5.96(-2)	6.17(-2)	6.16(-2)

TABLE 6

GAMMA RESPONSE MATRIX -  $R_{\gamma}$ 

E Incident Energy (MeV)	E' - Pulse Height (MeV)				
	<u>1.2</u>	<u>1.4</u>	<u>1.6</u>	<u>1.8</u>	<u>2.0</u>
0.2	0	0	0	0	0
0.4	0	0	0	0	0
0.6	0	0	0	0	0
0.8	0	0	0	0	0
1.0	2.56(-2)	7.10(-4)	0	0	0
1.2	6.22(-2)	2.96(-2)	1.08(-3)	0	0
1.4	6.77(-2)	4.07(-2)	3.02(-2)	1.44(-3)	0
1.6	9.46(-2)	8.08(-2)	4.80(-2)	2.91(-2)	3.92(-3)
1.8	8.97(-2)	9.74(-2)	7.04(-2)	5.15(-2)	2.74(-2)
2.0	9.90(-2)	8.68(-2)	9.10(-2)	6.25(-2)	5.15(-2)
2.2	1.21(-1)	9.09(-2)	7.98(-2)	8.35(-2)	5.61(-2)
2.4	9.17(-2)	9.83(-2)	8.77(-2)	7.51(-2)	7.75(-2)
2.6	7.16(-2)	7.89(-2)	1.02(-1)	7.78(-2)	6.85(-2)
2.8	6.48(-2)	5.79(-2)	8.72(-2)	9.61(-2)	6.79(-2)
3.0	6.21(-2)	5.03(-2)	5.35(-2)	9.87(-2)	8.78(-2)
3.2	6.09(-2)	4.68(-2)	4.09(-2)	6.73(-2)	1.06(-1)
3.4	6.27(-2)	5.02(-2)	3.45(-2)	3.72(-2)	8.38(-2)
3.6	6.05(-2)	4.97(-2)	3.25(-2)	2.89(-2)	4.82(-2)
3.8	5.73(-2)	5.15(-2)	3.83(-2)	2.57(-2)	2.52(-2)
4.0	5.89(-2)	5.30(-2)	3.97(-2)	2.37(-2)	2.32(-2)

TABLE 6

GAMMA RESPONSE MATRIX -  $R_{\gamma}$ 

E Incident Energy (MeV)	<u>E' - Pulse Height (MeV)</u>				
	<u>2.2</u>	<u>2.4</u>	<u>2.6</u>	<u>2.8</u>	<u>3.0</u>
0.2	0	0	0	0	0
0.4	0	0	0	0	0
0.6	0	0	0	0	0
0.8	0	0	0	0	0
1.0	0	0	0	0	0
1.2	0	0	0	0	0
1.4	0	0	0	0	0
1.6	7.70(-4)	0	0	0	0
1.8	3.33(-3)	8.70(-4)	0	0	0
2.0	1.66(-2)	2.58(-3)	9.90(-4)	0	0
2.2	4.74(-2)	1.64(-2)	2.53(-3)	9.70(-4)	0
2.4	5.10(-2)	4.60(-2)	1.86(-2)	2.36(-3)	1.01(-3)
2.6	7.06(-2)	4.86(-2)	3.73(-2)	1.46(-2)	3.06(-3)
2.8	6.17(-2)	6.17(-2)	4.94(-2)	3.22(-2)	1.29(-2)
3.0	5.90(-2)	5.62(-2)	5.64(-2)	4.61(-2)	2.87(-2)
3.2	7.25(-2)	4.92(-2)	4.88(-2)	5.25(-2)	3.90(-2)
3.4	9.90(-2)	5.47(-2)	4.85(-2)	4.49(-2)	5.06(-2)
3.6	1.05(-1)	8.34(-2)	4.25(-2)	4.14(-2)	3.71(-2)
3.8	6.65(-2)	1.10(-1)	9.28(-2)	4.46(-2)	3.46(-2)
4.0	2.39(-2)	8.61(-2)	1.12(-2)	5.65(-2)	3.62(-2)

TABLE 6

GAMMA RESPONSE MATRIX -  $R_\gamma$ 

<u>E</u> Incident Energy (MeV)	<u>E' - Pulse Height (MeV)</u>				
	<u>3.2</u>	<u>3.4</u>	<u>3.6</u>	<u>3.8</u>	<u>4.0</u>
0.2	0	0	0	0	0
0.4	0	0	0	0	0
0.6	0	0	0	0	0
0.8	0	0	0	0	0
1.0	0	0	0	0	0
1.2	0	0	0	0	0
1.4	0	0	0	0	0
1.6	0	0	0	0	0
1.8	0	0	0	0	0
2.0	0	0	0	0	0
2.2	0	0	0	0	0
2.4	0	0	0	0	0
2.6	1.15(-3)	0	0	0	0
2.8	3.24(-3)	1.28(-3)	7.40(-4)	0	0
3.0	6.37(-2)	3.97(-3)	1.57(-3)	8.20(-4)	0
3.2	2.33(-2)	1.33(-2)	5.11(-3)	1.74(-3)	8.00(-4)
3.4	3.13(-2)	1.92(-2)	1.16(-2)	4.82(-3)	1.63(-3)
3.6	4.58(-2)	3.22(-2)	1.63(-2)	1.03(-2)	5.37(-3)
3.8	3.25(-2)	3.95(-2)	2.36(-2)	1.52(-2)	1.08(-2)
4.0	3.05(-2)	3.13(-2)	3.94(-2)	2.02(-2)	1.56(-2)

TABLE 7

GAMMA EFFICIENCY MATRICES -  $\epsilon_r(\theta, \phi)$ 

E (MeV)	$\epsilon_r(\theta, \phi)$ (Counts/Photon - $\text{Cm}^{-2}$ )		
	$\theta, \phi = 0^\circ 0^\circ$	$\theta, \phi = 180^\circ, 0^\circ$	$\theta, \phi = 90^\circ, 0^\circ$
0.2	.720	.928	.046
0.4	.780	.820	.241
0.6	.768	.702	.501
0.8	.753	.690	.617
1.0	.733	.610	.630
1.2	.708	.595	.583
1.4	.685	.583	.517
1.6	.660	.568	.468
1.8	.638	.555	.439
2.0	.623	.545	.435
2.2	.610	.537	.435
2.4	.603	.532	.435
2.6	.601	.525	.435
2.8	.600	.519	.435
3.0	.600	.515	.435
3.2	.600	.510	.435
3.4	.600	.510	.435
3.6	.600	.510	.435
3.8	.600	.510	.435
4.0	.600	.510	.435

TABLE 8

GAMMA EFFICIENCY MULTIPLIERS

$\theta$ (deg)	$\phi$ (deg)	$N_{\theta, \phi} = \frac{\epsilon_r(\theta, \phi)}{\epsilon_r(90^\circ, 0^\circ)}$
45	0	0.83
45	45	0.86
45	90	0.83
45	135	0.84
45	180	0.85
45	225	0.79
45	270	0.88
45	315	0.90
90	0	1.00
90	45	0.88
90	90	0.68
90	135	1.08
90	180	1.13
90	225	1.11
90	270	1.00
90	315	1.07
135	0	0.96
135	45	0.61
135	90	0.76
135	135	0.97
135	180	1.01
135	225	1.00
135	270	0.86
135	315	0.83



TABLE 9

GAMMA CROSS-TALK RESPONSE MATRIX -  $C_Y$ 

<u>E</u> Incident Energy (MeV)	<u>E' - Pulse Height (MeV)</u>				
	<u>0.2</u>	<u>0.4</u>	<u>0.6</u>	<u>0.8</u>	<u>1.0</u>
0.2	3.32(-1)	0	0	0	0
0.4	3.65(-1)	6.88(-2)	0	0	0
0.6	3.62(-1)	1.42(-1)	2.45(-2)	0	0
0.8	3.36(-1)	1.88(-1)	6.39(-2)	1.25(-2)	0
1.0	3.13(-1)	2.08(-1)	9.31(-2)	3.06(-2)	9.88(-3)
1.2	2.85(-1)	2.10(-1)	1.16(-1)	5.17(-2)	2.03(-2)
1.4	2.55(-1)	2.06(-1)	1.33(-1)	7.31(-2)	3.58(-2)
1.6	2.30(-1)	1.96(-1)	1.43(-1)	3.98(-2)	5.04(-2)
1.8	1.93(-1)	1.76(-1)	1.43(-1)	1.06(-1)	7.24(-2)
2.0	1.68(-1)	1.57(-1)	1.35(-1)	1.09(-1)	8.32(-2)
2.2	1.39(-1)	1.34(-1)	1.23(-1)	1.07(-1)	8.92(-2)
2.4	1.20(-1)	1.14(-1)	1.06(-1)	9.64(-2)	8.53(-2)
2.6	1.01(-1)	9.49(-2)	8.95(-2)	8.40(-2)	7.86(-2)
2.8	8.80(-2)	7.98(-2)	7.60(-2)	7.66(-2)	7.60(-2)
3.0	7.63(-2)	7.45(-2)	7.05(-2)	7.22(-2)	7.28(-2)
3.2	7.05(-2)	6.53(-2)	6.30(-2)	6.36(-2)	6.36(-2)
3.4	6.48(-2)	6.32(-2)	5.93(-2)	5.93(-2)	5.99(-2)
3.6	5.80(-2)	5.75(-2)	5.65(-2)	5.60(-2)	5.60(-2)
3.8	5.33(-2)	5.33(-2)	5.28(-2)	5.24(-2)	5.18(-2)
4.0	5.24(-2)	5.24(-2)	5.14(-2)	4.86(-2)	4.95(-2)

TABLE 9

GAMMA CROSS-TALK RESPONSE MATRIX -  $C_{\gamma}$  (Con't)

<u>E</u> Incident Energy (MeV)	<u>E' - Pulse Height (MeV)</u>				
	<u>1.2</u>	<u>1.4</u>	<u>1.6</u>	<u>1.8</u>	<u>2.0</u>
0.2	0	0	0	0	0
0.4	0	0	0	0	0
0.6	0	0	0	0	0
0.8	0	0	0	0	0
1.0	0	0	0	0	0
1.2	9.11( 3)	0	0	0	0
1.4	1.78(-2)	9.64(-3)	0	0	0
1.6	2.74(-2)	1.55(-2)	9.27(-3)	0	0
1.8	4.48(-2)	2.78(-2)	1.89(-2)	1.31(-2)	8.88(-3)
2.0	6.10(-2)	4.30(-2)	2.97(-2)	2.05(-2)	1.39(-2)
2.2	7.16(-2)	5.60(-2)	4.34(-2)	3.30(-2)	2.46(-2)
2.4	7.46(-2)	6.45(-2)	5.10(-2)	4.68(-2)	3.86(-2)
2.6	7.35(-2)	6.83(-2)	6.25(-2)	5.67(-2)	5.06(-2)
2.8	7.22(-2)	6.65(-2)	6.20(-2)	6.14(-2)	5.79(-2)
3.0	6.99(-2)	6.00(-2)	5.74(-2)	5.76(-2)	5.88(-2)
3.2	6.25(-2)	5.96(-2)	5.62(-2)	5.56(-2)	5.73(-2)
3.4	5.93(-2)	5.77(-2)	5.60(-2)	5.36(-2)	5.27(-2)
3.6	5.44(-2)	5.28(-2)	5.23(-2)	5.08(-2)	4.92(-2)
3.8	5.09(-2)	5.04(-2)	4.99(-2)	4.91(-2)	4.76(-2)
4.0	4.91(-2)	4.76(-2)	4.72(-2)	4.62(-2)	4.54(-2)

TABLE 9

GAMMA CROSS-TALK RESPONSE MATRIX -  $C_{\gamma}$  (Con't)

E Incident Energy (MeV)	E' - Pulse Height (MeV)				
	<u>2.2</u>	<u>2.4</u>	<u>2.6</u>	<u>2.8</u>	<u>3.0</u>
0.2	0	0	0	0	0
0.4	0	0	0	0	0
0.6	0	0	0	0	0
0.8	0	0	0	0	0
1.0	0	0	0	0	0
1.2	0	0	0	0	0
1.4	0	0	0	0	0
1.6	0	0	0	0	0
1.8	0	0	0	0	0
2.0	9.31(-3)	0	0	0	0
2.2	1.77(-2)	1.21(-2)	8.38(-3)	0	0
2.4	3.07(-2)	2.34(-2)	1.63(-2)	9.77(-3)	0
2.6	4.41(-2)	3.66(-2)	2.72(-2)	1.76(-2)	9.96(-2)
2.8	5.19(-2)	4.43(-2)	3.67(-2)	2.78(-2)	1.80(-2)
3.0	5.71(-2)	5.18(-2)	4.40(-2)	3.64(-2)	2.80(-2)
3.2	5.79(-2)	5.53(-2)	5.10(-2)	4.53(-2)	3.72(-2)
3.4	5.49(-2)	5.38(-2)	5.11(-2)	4.75(-2)	4.34(-2)
3.6	4.98(-2)	5.08(-2)	4.92(-2)	4.66(-2)	4.43(-2)
3.8	4.66(-2)	4.69(-2)	4.69(-2)	4.56(-2)	4.41(-2)
4.0	4.46(-2)	4.39(-2)	4.29(-2)	4.20(-2)	4.10(-2)

TABLE 9

GAMMA CROSS-TALK RESPONSE MATRIX -  $C_{\gamma}$  (Con't)

E Incident Energy (MeV)	E' - Pulse Height (MeV)				
	<u>3.2</u>	<u>3.4</u>	<u>3.6</u>	<u>3.8</u>	<u>4.0</u>
0.2	0	0	0	0	0
0.4	0	0	0	0	0
0.6	0	0	0	0	0
0.8	0	0	0	0	0
1.0	0	0	0	0	0
1.2	0	0	0	0	0
1.4	0	0	0	0	0
1.6	0	0	0	0	0
1.8	0	0	0	0	0
2.0	0	0	0	0	0
2.2	0	0	0	0	0
2.4	0	0	0	0	0
2.6	0	0	0	0	0
2.8	1.00(-2)	0	0	0	0
3.0	1.83(-2)	9.90(-3)	0	0	0
3.2	2.95(-2)	2.03(-2)	1.05(-2)	0	0
3.4	3.74(-2)	2.99(-2)	2.03(-2)	1.02(-2)	0
3.6	4.12(-2)	3.73(-2)	3.11(-2)	2.36(-2)	1.58(-2)
3.8	4.24(-2)	3.94(-2)	3.59(-2)	3.09(-2)	2.44(-2)
4.0	3.96(-2)	3.99(-2)	3.87(-2)	3.61(-2)	3.18(-2)

TABLE 10  
GAMMA CROSS-TALK EFFICIENCY MATRIX -  $f_{\gamma}$

E (MeV)	$f_{\gamma}$
.2	.0044
.4	.0053
.6	.0062
.8	.0074
1.0	.0088
1.2	.0105
1.4	.0131
1.6	.0165
1.8	.0205
2.0	.0260
2.2	.0325
2.4	.041
2.6	.051
2.8	.064
3.0	.080
3.2	.100
3.4	.125
3.6	.158
3.8	.200
4.0	.250

TABLE 11

SYSTEM CHANNEL BOUNDARIES

Calibration Reference - 2.615 MeV = 4.00 volts

Bremsstrahlung Channels

<u>Channel Number</u>	<u>Lower (volts)</u>	<u>Upper (volts)</u>	<u>Width (volts)</u>
1	0.345	0.427	0.082
2	0.427	0.764	0.336
3	0.764	1.709	0.945
4	1.709	2.627	0.918
5	2.627	5.491	2.864

Beta Channels

<u>Channel Number</u>	<u>Lower (volts)</u>	<u>Upper (volts)</u>	<u>Width (volts)</u>
1	0.296	0.709	0.413
2	0.709	1.727	1.018
3	1.727	2.854	1.127
4	2.854	4.236	1.382
5	4.236	5.491	1.254









4

3

2

1

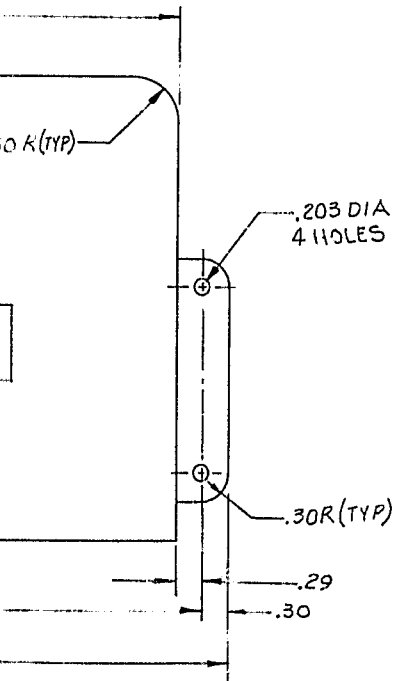
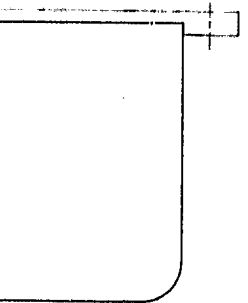
ZONE	TR	REVISIONS DESCRIPTION	DATE	APPROVED

D

C

B

N100-00920



QUANTITY REQUIRED	ZONE	ITEM	CODE IDENT NO.	PART OR IDENTIFYING NO.	NOMENCLATURE OR DESCRIPTION	MATERIAL AND FINISH OR NOTE OR REF DES.

LIST OF MATERIAL OR PARTS LIST

QTY PER MAJOR ASSY	NEXT ASSEMBLY	USED ON	UNLESS OTHERWISE SPECIFIED	PROJ ENGR	<b>LTV RESEARCH CENTER</b> CASE OUTLINE β-γ SPECTROMETER
	N100-00000	N100-00000	TOLERANCES UNLESS OTHERWISE SPECIFIED: 2 PLACE DEC 1 PLACE DEC .02 .010 ANGLES 2° 15' 2° 30' MACHINED FORMED SHEARED HOLE TOLERANCE PER AND H387 SURFACE ROUGHNESS PER MIL-STD-19 MACHINED SURFACE FINISH DIMENSIONING AND TOLERANCING PER MIL-STD-19 ECCENTRICITY BETWEEN ANY DIAM ON THE SAME CENTERLINE SHALL NOT EXCEED .010 TOTAL INDICATOR READING ALL DIM. ARE IN INCHES UNLESS OTHERWISE SPECIFIED WELD SYMBOLS PER MIL-STD-19 RIVET CODE PER NAS 393 THREADS PER MIL-STD-19 MARK PER MIL-STD-19 REMOVE ALL BURRS AND SHARP EDGES SPECIFICATIONS:	COMP ENGR MATEL/PROC ENGR STRUCT WTS GROUP APP CHECKED BY DRAWN BY ENGR GRJUP	
					SIZE CODE IDENT NO. D 1181 N100-00920
					SCALE: FULL REV. SHEET

A





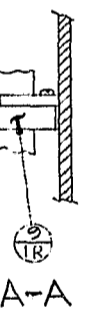
4 3 2 1

NOTES

1. ASSEMBLE & SOLDER PER NASA SPEC NPC 200-4
2. BARRY CONTROLS, DIV OF BARRY-WRIGHT INC, WATERTOWN, MASS.
3. BOND ITEM 12 TO ITEM 4 USING ITEM 36
4. BOND ITEM 21 TO TOP OF ITEMS 6 & 7 AFTER INSTALLATION OF SPACERS.
5. STRING TIE ITEM 11 TO ITEM 3 AND CONNECTORS J101, J102 & J103 USING ITEM 20
6. CONFORMAL COAT AND SECURE COMPONENTS PER 408-00060.
7. CONFORMAL COAT BOTH SIDES OF BOARD AND SECURE COMPONENTS AND WIRES ON PE5400 POWER SUPPLY PER 408-00060. MASK OFF MOUNTING AREAS AND TACK SECURE PE5400 PWR SUPPLY IN THREE PLACES
8. TORQUE SCREWS UNTIL RUBBER COMPRESSES OUT AROUND ENTIRE MOUNTING PERIPHERY.

REVISIONS				
ZONE	LTR	DESCRIPTION	DATE	APPROVED
	A	1. ADDED ITEMS 16 & 3A TO L/M & F/D 2. ITEM 24 WAS AN507-G32RIO IN L/M 3. ITEM 27 WAS NAS601-16P	8-19-66 8-31-66	CARTWRIGHT JH
AS	B	ADDED HIDDEN VIEW OF CAPACITOR.	1-12-67 1/29/67	St. Lowe CHK BY Rb. Brown

QTY	ZONE	ITEM	CODE IDENT NO.	PART OR IDENTIFYING NO.	NOMENCLATURE OR DESCRIPTION	MATERIAL AND FINISH OR NOTE OR REF DES
	AI	40		GRADE C	SEALANT	MIL-S-22473
	AI	39		GRADE N, FM-R, GRN	PRIMER	MIL-S-22473
		38				
		37				
	AR	36		RTV102	SEALANT	GENERAL ELECTRIC, WATERFORD, N.Y.
		35				
	AR	34		24 AWG	WIRE, SAFETY	QQ-W-423
		33				
		32		MS9021-019	O-RING	
		31		NAS1352C04-12	SCREW	
		30		NAS620-6	WASHER, FLAT	
		29		NAS620-4	WASHER, FLAT	
		28		NAS601-9P	SCREW	
		27		AN526-14	SCREW	
		26		NAS600-6P	SCREW	
		25		NAS600-8P	SCREW	
		24		AN507-440RIO	SCREW	
		23				
		22				
	AR	21		CHR-700	SILICONE RUBBER	LONGHORN GASKET, DALLAS, TEX
	AR	20		TYPE P, WAXED, CL2 NAT	TWINE	MIL-T-713
		19				
		18				
		17				
		16		10-101964-123	CAP, DUST	BENDIX SCINTILLA DIV. SIDNEY, N.Y.
		15		20150-1	SLIDE, CARD	NOTE 2 (LENGTH IN INCHES)
		14				
		13		N100-10300-01	INTERCONNECT ASSY	
		12		N100-10015-02	GASKET	
	REF	11		N100-10200-01	WIRE HARNESS	
		10		N100-10016-06	SPACER	
		9		N100-10016-05	CLAMP	
		8		N100-10016-04	CLAMP	
		7		N100-10016-03	SPACER	
		6		N100-10016-02	SPACER	
		5		N100-10004-01	CASE	
		4		N100-10002-01	COVER, BOTTOM	
	REF	3		N100-10001-01	TUBE ASSY	CALL OUT ON DWG N100-10300
		2				
		1		-01	ASSY	



BOND TO CONNECTOR PER NOTE 6.



QTY PER MAJOR ASSY	NEXT ASSEMBLY	USED ON	UNLESS OTHERWISE SPECIFIED	PROJ ENGR	COMP ENGR	DATE	SIZE	CODE IDENT NO.
	N100-00000	N100-00000	TOLERANCES UNLESS OTHERWISE SPECIFIED: 2 PLACE DEC 3 PLACE DEC 2.00 2.010 ANGLES 30° 45° MACHINED 2° 15' FORMED 2° 30' SHEARED 2° 30' HOLE TOLERANCE PER ANSI B3.1 SURFACE ROUGHNESS PER MIL-STD-10 MACHINED SURFACE FINISH 125 DIMENSIONING AND TOLERANCING PER MIL-STD-10 ECCENTRICITY BETWEEN ANY DIAMS ON THE SAME CENTERLINE SHALL NOT EXCEED .010 TOTAL INDICATOR READING ALL DIMENSIONS IN INCHES UNLESS APPLIED FINISH WELD SYMBOLS PER MIL-STD-10 RIVET CODE PER NAS 313 THREADS PER MIL-STD-18 MARK PER MIL-STD-18 REMOVE ALL BURRS AND SHARP EDGES SPECIFICATIONS				D	11817
								N100-10000
							SCALE: 1/1	REV. B

LTV RESEARCH CENTER  
COMPONENT ASSY









4

3

2

1

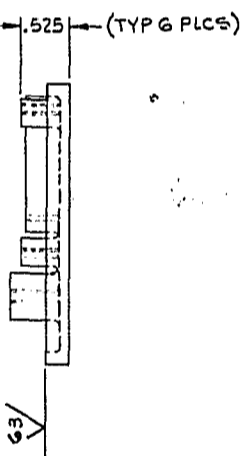
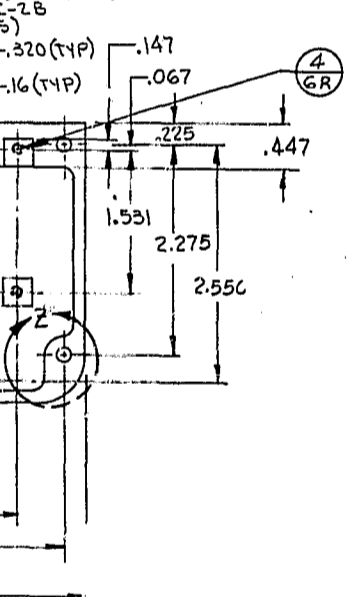
NOTES:  
 1. GLASS PEEN PER AERO SPEC 13-401  
 2. BLEACH ALODINE 12005 PER SPECVA9-18  
 3. INSTALL HELICOILS AFTER FINISH

ZONE		LTR	REVISIONS DESCRIPTION	DATE	APPROVED
	A		INCREASED HOLE DIA TO .800 (WAS .600.)	1/19/67 1/24/67	David G. [Signature] Chk. by [Signature]

.150 DIA THRU  
 CORE .285 DIA X .100 DP  
 5 HOLES



(.1700) X 2.62 DEEP



D  
C  
B  
A  
N100-10002

QUANTITY REQUIRED	ZONE	ITEM	CODE IDENT NO.	PART OR IDENTIFYING NO.	NOMENCLATURE OR DESCRIPTION	MATERIAL AND FINISH OR NOTE OR REF DES
	2	5		3585-06CN-0207	HELICOIL	NOTE 3
	6	4		3585-04CN-0224	HELICOIL	NOTE 3
		3				
		2				
	1	1		-01	COVER	7075-T6 AL NOTE 1 & 2

QTY PER MAJOR ASSY	NEXT ASSEMBLY	USED ON	UNLESS OTHERWISE SPECIFIED:	PROJECT	COMP ENGR	STRUCT	WTS	GROUP APP	CHECKED BY	DRAWN BY	ENGR GROUP	SIZE	CODE IDENT NO.	SCALE	REV.	DMST
-	N100-10000	N100-0000	TOLERANCES UNLESS OTHERWISE SPECIFIED: 2 PLACE DEC 3 PLACE DEC 1.92 2.918 ANGLES MACHINED FORMED SHEARED 2° 30' 2° 30' 5° 30' HOLE TOLERANCE PER AND HST SURFACE ROUGHNESS PER MIL-STD-19 MACHINED SURFACE FINISH DIMENSIONING AND TOLERANCING PER MIL-STD-19 ECCENTRICITY BETWEEN ANY DIA(S) ON THE SAME CENTRELINE SHALL NOT EXCEED .018 TOTAL INCL. LATOR READING ALL DIM. ARE IN INCHES UNLESS OTHERWISE APPLIED FINISH HELD SYMBOLS PER MIL-STD-19 RIVET CODE PER AS 21 THREADS PER MIL-STD-745 MARK PER MIL-STD-150 REMOVE ALL BURRS AND SHARP EDGES SPECIFICATIONS:									D	11817	1/1	A	
												N100-10002				

LTV RESEARCH CENTER

COVER - BOTTOM SPECTROMETER

LTVC 410

8

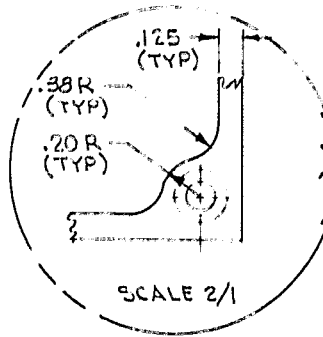
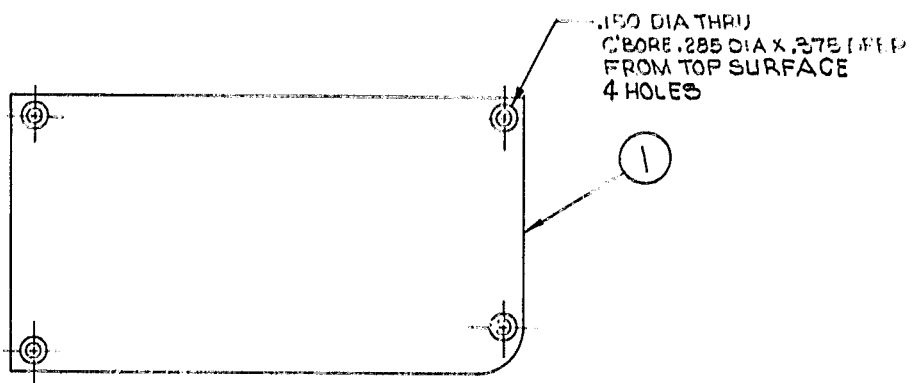
7

6

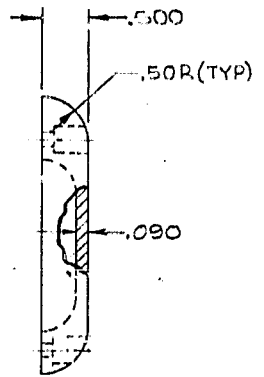
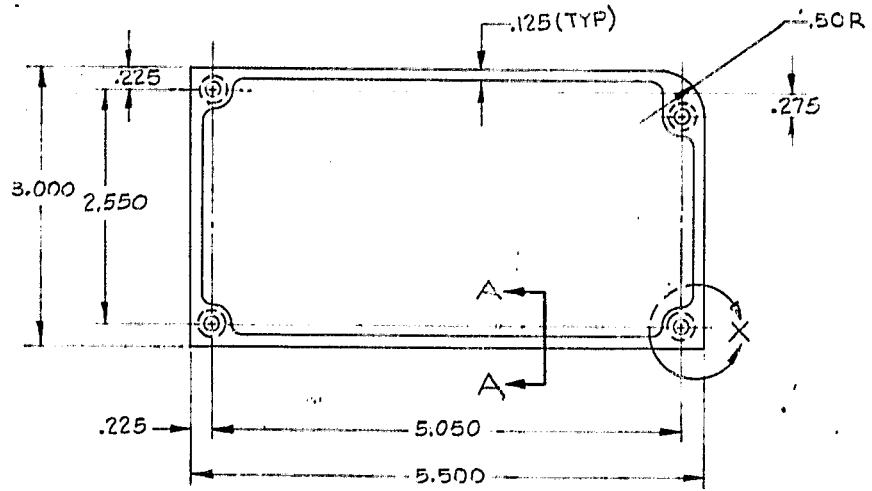
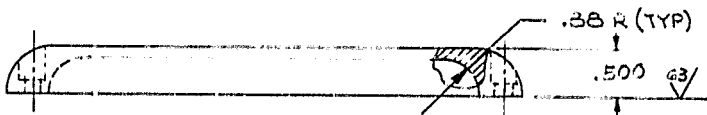
5

4

D



C



B

A

QTY PER MAJOR ASSY	NEXT ASSY
	N100-

1

4

3

2

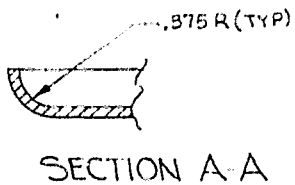
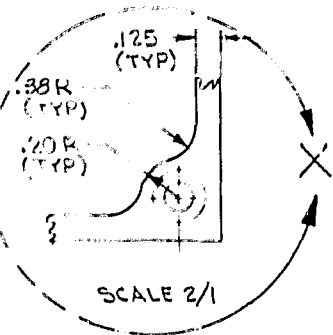
1

NOTES:  
 1. GLASS PEEN PER AERO SPEC 13-401  
 2. BLEACH ALODINE 1200S PER CVA9-18

ZONE	LTR

REVISIONS  
 DESCRIPTION

DATE APPROVED



D

C

B

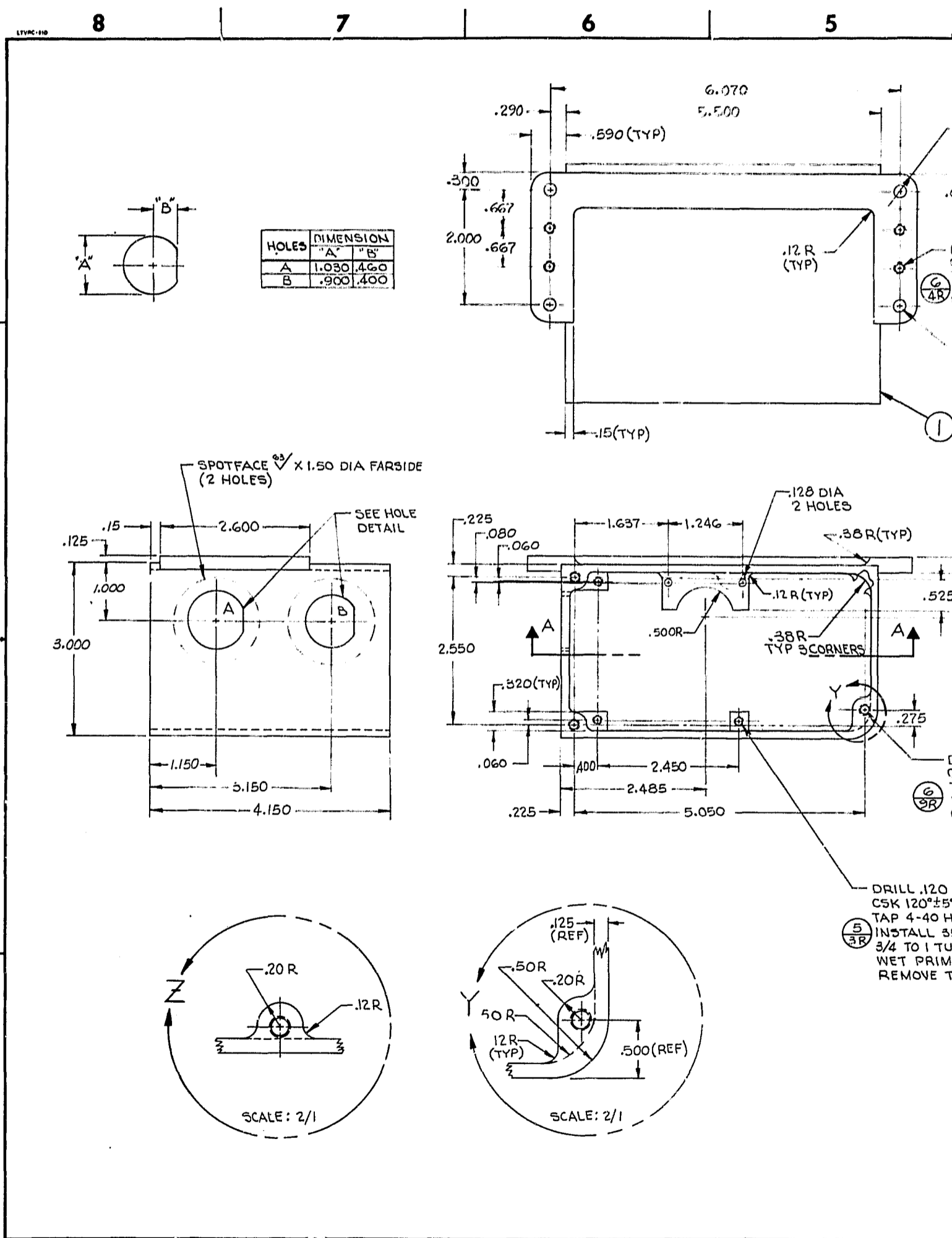
N100-1000

QUANTITY REQUIRED	ZONE	ITEM	CODE IDENT NO.	PART OR IDENTIFYING NO.	NOMENCLATURE OR DESCRIPTION	MATERIAL AND FINISH OR NOTE OR REF DES
	-01	1		-01	COVER	7075-T6 AL SEE NOTE 1 & 2

LIST OF MATERIAL OR PARTS LIST

QTY PER MAJOR ASSY	NEXT ASSEMBLY	USED ON	UNLESS OTHERWISE SPECIFIED		PROJ ENGR	LTV RESEARCH CENTER
	N100-00000	N100-00000	TOLERANCES ON: 2 PLACE DEC 3 PLACE DEC ANGLES MACHINED FORMED SHEARED HOLE TOLERANCE PER AND H87 SURFACE ROUGHNESS PER MIL-STD-18 DIMENSIONING AND TOLERANCING PER MIL-STD-8 ECCENTRICITY BETWEEN ANY DIA(S) ON THE SAME CENTERLINE SHALL NOT EXCEED .018 TOTAL INDICATOR READING ALL DIM. ARE IN INCHES INCLUDE APPLIED FINISH GOLD SYMBOLS PER MIL-STD-19 RIVET CODE PER NAS 113 THREADS PER MIL-S-7742 MARK PER MIL-STD-130 REMOVE ALL BURRS AND SHARP EDGES	COMP ENGR MACH ENGR STRUCT WTS GROUP APP CHECKED BY DRAWN BY ENGR GROUP		
						SIZE CODE IDENT NO. D 11817 N100-10003
						SCALE: VI REV. DWG

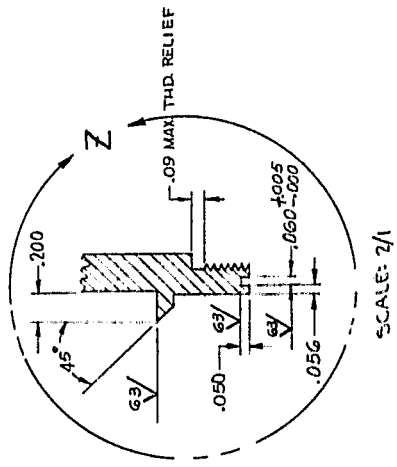
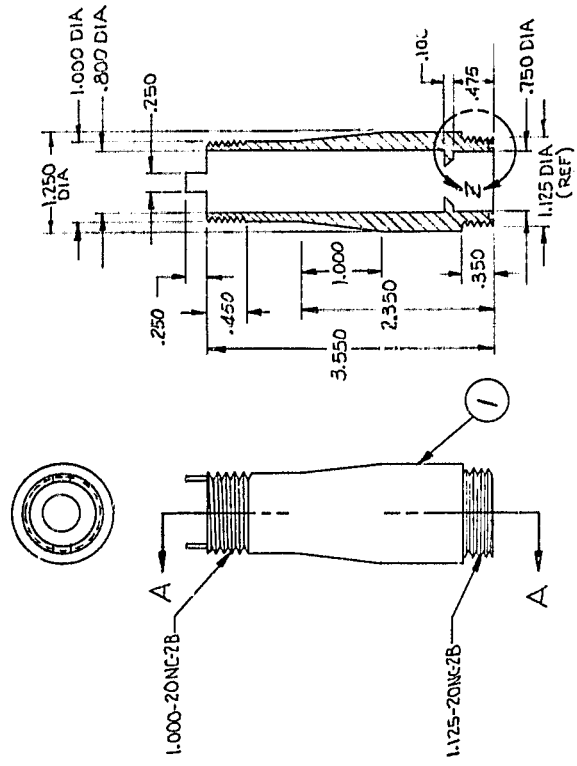
A





REVISED		DATE		APPROVED	
ZONE	LTR	DESCRIPTION	DATE	BY	DATE
A		INCORPORATED EO. 1100.2	1-3-67	8	1-3-67
			1/24/67	8	1-24-67

NOTES:  
1. MATL: TANTALUM; MAY BE PURCHASED FROM RYERSON STEEL, CHICAGO, ILL.



OTHER MADE BY		NEXT ASSEMBLY		USED ON		QUANTITY REQUIRED		ZONE		CODE		PART OR IDENTIFYING NO.		NOMENCLATURE OR DESCRIPTION		MATERIAL AND FINISH OR NOTE OR REF DES		
		N100-1000.1		N100-00000														
LIST OF MATERIAL OR PARTS LIST																		
LTPV RESEARCH CENTER																		
SHIELD DETECTOR ASSEMBLY																		
SCALE: FULL REV. A																		
C 11817 N100-10005																		







4	3	2	1
REVISIONS ZONE LTR DESCRIPTION DATE APPROVED			
NOTES: 1. BLEACH ALODINE 1200S PER SPEC CVA9-18			
80001-001N			
D		C	
B		A	

QUANTITY REQUIRED	2	1	CODE	IDENT NO.	IDENTIFYING NO.	PART OR DESCRIPTION	NOMENCLATURE OR REF DES	7075-T6 AL	NOTE 1
LIST OF MATERIAL OR PARTS LIST									
UNLESS OTHERWISE SPECIFIED 1. ALL DIMENSIONS ARE IN INCHES 2. ALL DIMENSIONS ARE TO BE TAKEN TO THE CENTERLINE UNLESS OTHERWISE SPECIFIED 3. ALL DIMENSIONS ARE TO BE TAKEN TO THE SURFACE UNLESS OTHERWISE SPECIFIED 4. ALL DIMENSIONS ARE TO BE TAKEN TO THE CENTERLINE UNLESS OTHERWISE SPECIFIED 5. ALL DIMENSIONS ARE TO BE TAKEN TO THE SURFACE UNLESS OTHERWISE SPECIFIED 6. ALL DIMENSIONS ARE TO BE TAKEN TO THE CENTERLINE UNLESS OTHERWISE SPECIFIED 7. ALL DIMENSIONS ARE TO BE TAKEN TO THE SURFACE UNLESS OTHERWISE SPECIFIED 8. ALL DIMENSIONS ARE TO BE TAKEN TO THE CENTERLINE UNLESS OTHERWISE SPECIFIED 9. ALL DIMENSIONS ARE TO BE TAKEN TO THE SURFACE UNLESS OTHERWISE SPECIFIED 10. ALL DIMENSIONS ARE TO BE TAKEN TO THE CENTERLINE UNLESS OTHERWISE SPECIFIED									
DTYPER	HEAT ASSEMBLY	USED ON							
MAJOR	N100 - 10001	N100 - 11000							
LTV RESEARCH CENTER SPACER, COLLIMATOR DETECTOR ASSY									
								SIZE	C 11817
								CONTRACT NO.	N100-10008
								SCALE	2/1
								DATE	

LTARC-81D

8

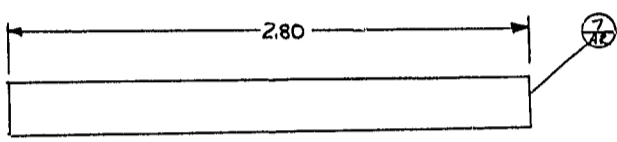
7

6

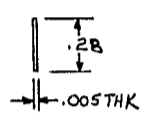
5

4

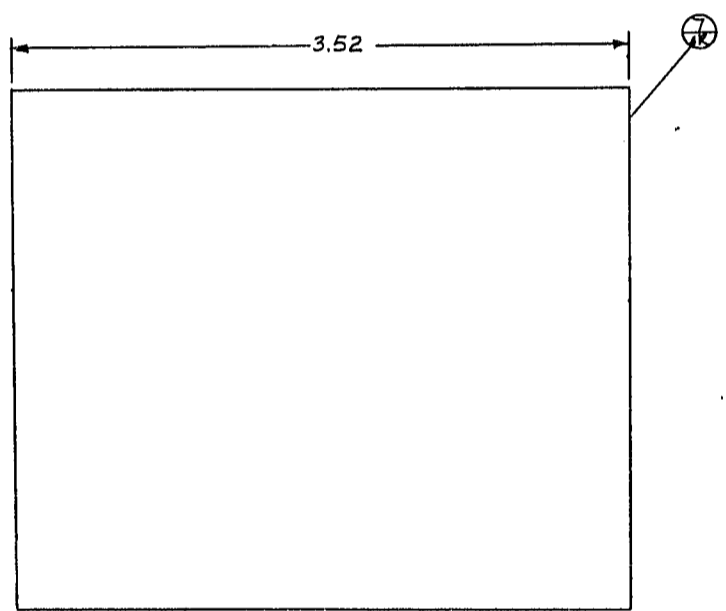
D



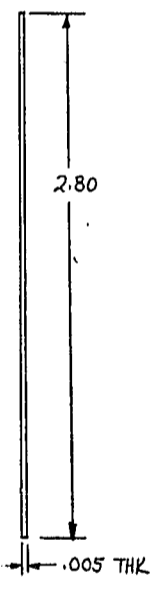
-01 SPACER



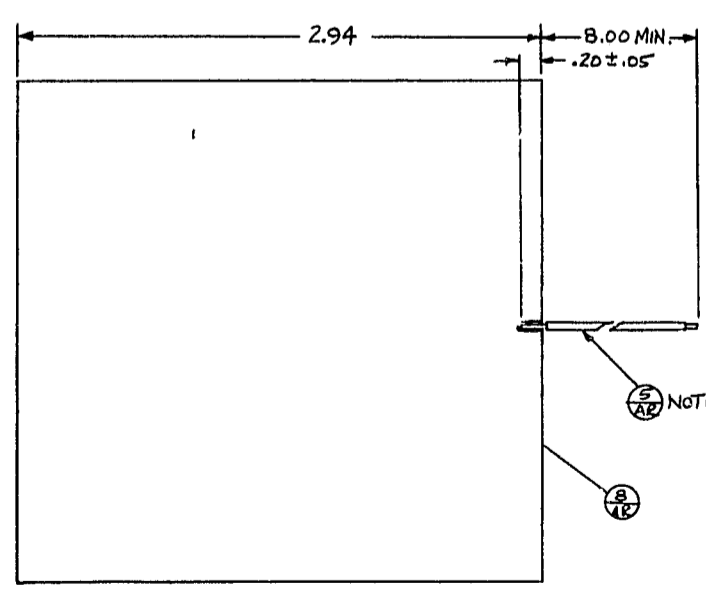
C



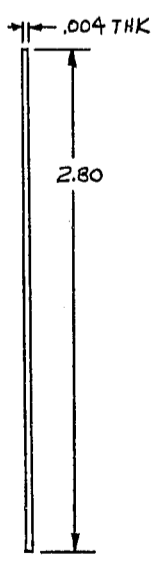
-02 INSULATOR



B



-03 SHIELD



A

NOTE 3

QTY PER MAJOR ASSY	NEXT ASSEMBLY
	N100-100

4

3

2

1

NOTES:  
 1. PERFECTION MICA CO., CHICAGO, ILL.  
 2. C.P. WAGGONER SALES CO., GRAND PRAIRIE, TEXAS.  
 3. SOLDER WIRE TO CO-NETIC. MAKE AS FLAT AS POSSIBLE.

ZONE		LTR	REVISIONS		
			DESCRIPTION	DATE	APPROVED

D

C

B

N100-10010

QUANTITY REQUIRED	-03	-02	-01	ZONE	ITEM	CODE IDENT NO.	PART OR IDENTIFYING NO.	NOMENCLATURE OR DESCRIPTION	MATERIAL AND FINISH OR NOTE OR REF DES.
					8		.004 THK-SHT.	CO-NETIC -	NOTE 1
					7		.005 THK X 4 IN.	TAPE - CLEAR,	NON-ADHESIVE, NOTE 2
					6				
					5		E26-BLK	WIRE	MIL-W-16878
					4				
					3		- 03	SHIELD	
					2		- 02	INSULATOR	
					1		- 01	SPACER	

LIST OF MATERIAL OR PARTS LIST

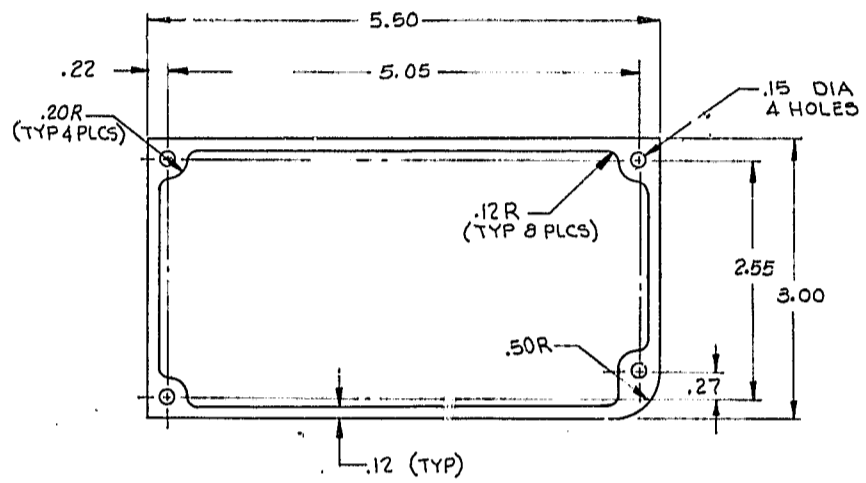
QTY PER MAJOR ASSY	NEXT ASSEMBLY	USED ON	UNLESS OTHERWISE SPECIFIED	PROJ ENGR	LTV RESEARCH CENTER	
	N100-10001	N100-00000	TOLERANCES UNLESS OTHERWISE SPECIFIED: 2 PLACE DEC 3 PLACE DEC ANGLES MACHINED 1/16" FORMED 1/32" SHEARED 1/32" HOLE TOLERANCE PER AND 1017 SURFACE ROUGHNESS PER MIL-STD-10 MACHINED SURFACE FINISH DIMENSIONING AND TOLERANCING PER MIL-STD-10 ECCENTRICITY BETWEEN ANY DIA(S) ON THE SAME CENTERLINE SHALL NOT EXCEED .010 TOTAL INDICATOR READING ALL DIM. AND DIMENSIONS INCLUDE APPLIED FINISH WELD SYMBOLS PER MIL-STD-10 RIVET CODE PER MIL-STD-10 THREADS PER MIL-STD-10 MARK PER MIL-STD-10 REMOVE ALL BURRS AND SHARP EDGES SPECIFICATIONS:	COMP ENGR		DETAILS MYLAR & CO-NETIC
				GROUP APP	SIZE	
				CHECKED BY	D	11817
				DRAWN BY	N100-10010	
				ENGR GROUP	SCALE: 2/1	REV.
					SHEET	

A

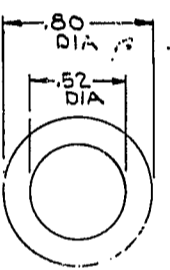
LTVC-110

8 7 6 5 4

D

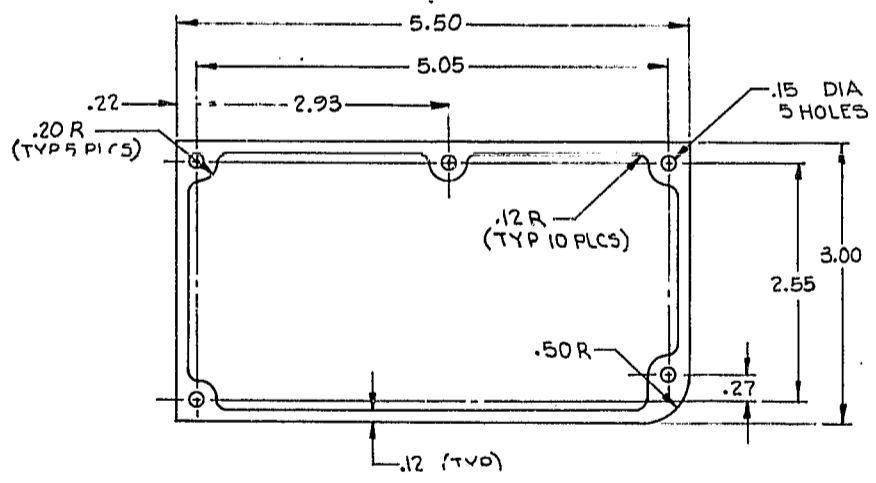


-01 GASKET  
SCALE: 1/1



-03 GASKET  
SCALE: 2/1

C



-02 GASKET  
SCALE: 1/1

B

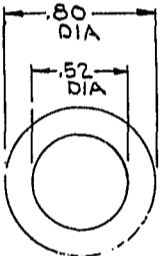
A

QTY PER MAJOR ASSY *	NEXT
-01	N100-
-02	N100-
-03	N100-
-04	N100-

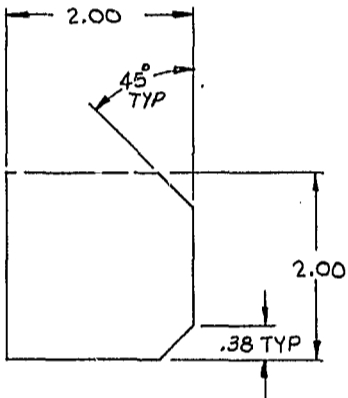
4 3 2 1

ZONE		LTR	REVISIONS	DATE	APPROVED
DESCRIPTION					

D  
C  
B  
N100-10015



-03 GASKET  
SCALE: 2/1



-04 GASKET  
SCALE: 1/1

QUANTITY REQUIRED	ZONE	ITEM	CODE IDENT NO.	PART OR IDENTIFYING NO.	NOMENCLATURE OR DESCRIPTION	MATERIAL AND FINISH OR NOTE OR REF DES.
	4			-04	GASKET	.063 THK SILICONE RUBBER
	3			-03	GASKET	.032 THK SILICONE RUBBER
	2			-02	GASKET	.063 THK SILICONE RUBBER
	1			-01	GASKET	.063 THK SILICONE RUBBER

QTY PER MAJOR ASSY	NEXT ASSEMBLY	USED ON	UNLESS OTHERWISE SPECIFIED	PROJ ENGR	COMP ENGR	DATE	SCALE	NOTED	REV.	SHEET
-01	N100-00000	N100-00000	TOLERANCES ON: 2 PLACE DEC 3 PLACE DEC 2.00 2.010							
-02	N100-10000	N100-00000	ANGLES MACHINED 2° 15' FORMED 2° SHEARED 2° 30'							
-03	N100-10001	N100-00000	HOLE TOLERANCE PER AND M197 SURFACE ROUGHNESS PER MIL-STD-19 MACHINED SURFACE FINISH							
-04	N100-0000	N100-00000	DIMENSIONING AND TOLERANCING PER MIL-STD-19 ECCENTRICITY BETWEEN ANY DIAM(S) ON THE SAME CENTERLINE SHALL NOT EXCEED .010 TOTAL INDICATOR READING ALL DIM. ARE IN INCHES UNLESS OTHERWISE SPECIFIED HOLE SYMBOLS PER MIL-STD-19 W/LET CODE PER NAS 832 THREADS PER MIL-STD-19 FINISH PER MIL-STD-19 REMOVE ALL BURRS AND SHARP EDGES MATERIAL SPECIFICATIONS							
				<b>LTV RESEARCH CENTER</b> <b>GASKETS</b>						
				CODE IDENT NO. <b>11817</b>		<b>N100-10015</b>				

LTVC-410

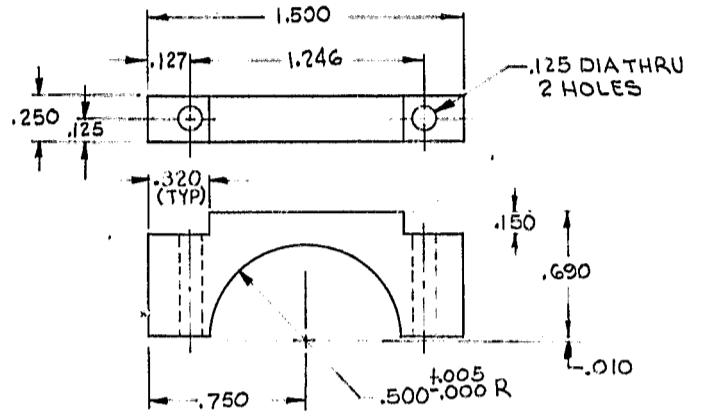
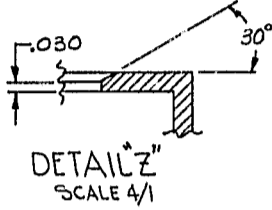
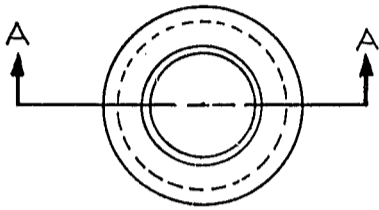
8

7

6

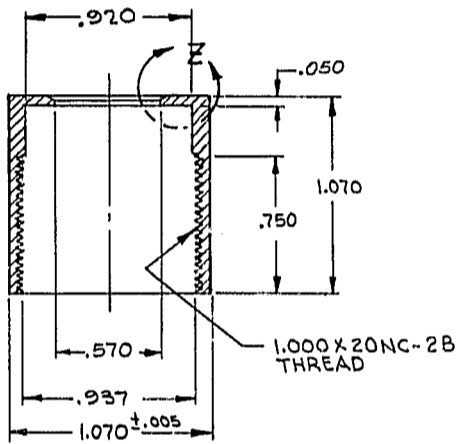
5

D

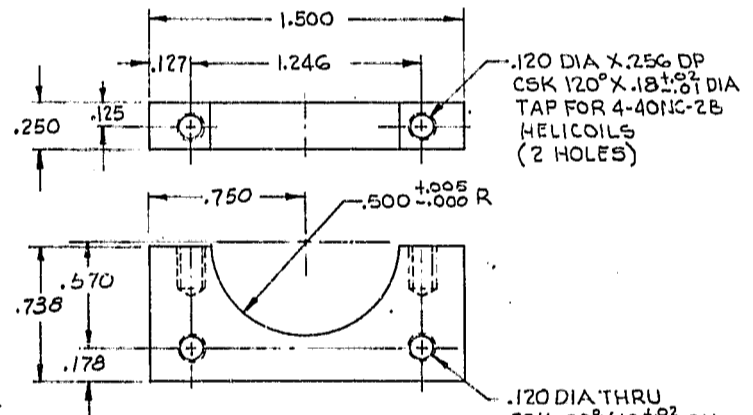


DETAIL -04  
SCALE 2/1

C

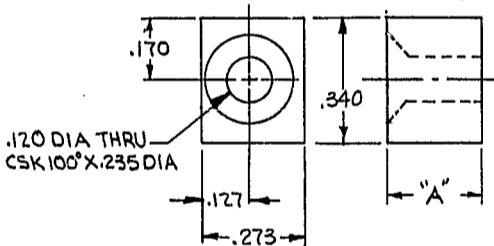


DETAIL -01  
SCALE 2/1



DETAIL -05  
SCALE 2/1

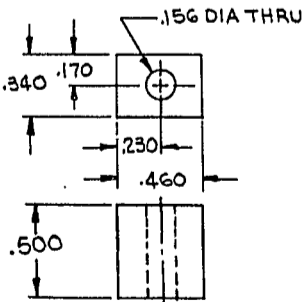
B



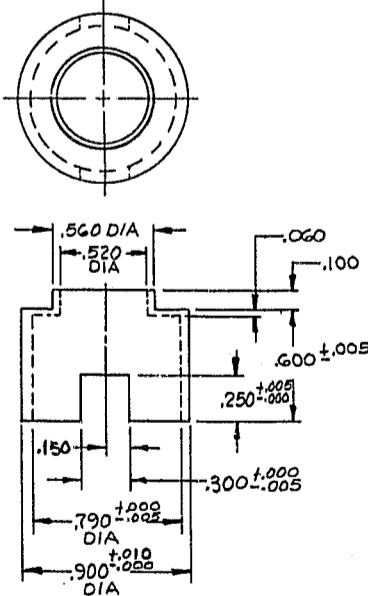
DETAIL -02 & -03  
SCALE: 4/1

DASH NO.	"A" DIM
-02	.208
-03	.190

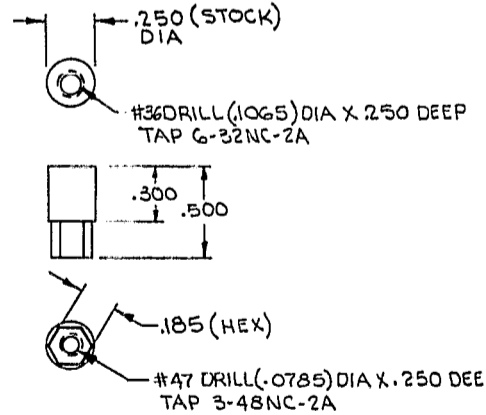
A



DETAIL -06  
SCALE 2/1  
2 REQD



DETAIL -07  
SCALE: 2/1



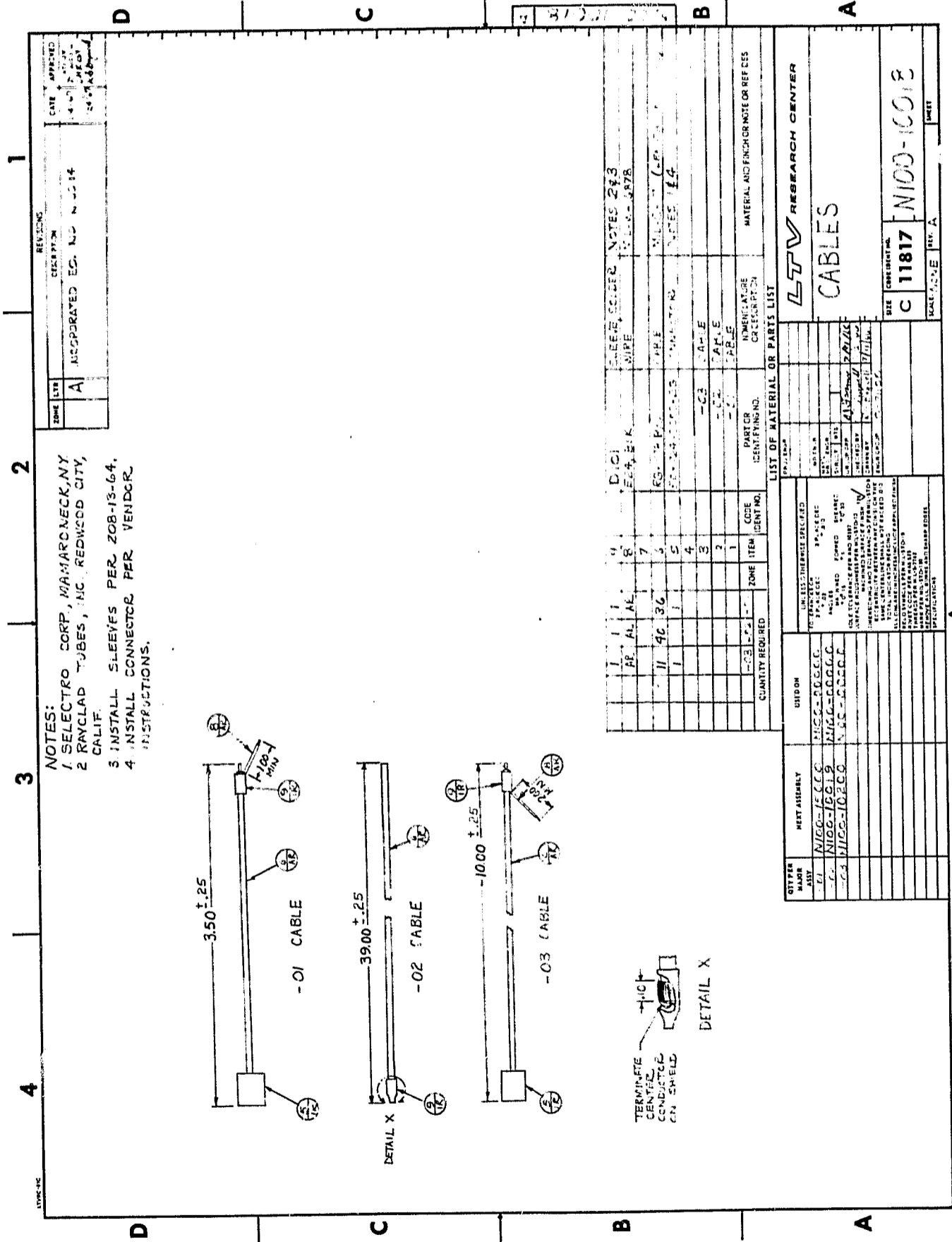
DETAIL -08  
SCALE: 2/1

QTY PER MAJOR ASSY	
-01	NI
-02	NI
-03	NI
-04	NI
-05	NI
-06	NI
-07	NI
-08	NI
-09	NI









NOTES:  
 1. SELECTRO CORP, MAMARONECK, NY  
 2. RAYCLAD TUBES, INC. REDWOOD CITY, CALIF.  
 3. INSTALL SLEEVES PER ZOB-13-64.  
 4. INSTALL CONNECTOR PER VENDOR INSTRUCTIONS.

ZONE LTR	REVISED	DATE
A	INCORPORATED EC. NO. N-0014	4-27-64

QTY	REMARKS	UNIT	ZONE	ITEM	CODE	IDENTIFYING NO.	PART OR DESCRIPTION	NUMERICAL OR REFERENCE	MATERIAL AND FINISH OR NOTE OR REF DES
1	RE-AL		1	1			DIOL		
1	AL		1	2			WIRE		
1	36		1	3			RG-58		
1	1		1	4			CONNECTOR		
1	1		1	5			SLIP		
1	1		1	6			SLIP		
1	1		1	7			SLIP		
1	1		1	8			SLIP		
1	1		1	9			SLIP		
1	1		1	10			SLIP		

QTY	REMARKS	UNIT	ZONE	ITEM	CODE	IDENTIFYING NO.	PART OR DESCRIPTION	NUMERICAL OR REFERENCE	MATERIAL AND FINISH OR NOTE OR REF DES
1	RE-AL		1	1			DIOL		
1	AL		1	2			WIRE		
1	36		1	3			RG-58		
1	1		1	4			CONNECTOR		
1	1		1	5			SLIP		
1	1		1	6			SLIP		
1	1		1	7			SLIP		
1	1		1	8			SLIP		
1	1		1	9			SLIP		
1	1		1	10			SLIP		

QTY	REMARKS	UNIT	ZONE	ITEM	CODE	IDENTIFYING NO.	PART OR DESCRIPTION	NUMERICAL OR REFERENCE	MATERIAL AND FINISH OR NOTE OR REF DES
1	RE-AL		1	1			DIOL		
1	AL		1	2			WIRE		
1	36		1	3			RG-58		
1	1		1	4			CONNECTOR		
1	1		1	5			SLIP		
1	1		1	6			SLIP		
1	1		1	7			SLIP		
1	1		1	8			SLIP		
1	1		1	9			SLIP		
1	1		1	10			SLIP		

LTV RESEARCH CENTER	
CABLES	
SIZE	C 11817 N100-10018
SCALE	1:1
REV.	A
SHEET	











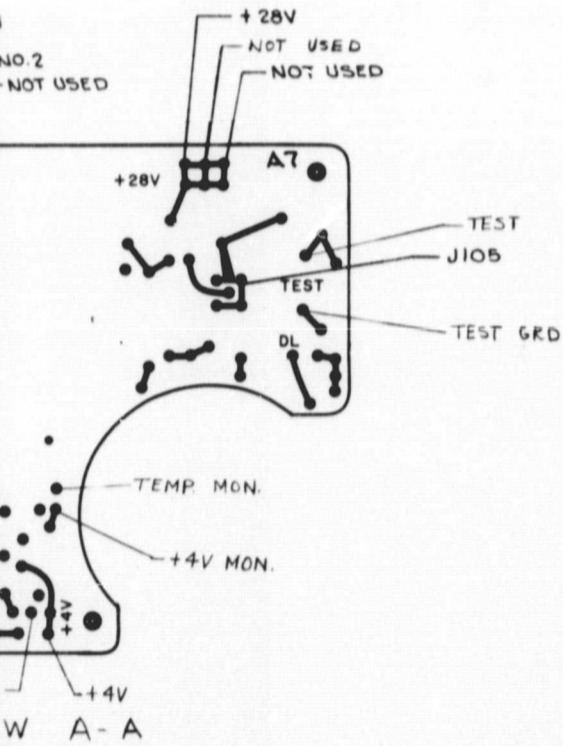
4

3

2

1

ZONE		REVISIONS		DATE	APPROVED
LTR	DESCRIPTION				
A	ADDED ITEM 19			1-24-67	EDWARD GLENN
				1/24/67	CHK BY R. B. Boyd



D  
C  
B  
A  
N100-10200

QUANTITY REQUIRED	ZONE	ITEM	CODE IDENT NO.	PART OR IDENTIFYING NO.	NOMENCLATURE OR DESCRIPTION	MATERIAL AND FINISH OR NOTE OR REF DES
		2		SEE SHT 1		

QTY PER MAJOR ASSY	NEXT ASSEMBLY	USED ON	UNLESS OTHERWISE SPECIFIED	PROJ ENGR	COMP ENGR	WATER PROOF ENGR	STRUCT WTS	GROUP APP	CHECKED BY	DRAWN BY	ENGR GROUP	SIZE	CODE IDENT NO.	SCALE	REV.	SHEET	
			TOLERANCES UNLESS OTHERWISE SPECIFIED: 2 PLACE DEC 1 PLACE DEC .00 .01 ANGLES MACHINED FORMED SHEARED 1/2° 1° 1/2° HOLE TOLERANCES PER ANSI 1927 SURFACE ROUGHNESS PER MIL-STD-15 MACHINED SURFACE FINISH DIMENSIONING AND TOLERANCING PER MIL-STD-15 ECCENTRICITY BETWEEN ANY DIAMS ON THE SAME CENTERLINE SHALL NOT EXCEED .010 TOTAL INDICATOR READING ALL DIM. ARE IN INCHES UNLESS APPLIED FINISH WELD SYMBOLS PER MIL-STD-15 RIVET CODE PER NAS 322 THREADS PER MIL-STD-15 MARK PER MIL-STD-15 REMOVE ALL BURRS AND SHARP EDGES SPECIFICATIONS										D	11817	NONE	A	2 OF 2

**LTV RESEARCH CENTER**

**HARNESS, WIRING**

SIZE: D CODE IDENT NO.: 11817 N100-10200

SCALE: NONE REV.: A SHEET: 2 OF 2











8

7

6

5

4

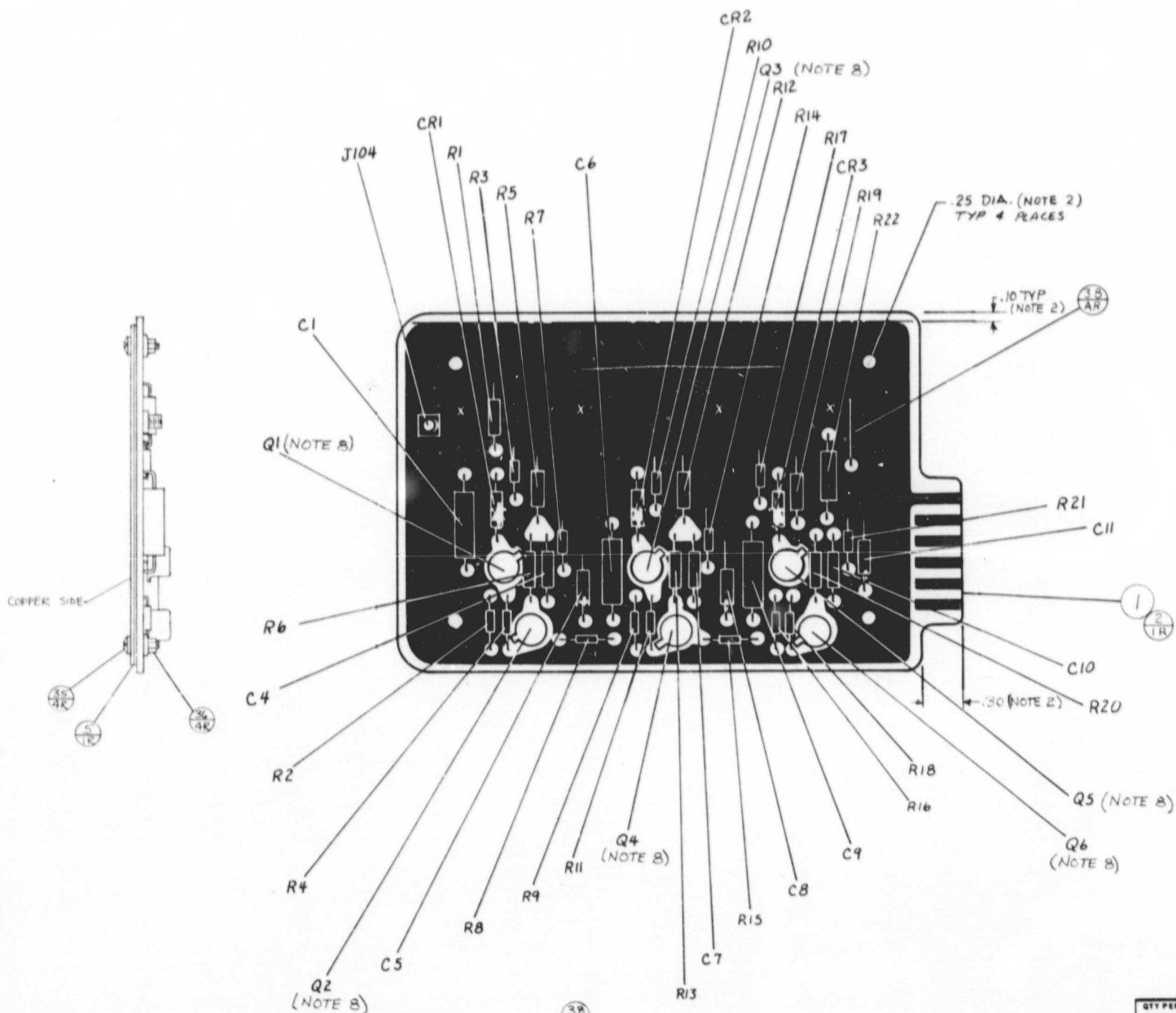
D


C

B

A

COPPER SIDE



  
 X - DENOTES INTERFACIAL CONNECTION

QTY PER MAJOR ASSY	NEXT ASSEMBLY
	N100-0000



8

7

6

5

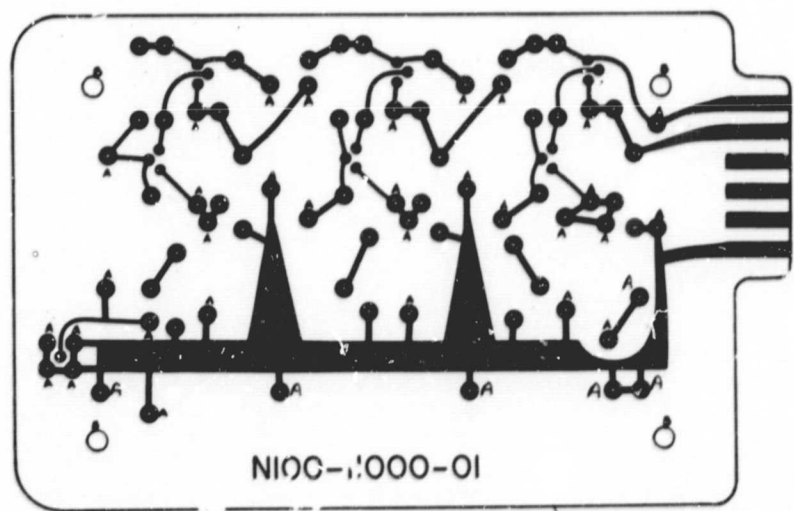
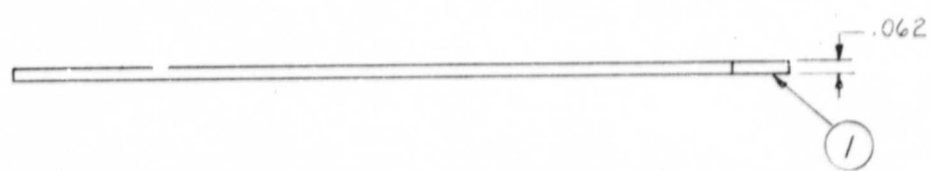
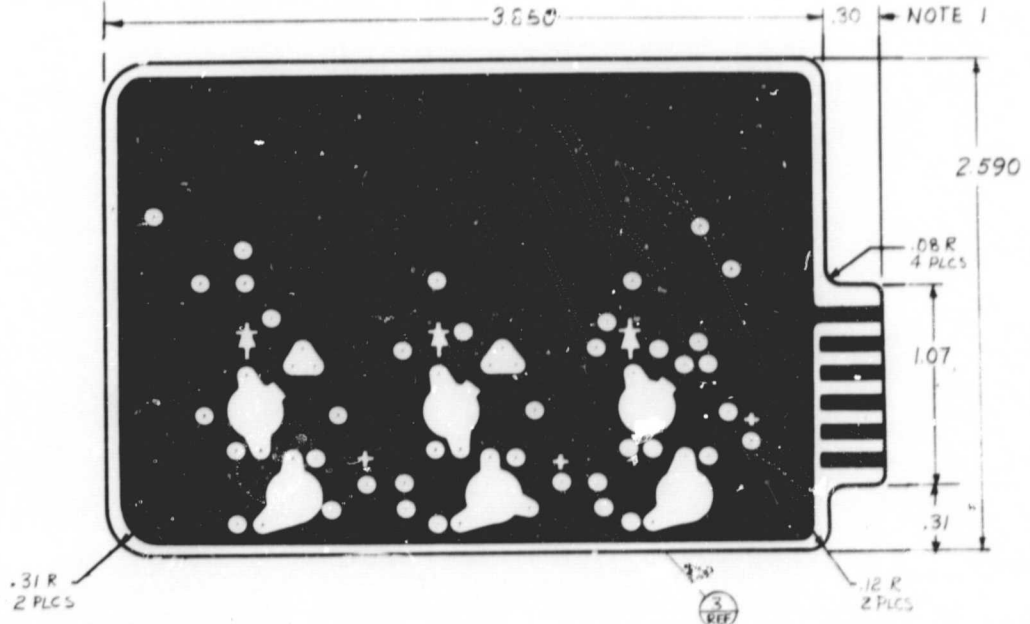
4

D

C

B

A

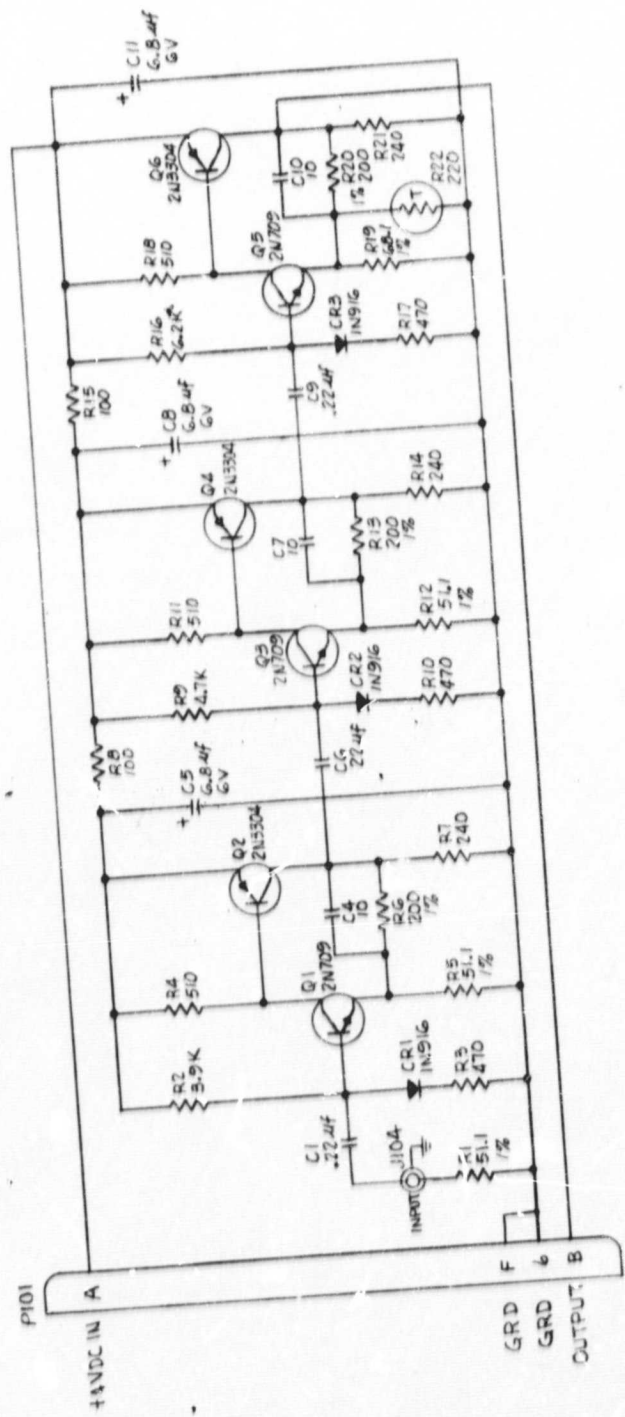


CODE	HOLE SIZE (INCHES)
NO CODE	.025 DIA.
A	.031 DIA.
B	.128 DIA.

QTY PER MAJOR ASSY	HEAT ASSEMBLY
	NI00-1100



REVISIONS		DATE	APPROVED
4	A	5-11-64	J.F.C.
DESCRIPTION		REVISED P.W. LOCATION OF PI01	



1. UNLESS OTHERWISE SPECIFIED:  
 ALL RESISTANCES ARE IN OHMS, 1/8 W, 5%  
 ALL CAPACITANCES ARE IN PF  
 NOTES:

ZONE	ITEM	QUANTITY REQUIRED	CODE	IDENTIFYING NO.	NOMENCLATURE OR DESCRIPTION	MATERIAL AND FINISH OR NOTE OR REF DES
1	1					
2	2					
3	3					
4	4					

LIST OF MATERIAL OR PARTS LIST

USED ON: N100-11900

NET ASSEMBLY: N100-11900

NET PARTS: N100-11900

DATE: 5-11-64

BY: J.F.C.

SCALE: 1:1

SIZE: C 11817

WORK CENTER NO.: N100-11900

WORK CENTER: A

WORK CENTER: A

LTV RESEARCH CENTER  
 SCHEMATIC  
 HIGH SPEED AMPL  
 AI

00611-001N









4

3

2

1

NOTES:  
 1. RHODIUM PLATE CONNECTOR AREA PER MIL-STD-275.  
 2. FABRICATE AND SOLDER PLATE PER MSFC-STD-154.

ZONE		LTR	REVISIONS	DATE	APPROVED
		A	INCREASED HOLE SIZE TO .031 11 PLACES. (WAS .025)	7/18/66	DWG BY P.G. Bignell CHK BY H. FORTNEY APP BY P.J. Janner

MENT SIDE)

HOLE SIZE (INCHES)
.025 DIA.
.031 DIA.

C  
 B  
 A  
 N100-12001 A B

QUANTITY REQUIRED	ZONE	ITEM	CODE IDENT NO.	PART OR IDENTIFYING NO.	NOMENCLATURE OR DESCRIPTION	MATERIAL AND FINISH OR NOTE OR REF DES
		REF	3		N100-12006-01 ARTWORK	
		REF	2		N100-12005-01 ARTWORK	
		-01	1		-01 BOARD	.062 THK-2/20Z. MIL-P-13949 GEF.

LIST OF MATERIAL OR PARTS LIST

QTY PER MAJOR ASSY	NET ASSEMBLY	USED ON	UNLESS OTHERWISE SPECIFIED	PROJ ENGR	COMP ENGR	WELDR	PROCESSOR	STRUCT	WTS	GROUP APP	CHECKED BY	DRAWN BY	ENGR GROUP	SIZE	CODE IDENT NO.	SCALE	REV.	DATE	
	N100-12000	N100-00000	2 PLACE DEC 1.01 3 PLACE DEC 1.010 1 INCHES 1" 0' MACHINED 1/8" FORMED 1/8" SHEARED 1/8" HOLE TOLERANCE PER AMS 1913T SURFACE ROUGHNESS PER MIL-STD-15 DIMENSIONING AND TOLERANCING PER MIL-STD-15 ECCENTRICITY BETWEEN ANY QUER IN THE SAME CENTERLINE SHALL NOT EXCEED .015 TOTAL INDICATOR READING ALL DIM. PER IN INCHES INCLUDE APPLIED FINISH WELD SYMBOLS PER MIL-STD-15 RIVET CODE PER NAS 353 THREADS PER MIL-STD-15 MARK PER MIL-STD-15 FINISHES, ALL SURFS AND SHARP EDGES SPECIFICATIONS												D	11817	2/1	A	
															N100-12001				











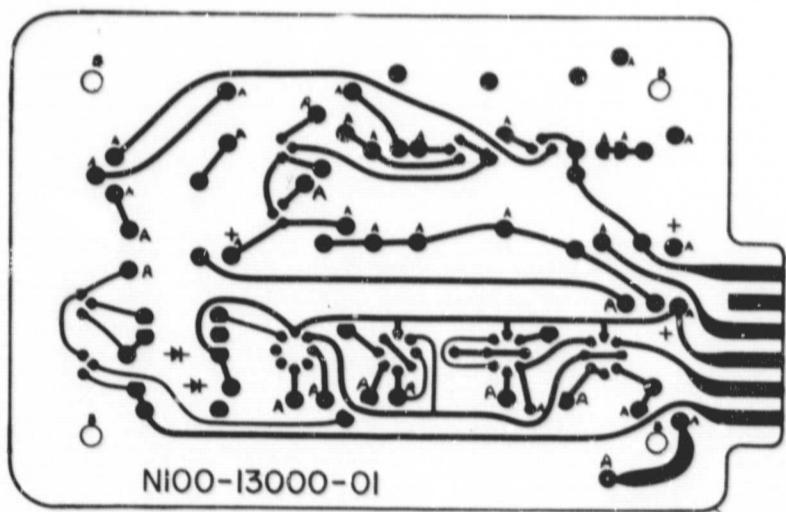
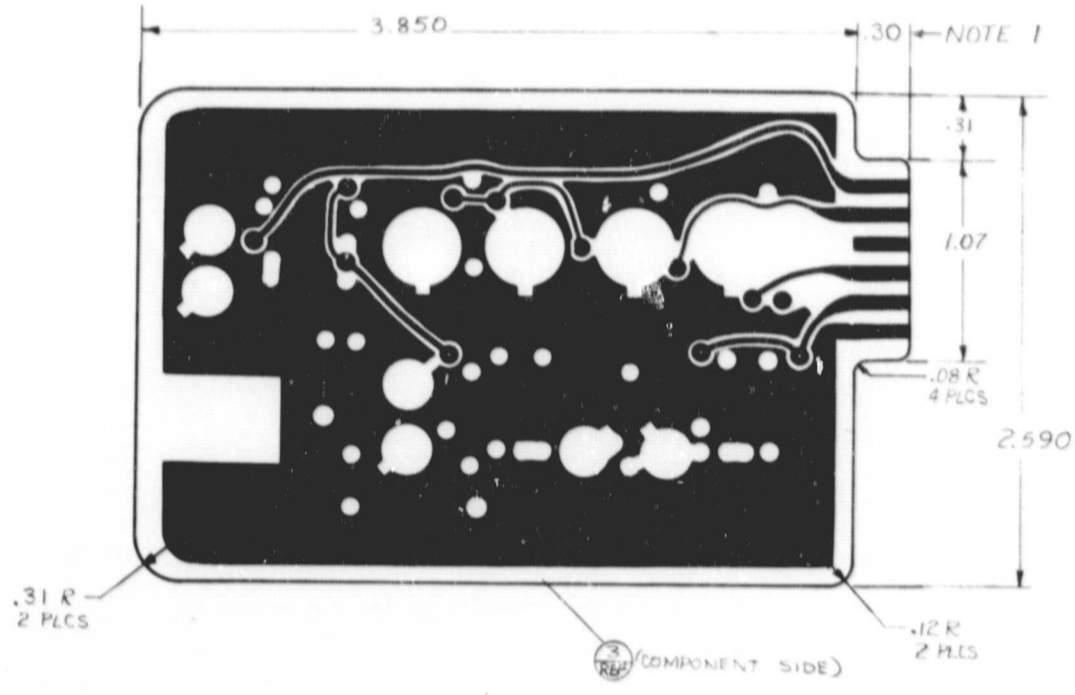
8 | 7 | 6 | 5

D

C

B

A



(2) REF (CIRCUIT SIDE)

CODE	HOLE SIZE (INCHES)
M CODE	.025 DIA.
A	.031 DIA.
B	.128 DIA.

QTY PER MAJOR ASSY	
	N/A

4

3

2

1

NOTES:  
 1. RHODIUM PLATE CONNECTOR AREA PER MIL-STD-275.  
 2. FABRICATE AND SOLDER COAT PER MSFC-STD-154.

ZONE		LTR	DESCRIPTION	DATE	APPROVED
A			1. INCREASED HOLE SIZE TO .031 12 PLS. (WAS .025) 2. CHANGED VIEW OF "B" SIZE HOLES	7/12/64 10/2/66 7/12/64	DWG BY R.C. Bagwell CHK BY U. FOREST APP. BY R.C. Bagwell

D

C

B

A

N/00-13001

CODE	HOLE SIZE (INCHES)
CODE	.025 DIA.
A	.031 DIA.
B	.128 DIA.

QUANTITY REQUIRED	ZONE	ITEM	CODE IDENT NO.	PART OR IDENTIFYING NO.	NOMENCLATURE OR DESCRIPTION	MATERIAL AND FINISH OR NOTE OR REF DES
		REF	3	N100-13006-01	ARTWORK	
		REF	2	N100-13005-01	ARTWORK	
			1	-01	BOARD	.062 THK-2/20Z, MIL-P-13949 GEE

LIST OF MATERIAL OR PARTS LIST

QTY PER MAJOR ASSY	NEXT ASSEMBLY	USED ON	UNLESS OTHERWISE SPECIFIED	PROJ ENGR	COMP ENGR	DATE	SCALE	REV.	SHEET
	N100-13000	N100-00000	TOLERANCES UNLESS OTHERWISE SPECIFIED: 2 PLACE DEC 3 PLACE DEC .02 .010 ANGLES MACHINED FORMED SHEARED ±.015 ±.015 ±.015 HOLE TOLERANCE PER AND HSBY SURFACE ROUGHNESS PER MIL-STD-10 MACHINED SURFACE FINISH DIMENSIONS AND TOLERANCING PER MIL-STD-883 ECCENTRICITY BETWEEN ANY DIAS (ON THE SAME CENTERLINE SHALL NOT EXCEED .010) TOTAL INDICATOR READING ALL DIM. ARE IN INCHES UNLESS OTHERWISE SPECIFIED WELD SYMBOLS PER MIL-STD-10 RIVET CODE PER MIL-STD-10 THREADS PER MIL-STD-10 MARKS PER MIL-STD-10 REMOVE ALL SHARP EDGES SPECIFICATIONS:						
			<b>LTV RESEARCH CENTER</b> <b>BOARD</b> <b>LOGIC &amp; LINEAR AMPL</b> <b>A4 &amp; A5</b>						
			CHECKED BY DRAWN BY ENGR GROUP		8-7100		SIZE CODE IDENT NO. <b>D 11817</b>		<b>N100-13001</b>
							SCALE: 2/1		REV. A

A











4

3

1

NOTES:

- 1. SOLDER & ASSEMBLE PER NPC 200-4
- 2. MOTOROLA INC., PHOENIX, ARIZONA
- 3. BOURNS INC., RIVERSIDE, CALIF.
- 4. MOUNT BOTTOM OF TRANSISTORS .02±.03 FROM BOARD.
- 5. SELECTED COMPONENT

REVISIONS		
DESCRIPTION	DATE	APPROVED
DATE NO. N100.5	1-1-67	APPROVED BY C.R. BROWN
	1/29/67	APPROVED BY R.B. BROWN

D

C

QTY PER MAJOR ASSY	ZONE	ITEM	CODE IDENT NO.	PART OR IDENTIFYING NO.	NOMENCLATURE OR DESCRIPTION	MATERIAL AND FINISH OR NOTE OR REF DES
	AR	27		24 AWG, SOFT, TIN/50 WIRE, BARE	QQ-W-343, TYPE 5	
1		26		1N751 A	DIODE JEDEC	CR3
1		25		1N754 A	DIODE JEDEC	CR1
		24				
1		23		2N3947	TRANSISTOR JEDEC	Q4
1		22		2N2913	TRANSISTOR JEDEC	Q2
1		21		2N3811	TRANSISTOR NOTE 2	Q1
		20				
1		19		8005-000-0060-270K	CAPACITOR	C3
1		18		8005-000-W5R0-221K	CAPACITOR	C2
		17				
1		16		3R80W-1-502	POTENTIOMETER NOTE 3	R2
1		15				
1		14		RN55D-5112 F	RESISTOR MIL-R-10509, NOTE 5	R1
		13				
1		12		RN55D 5112 F	RESISTOR MIL-R-10509	R10
2		11		RN55D 1213 F	RESISTOR MIL-R-10509	R3, R11
		10				
1		9		RC056F 221J	RESISTOR MIL-R-11	R9
1		8		622J		R14
2		7		103J		R6, R7
1		6		204J		R5
2		5		RC056F 105J	RESISTOR MIL-R-11	R4, R8
		4				
	REF	3		N100-14900	SCHEMATIC	
1		2		N100-14003-01	BOARD	
		1		-01	BOARD ASSY	

N100-14001

A

LIST OF MATERIAL OR PARTS LIST

QTY PER MAJOR ASSY	NEXT ASSEMBLY	USED ON	PROJ ENGR	LTV RESEARCH CENTER	
	N100-14000	N100-00000	COMP ENGR	COMP BD ASSY	
			DRY ENGR	LOW VOLTAGE PWR SUPPLY	
			STRUCT	TOP BOARD	
			GROUP APP	SIZE	CODE IDENT NO.
			CHECKED BY	D	11817
			DRAWN BY	N100-14001	
			ENGR GROUP	SCALE: 2/1	REV. A
				SHEET	

A



8

7

6

5

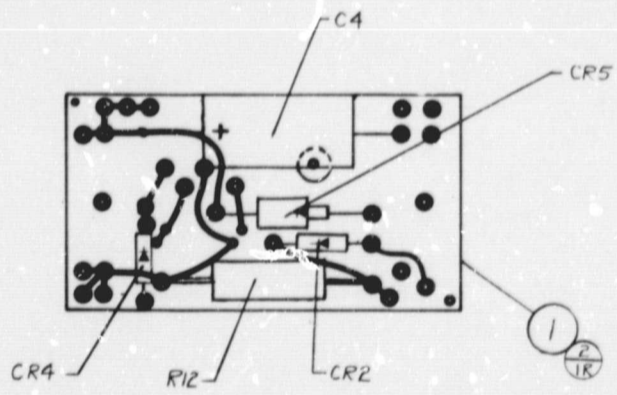
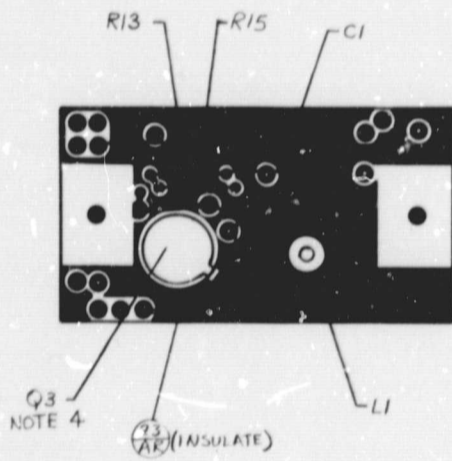
4

D

C

B

A



QTY PER MAJOR ASSY	HEX
	N100

1

4

3

2

1

NOTES:  
 1. SOLDER & ASSEMBLE PER NPC200-4  
 2. MOTOROLA INC., PHOENIX, ARIZONA  
 3. TOROTEL INC., KANSAS CITY, MO.  
 4. MOUNT BOTTOM OF TRANSISTORS  
 .02±.03 FROM BOARD.  
 5. FAIRCHILD SEMICONDUCTOR INC. SAN RAFAEL  
 CALIFORNIA.

REVISIONS				
ZONE	LTR	DESCRIPTION	DATE	APPROVED
A		INCORPORATED EO. NO. N100.6 N100.10	1-3-67 1/24/67	Lowell CHE 87 Kob. Braggitt

QTY PER MAJOR ASSY	ZONE	ITEM	CODE IDENT NO.	PART OR IDENTIFYING NO.	NOMENCLATURE OR DESCRIPTION	MATERIAL AND FINISH OR NOTE OR REF DES
	AR	23		24 AWG, SOFT, TINNED WIRE, BARE	QQ-W-343, TYPE S	
		22				
		21		3-48NC-2A-3/8L6 SCREW (COM'L)	100° FLAT HEAD SLOTTED, CKFC	
		20				
		19		P50-3	INDUCTOR	NOTE 3 LI
		18				
		17		1N3829	DIODE	JEDEC CR5
		16		FDH600	DIODE	NOTE 5 CR4
		15		1N751A	DIODE	JEDEC CR2
		14				
		13		2N3720	TRANSISTOR	NOTE 2 Q3
		12				
		11				
		9		CL65CH151MP3	CAPACITOR	MIL-C-3965 C1,C4
		8				
		7		RC32GF361J	RESISTOR	MIL-R-11 R12
		6		RC05GF152J	RESISTOR	MIL-R-11 R15
		5		RC05GF102J	RESISTOR	MIL-R-11 R13
		4				
	REF	3		N100-1400	SCHEMATIC	
		2		N100-14004-01	BOARD	
		1				
		1		-01 BOARD ASSY		

D  
C  
B  
A  
N100-14002

QTY PER MAJOR ASSY		NEXT ASSEMBLY	USED ON	UNLESS OTHERWISE SPECIFIED		LTV RESEARCH CENTER	
		N100-14000	N100-00000	TOLERANCES UNLESS OTHERWISE SPECIFIED	PROJ ENGR		COMP BD ASSY LOW VOLTAGE PWR SUPPLY LWR BOARD
				2 PLACE DEC 3 PLACE DEC 1/16 1/32 ANGLES MACHINED FORMED SHEARED 1/16 1/32 1/16 1/32 HOLE TOLERANCE PER ANSI B91.1 SURFACE ROUGHNESS PER MIL-STD-19 DIMENSIONING AND TOLERANCING PER MIL-STD-113 ECCENTRICITY BETWEEN ANY DIA'S ON THE SAME CENTRALLINE SHALL NOT EXCEED .010 TOTAL INDICATOR READING ALL DIM. ARE IN INCHES UNLESS APPLIED FINISH WELD SYMBOLS PER MIL-STD-19 HOLE CODE PER ANSI Z39.53 THREADS PER MIL-STD-183 MARKS PER MIL-STD-190 REMOVE ALL BURRS AND SHARP EDGES SPECIFICATIONS	COMP ENGR MKTG PROJ ENGR STRUCT WYS GROUP APP CHECKED BY DRAWN BY ENGR GROUP		
							SIZE CODE IDENT NO. D 11817 N100-14002
							SCALE: 2/1 REV. A SHEET



4

3

2

1

NOTES:  
1. FABRICATE AND SOLDER COAT PER  
MSFC-STD-275.

REVISIONS			
ZONE	LTR	DESCRIPTION	DATE
A		INCORPORATED EO. NO. N100.7	1-5-67
			1/29/67
			CHK BY R. B. B. - d

D

C

B

A

N:00-14003

QTY	REF	ZONE	ITEM	CODE IDENT NO.	PART OR IDENTIFYING NO.	NOMENCLATURE OR DESCRIPTION	MATERIAL AND FINISH OR NOTE OR REF DES
	REF		3		N100-14006-01	ARTWORK	
	REF		2		N100-14005-01	ARTWORK	
			1		- 01	BOARD	.062THK 2/20Z MIL-P-13949 GEE

LIST OF MATERIAL OR PARTS LIST

QTY PER MAJOR ASSY	NEXT ASSEMBLY	USED ON	UNLESS OTHERWISE SPECIFIED	PROJ ENGR	COMP ENGR	STRUCT WTS	GROUP APP	CHECKED BY	DRAWN BY	ENGR GROUP	SIZE	CODE IDENT NO.	
	N100-14001	N100-00000	TOLERANCE UNLESS OTHERWISE SPECIFIED 2 PLACE DEC 1.00 3 PLACE DEC 0.010 ANGLES MILCHINE 1/8" 1/16" 1/32" FORMED 1/8" 1/16" 1/32" SHEARED 1/8" 1/16" 1/32" HOLE TOLERANCE PER AND 13387 SURFACE ROUGHNESS PER MIL-STD-10 MACHINED SURFACE FINISH DIMENSIONING AND TOLERANCING PER MIL-STD-8 ECCENTRICITY BETWEEN ANY DIAS IN THE SAME CENTRALING SHALL NOT EXCEED .010 TOTAL INDICATOR READING ALL DIMS ARE IN UNLESS INCLUDE APPL. ED FINISH WELD SYMBOLS PER MIL-STD-10 RIVET CODE PER NAS 373 THREADS PER MIL-STD-172 MARK PER MIL-STD-10 REMOVE ALL BURRS AND SHARP EDGES SPECIFICATIONS:									D	11817
											LTV RESEARCH CENTER		
											BOARD		
											LOW VOLTAGE PWR SUPPLY		
											TOP BOARD		
											N100-14003		
											SCALS: 2/1 REV: A SHEET		

A

LT96-80

8

7

6

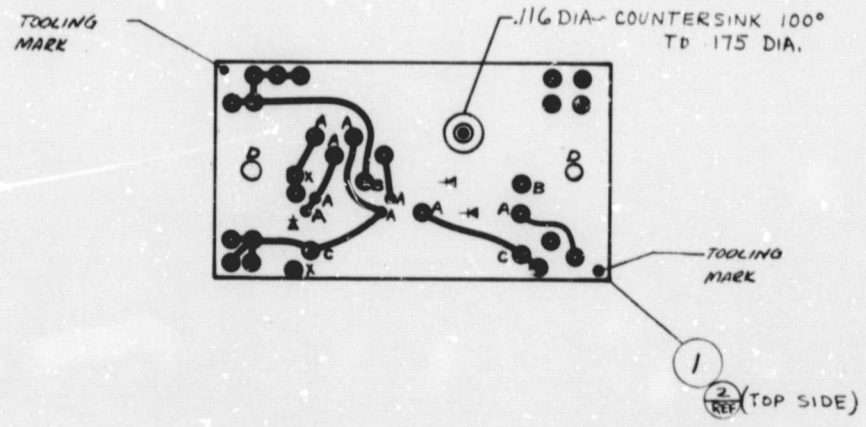
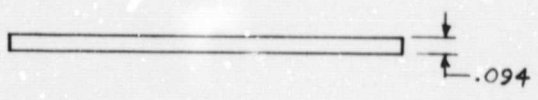
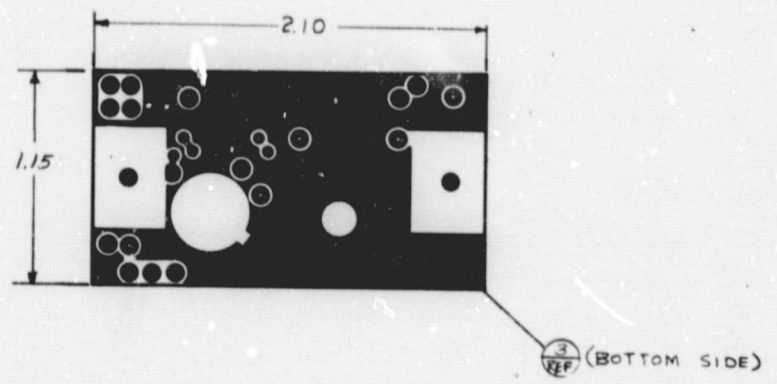
5

D

C

B

A



CODE	HOLE SIZE
NO CODE	.031 DIA
A	.025 DIA
B	.040 DIA
C	.047 DIA
D	.156 DIA

4

3

2

1

NOTES:  
1. FABRICATE AND SOLDER COAT PER  
MSFC-STD-275.

ZONE		LTR		REVISIONS		DATE	APPROVED
				DESCRIPTION			
	A			INCORPORATED ED. NO. N100-6		1-12-66 1/24/67	APPROVED BY A. H. LONG CHK BY E. H. BROWN

D

C

B

NICO-14004

REF	ZONE	ITEM	CODE IDENT NO.	PART OR IDENTIFYING NO.	NOMENCLATURE OR DESCRIPTION	MATERIAL AND FINISH OR NOTE OR REF DES
REF		3		N100-14006-02	ARTWORK	
REF		2		N100-14005-03	ARTWORK	
		1		-01	BOARD	.094 THK 2/20Z. MIL-P-13949 GEE

LIST OF MATERIAL OR PARTS LIST

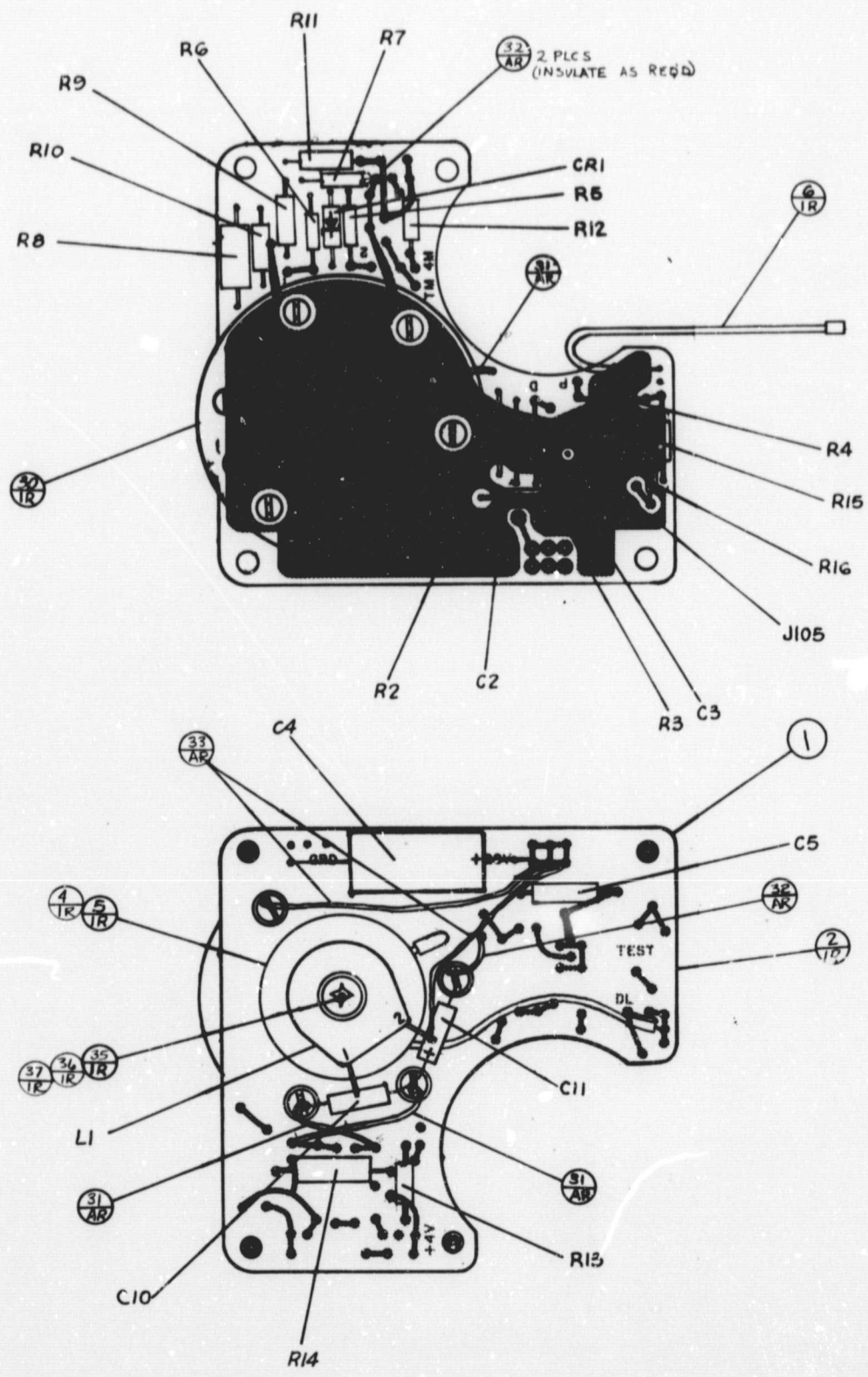
QTY PER MAJOR ASSY	NEXT ASSEMBLY	USED ON	UNLESS OTHERWISE SPECIFIED	PROJ ENGR	DATE	SCALE	REV.	SHEET	
	N100-14002	N100-00000	TOLERANCES UNLESS OTHERWISE SPECIFIED: 2 PLACE DEC 1 PLACE DEC .02 .015 ANGLES 2° 1° MACHINED FORMED SHEARED ±.015 ±.01 ±.015 HOLE TOLERANCE PER AND USE: SURFACE ROUGHNESS PER MIL-STD-15 MACHINED SURFACE FINISH DIMENSIONING AND TOLERANCING PER MIL-STD-15 ECCENTRICITY BETWEEN ANY DIAMS ON THE SAME CENTERLINE SHALL NOT EXCEED .015 TOTAL INDICATOR READING ALL DIMS ARE IN INCHES UNLESS APPLIED FINISH WELD SYMBOLS PER MIL-STD-15 RIVET CODE PER NAS 225 THREADS PER MIL-STD-15 BARR PER MIL-STD-15 BREAK ALL SHARP AND SHARP EDGES SPECIFICATIONS	COMP ENGR DESIGNED STRUCT ENGR GROUP APP CHECKED BY DRAWN BY ENGR GROUP	6-27-66 6/24/66 6-22-66 0-71100	<b>LTV RESEARCH CENTER</b> <b>BOARD</b> <b>LOW VOLTAGE PWR SUPPLY</b> <b>LWR BOARD</b>	D 11817	N100-14004	2/1 A 1

A



8 | 7 | 6 | 5

D  
C  
B  
A



QTY PER MAJOR ASSY	
	N

1







5 | 4 | 3 | 2 | 1

NOTES:  
1. FABRICATE & SOLDER COAT PER  
MFSC-STD-154

REVISIONS				
ZONE	LTR	DESCRIPTION	DATE	APPROVED
	A	INCORPORATED ED. NO. N100.11	1-5-67 1/14/67	B. Lowe C.H. HX R.B. Bannell

CODE	HOLE SIZE (INCHES)
NO CODE	.031
A	.025
B	.128
C	.195
D	.150

D  
C  
B  
A  
N100-15001

QUANTITY REQUIRED	ZONE	ITEM	CODE IDENT NO.	PART OR IDENTIFYING NO.	NOMENCLATURE OR DESCRIPTION	MATERIAL AND FINISH OR NOTE OR REF DES
		4				
	REF	3		N100-15006	ARTWORK	
	REF	2		N100-15005	ARTWORK	
		1		-01	BOARD	

QTY PER MAJOR ASST	NEXT ASSEMBLY	USED ON	TOLERANCES UNLESS OTHERWISE SPECIFIED		PROJ ENGR	LTV RESEARCH CENTER	
	N100-15000	N100-00000	2 PLACE DEC ±.02	3 PLACE DEC ±.010		BOARD HIGH VOLTAGE PWR SUPPLY A7	
			ANGLES MACHINED 1° 15'	FORMED 1°	COMP ENGR	SIZE	CODE IDENT NO.
			HOLE TOLERANCE PER AND HSB	SURFACE ROUGHNESS PER MIL-STD-10	MAT'L	D	11817
			MACHINED SURFACE FINISH	DIMENSIONING AND TOLERANCING PER MIL-STD-10	STRUC ENGR	N100-15001	
			ECCENTRICITY BETWEEN ANY DIAM ON THE SAME CENTERLINE SHALL NOT EXCEED .010	TOTAL INDICATOR READING	GROUP APP	SCALE:	REV. A
			ALL DIM. ARE IN INCHES UNLESS OTHERWISE APPLIED FINISH	WELD SYMBOLS PER MIL-STD-10	CHECKED BY	SHEET	
			RIVET CODE PER NAS 13	REMOVE ALL BURRS AND SHARP EDGES	DRAWN BY		
			MARK PER MIL-STD-10	SPECIFICATIONS	ENGR GROUP		